NASA TECHNICAL MEMORANDUM NASA TM-75497

N79-31779

INVESTIGATION OF A GENERATOR SYSTEM FOR GENERATING ELECTRICAL POWER, TO SUPPLY DIRECTLY TO THE PUBLIC NETWORK, USING A WINDMILL

C. Tromp

Translation of "Onderzoek aan een generatorsystem voor het opwekken van - direkt aan het openbare net te leveren - elektrische energie net behulp van een windmolen," Delft, The Netherlands, State University of Technology, Power Electronics Laboratory, Department of Electrical Engineering, May 1957, 122 pages.

NATIONAL AERONATUTICS AND SPACE ADMINISTRATION
WASHINGTON, D.C. AUGUST 1979

(Abstract continued)

view of the network, behaves like a normal, synchronous generator and that the converter only needs to be designed for about 15% of the rated power of the generator.

Contents

		Page
I.	General Introduction	1
1.a.	Wind Energy	1
1.a.1.	Introduction	1
1.a.2.	Properties of wind energy	1
1.a.3.	Properties of energy conversion using a windmill	4
1.b.	Generation of Electrical Power Using a Windmill	5
1.b.1.	Electrical part; tasks, requirements	5
1.b.2.	Electrical part; possibilities	8
II.	Method Investigated	12
2.a.	Theoretical Considerations	12
2.a.1.	Description of the method investigated	12
2.a.2.	Power balance as a function of wind velocity	16
2.a.3.	Derivation of the machine equations	20
	Power balance; the electromagnetic couple	29
	Similarity to a normal, synchronous generator	33
	Similarity to a transformer	38
2.a.4.	Special properties of a combination windmill-DSG	47
	Control of the maximum capacity point by controlling the converter frequency ω_2	48
	Control of cos φ network with converter voltage	49
	Overload capacity of the generator	51
	Copper and iron losses in a DSG	60
2.a.5.	The Converter	64
2.b.	Practical Section	66
2.b.1.	Description of the experimental set-up	66
	The generators used	67
	The converter used	69
2.b.2.	Findings in the experiment	70
2.b.3.	Measurement results	73
2.b.4.	Effect of non-perfect system parts the behavior of the machine	75
2.b.5.	Calculation method	82
Conclusions		88

INVESTIGATION OF A GENERATOR SYSTEM FOR GENERATING ELECTRICAL POWER, TO SUPPLY DIRECTLY TO THE PUBLIC NETWORK, USING A WINDMILL

C. Tromp
Power Electronics Laboratory

I. General Introduction

I.a. Wind Energy

1.a.1. Introduction

The transformation of wind energy into electrical energy proceeds in two stages: /1*

wind energy is transformed into mechanical energy by means of a windmill.

the mechanical energy is transformed into electrical energy using a generator whose lower part is made up of what we shall call the "electrical part" of the system.

The mechanical energy is presented to the electrical part by means of a turning shaft. Defining the power (the couple and the revolution) which can be presented, we have:

the properties of the wind energy itself,

the properties of the energy transformation using a mill.

Studying this is thus a first requirement. A detailed consideration given over to wind energy falls outside the specifications of this report. Only what is of immediate interest for the system concerned here is explained further. For a detailed treatment, consult the literature, for example [1].

1.a.2. Properties of Wind Energy

The kinetic energy per second, for an amount of air which flows at a certain velocity V_w perpendicular to a specified surface, is:

$$P_w = 0{,}64\ A\ v_w^3 \qquad [\text{watt}] \qquad (1) \qquad (1)$$

---

* Numbers in the margin indicate pagination in the foreign text.

where: P_W = the wind capacity (energy per second)
A = the size of the given surface (m^2)
V_W = the wind speed perpendicular to surface A (m/sec)

The constants in eq. (1) are determined by specific mass of the air, which depends on various factors. As an average value, we here take $\rho = 1.29\ kg/m^3$.

In the case of the windmill, A is the circular surface which is drawn by the vanes (Fig. 1) and P is the power which the mill offers.

If D is the diameter of the surface A, then:

$$P_W = 0.503\ D^2 v_W^3\ ,$$

or simply:

$$P_W \simeq \tfrac{1}{2}\ D^2 v_W^3 \qquad (2)$$

The power is thus very highly dependent on wind velocity. /2
In general, it may be said that wind velocity:

depends strongly on the location on earth, due to climatological circumstances,

increases with height above the earth's surface (naturally not unlimited),

is greater on the coast and at sea than inland.

Because of this, there is a need for information in a clear form on the behavior of the wind at a particular site. This information must relate to wind velocity. Wind direction is left out of consideration, because a windmill can always be directed into the wind.

The wind velocity distribution curve gives the information in question. Along the abscissa is set the wind velocity V_W, where this is divided into small increments ΔV. Along the ordinate is hours per year (see Fig. 2). The graph, which consequently is a histogram, gives the number of hours per year for each area ΔV that the wind velocity occurring at the site where it is measured lies within the area ΔV. By selecting a sufficiently large number of areas ΔV, the histogram turns into a continuous line. Along the ordinate one also sees well marked the probability that wind velocity lies within ΔV. In this case one speaks of a probability density function.

It is clear that, for a reliable curve, many years must be measured.

Fig. 3a (taken from [1]) gives an example of a wind /3

velocity distribution curve measured on the coast of Wales (GB) at a good 40 meters high. The wind velocity is given in meters per second. Because use is often made of the Beaufort scale (wind power), this is taken up in the appendix at the back.

The most often occurring wind velocity (top of the graph in Fig. 3a) is always lower than the average wind velocity (here, 7.24 m/sec).

On the graphs made at other sites, the top may lie more to the left or right. The latter naturally is more favorable. Moreover, the graphs may be smaller and higher, or wider and lower.

The surface under the curve is, however, constant, because it is defined by the number of hours in a year.

Fig. 3b gives the power P_W (= $0.64\ Av_W^3$) as a function of v_W where $A = 1\ m^2$.

Fig. 3c is obtained using Figs. 3a and 3b. In Fig. 3a, for each area ΔV, the number of hours per year is given for which v_W lies within that area. The curve in Fig. 3c is obtained by multiplying that number by the corresponding P_W from Fig. 3b. We then obtain the number kWh/year/m^2 as a function of the wind velocity with which this energy passes through surface A.

Although Figures 3a and 3c alone are valid for the measuring site names, it can still be used for individual general conclusions, because its form is very characteristic.

So we see that a more or less regular energy yield is out of the question; for a given curve, it holds true that the maximum power put out ($v_W \simeq 25$ m/sec) is about 125 times as great as the power for the most often occurring wind velocity ($V_W \simeq 5$ m/sec).

Fig. 3c shows that right at less frequently occurring, high wind velocities, the greatest yearly energy yield is expected. /5

Without the chance of an increase in one form or another, or a replenishing energy source for periods with little wind, wind energy is therefore not useful. In addition, it holds true that, as a result of a strong increase in P_W for an increase in V_W (Fig. 3c), it is also not obtainable for each V_W to use all the energy put out.

Mass inertia, friction, and loss make it so that each installation can be used only up to a certain minimum percentage of the full capacity.

An extensive study of meteorological data must decide how the installation must be sized for optimum profit.

1.a.3. Properties of Energy Conversion Using a Windmill

With detailed demonstration, it will be seen that all the kinetic energy flowing through surface A (Fig. 1) can never be given over to the vanes of the mill. In order to guarantee a permanent steeam of air, the "used wind" must always leave the area behind the mill at a certain speed.

The power that is given over to the mill vanes, provided through the power of the wind P_w, is given by the power coefficient C_p.

$$C_p \text{ is defined as } \frac{P_{delivered}}{P_{wind}} \quad \text{dimensionless} \qquad (3)$$

A. Betz held, at the beginning of this century, that the theoretical maximum value of C_p is equal to 16/27 = 0.593. That is, the theoretical power to gain is less than 60% of the power put out by the wind.

The maximum value of C_p, C_{po}, where C_{po} 16/27, appears as the ratio between vane shaft revolution and wind velocity, which we shall call μ with a special value μ_o assumed. That is, for each wind velocity, a certain vane shaft revolution is involved whereby C_p is maximum.

Using the following notation:

μ	= tip speed ratio	-
μ_o	= value of μ at $C_p = C_{po}$	-
v_{tip}	= circumferential speed of the tip of the vane	m/sec
ω_m	= angular velocity of the vane shaft	rad/sec
n_m	= revolutions of the vane shaft	r/sec

$$\mu \overset{def}{=} \frac{v_{tip}}{v_w} = \frac{\omega_m D/2}{v_w} = \frac{\pi n_m D}{v_w} \qquad (4)$$

The value of μ_0 and the decline of C_p as a function of μ is determined by the shape of the vanes and not by their size.

Fig. 4 gives the power coefficient for two types of mill, as a function of tip speed ratio.

For $C_p = C_{po}$, μ at the value μ_0 must be allowed to increase for a mill revolution proportional to V_w (Eq. 4).

If this requirement is satisfied, then for $\mu = \mu_0$, it follows that:

$$n_m = \frac{\mu_o}{\pi D} v_w \qquad (5)$$

The maximum of C_p, C_{po}, is much lower than the theoretical value 0.593. This is caused by aerodynamic loss.

If the length of the vane (D) was not determined for the value μ_0, from eq. (4) it appears that D is easily determined for the revolution for which the mill must operate for a certain wind velocity in order to obtain $C_p = C_{po}$.

From eq. (4) and the requirement that $\mu = \mu_0$, it is concluded that only for very small installations is the mill revolution high enough for the electrical generator to be driven directly with the vane shaft. At higher powers, a translation takes place to a higher revolution. This means extra losses. /7

Even more losses develop whereby it is not possible to keep C_p continuously equal to C_{po}. Because of the high inertial mass of the mill on the one hand and the strong fluctuating character of the wind on the other hand, $\mu \neq \mu_o$ will occur regularly, whereby the average value of C_p will be lower than C_{po}.

In Fig. 5, the final couple-drive curves are sketched for a certain windmill at three different wind velocities.

Point a gives the running couple and point b the maximum couple at the wind velocity concerned.

The ratio between the running couple and the maximum couple depends on the type of mill. With a type with high μ_o goes a small running couple in proportion.

At point b, $\mu < \mu_o$ holds (for each mill type), while somewhere to the right of b lies the point where $\mu = \mu_o$. The hyperbola which is exactly in contact with the couple-drive curve has this point as the contact point (Fig. 5, point m).

At point c, the couple-drive curve goes through the n-axis. At the mill revolution, the passing air does not discharge the propelling power out of the vanes (at the wind velocity which involves the curves concerned). If one increases the revolution (by driving), then the passing air will be propelled by the mill (fan).

Summing up:

for optimum energy yield, the mill revolution must be kept proportional to the wind velocity which occurs,

the wind energy output is highly irregular,

favorable places for windmills in this respect are on the coast and at sea,

because of the freakish character of the wind, use can only be made of wind energy: if the energy savings are of not inexhaustible sources; in fact, the annual output of a windmill-generation capability can therefore be better expressed in tons of oil, or in cubic meters of natural gas than in kilowatt-hours.

1.b. Generation of Electrical Power Using a Windmill

1.b.1. Electrical Part: Tasks, Requirements

The electrical part of the system has as its primary task the conversion of mechanical energy into electrical energy. An electrical generator is necessary for this. The choice of generator type, along with further necessary provisions, is

determined by a second task which the electrical part has to fulfill, namely:

> The adjustment of the characteristic properties of the energy source (wind) to that of the user network voltage, network frequency), in such a way that the power provided to the vanes for a given wind velocity is always at maximum, $C_p = C_{po}$.

This is the field of power electronics. The focus at which $C_p = C_{po}$ we call the maximum power point. The following input and output quantities of the electrical part play a role in this (see also Fig. 6).

ω_r - is the mechanical angular velocity of the generator in rad/sec. It is determined from the vane revolution n_m and the conversion ratio for the generator shaft. A variable conversion ratio is not practically realizable for high power. We therefore start out from the fact that always holds: $\omega_r \sim n_m$, and with eq. (5) for $C_p = C_{po}$: $\omega_r \sim v_w$. /10

Because of the large difference in P_w at high and low wind velocities (Chapter 1), one generally tries for $C_p = C_{po}$ between certain limits for v_w.

We shall call the lower limit of v_k/v_{min}, and the upper limit v_k (see the abscissa on Fig. 7).

The value of v_k/v_{min} follows from the ratio between P_w at v_k and P_w at v_{min}, which will be recorded through the properties of the installation itself, namely through the smallest percentage of the full capacity at which energy generation is possible (zero load loss).

The value of v_k, and thus the amount of electrical power to install per square meter of the vane circle A (Fig. 1) is determined by using meteorological data, with the criterion of maximum kWh output per year.

Furthermore, it is defined: v_{max} is the maximum wind velocity occurring, and the maximum wind velocity at which the mill can be kept in operation.

P_a - is the mechanical power to the generator, in watts. We call n_m the combined mechanical output of the windmill and the transfer at the generator shaft.

Then:

$$P = C_p n_m p_w \qquad (6)$$

In Fig. 7, the dotted line P_a is given as a function of v_w, if n_m is constant and $C_p = C_{po}$ in the whole area $0 \leq v \leq v_{max}$.

The solid line given P_a as a function of v_w for: /11

$0 \leq v_w < v_{min}$: $P_a = 0$; P_w is too small to cover the total zero load loss.

$v_{min} \leq v_w \leq v_k$ } $P_a \sim v_w^3$; this is attained by keeping $C_p = C_{po}$ in this area.

$v_k < v_w \leq v_{max}$: P_a is equal to the full capacity of the installation.

For the limits of P_a at full power for $v_k < v_w \leq v_{max}$, special provisions are necessary.

T_a - is the mechanical couple for the generator shaft in Nm. With the definitions given for T_a, P_a, and ω_r, it follows that:

$$T_a = P_a/\omega_r \qquad (7)$$

If $\omega_r \sim v_w$ and $P_a \sim v_w^3$, then:

$$T_a \sim v_w^2$$

U_{net} - is the effective value of the voltage, relative to ground for the output terminal of the electrical part, in volts.

This voltage is, possibly after a transformation constant, equal to the (constant) network voltage. By the network, we mean here the public, three-phase current network.

ω_1 - is the electrical angular frequency of the three-phase current network in rad/sec; $\omega_1 = 2\pi f_1$ (f_1 = 50 Hz network frequency). /12

cos φ_{net} - is the work factor. This is the cosine of the (phase) angle φ_{net} between U_{net} and I_{net}, if I_{net} is the current given by the electrical part. With this can be written, for the watt-power P_w given by the

electrical part:

$$P_{net} = 3U_{net}\, I_{net} \cos \varphi_{net} \quad (\text{"3" for 3 phases})$$

The requirements for the electrical part are summarized:

1. For $v_{min} \leq v_w \leq v_k$, the electrical part of the windmill must set that revolution whereby P_a is maximum for a given wind velocity ($C_p = C_{po}$; maximum power point).

2. Irrespective of that revolution, the electrical part must generate three-phase voltage with constant network amplitude and frequency.

We require, moreover:

3. The electrical part may not assume idle power; it is desirable to be able to deliver a certain amount of idle power.

For P_{net}, and therefore for I_{net}, no requirements may be set. Because the electrical part has no energy storage capability worth mentioning, P_{net} follows from the power P_a supplied.

It can even be required of the electrical part that the shaft power P_a be limited for $v_k < v_w \leq v_{max}$. For the present, we are not setting this requirement, because other, mechanical methods appear to be suitable for this.

In Fig. 6a, the electrical part is further worked out, using the requirements formulated in this chapter (compare Fig. 6).

The converter is a static transformer. It plays an important role in satisfying the requirements set.

1.b.2. Electrical Part: Possibilities /14

Method 1

We can build the electrical part so that the set requirements will be satisfied step by step. That is, without paying attention to voltage or frequency, the generator is adjusted so that the power delivered at the v_w occurring is maximum. Then, using a converter, the voltage (three phases) and the frequency are put at the correct value. We call this the cascade system.

Fig. 8 gives the block diagram. The converter builds up the load for the generator. Through its build-up, the converter

is in a state of its assumed power, and with it the generator current is adjusted. The generator current determines the (inhibiting) electromagnetic couple T_{el} of the generator. The generator will go around with the angular velocity ω_r, for which $T_a(\omega_r) = T_{el}$ (see Fig. 5a, NB: only the intersection at side bc gives a stationary position; compare the T-n curve for an asynchronous machine).

At point Q (Fig. 8), the electrical power delivered by the generator is measured. This is a measure for P_a (NB: $P_a = \omega_r T_a$).

By varying T_{el} (using the converter), we can find the setting at which the power at Q, and thus P_a, is maximum.

With the aid of the text for Fig. 5 on page 101, it is plain to see that we come point m again (see also Fig. 5a), for which: P_a is maximum, $\mu = \mu_o$, $C_p = C_{po}$.

Requirement 1 of Section 1.b.1 is thus satisfied.

Fig. 9 gives an example of a three-phase DC → AC converter /15
with voltage adjustment, which satisfies requirement 2 in Section 1.b.1.

Voltage Regulation:

U_G depends on the generator (mill) revolution, but must always be greater than the usual value of U_o.

The CSS is a controlled semiconductor switch (transistor, or thyristor with an idle circuit).

If the CSS is closed, a current passes which loads the condenser, upon which $u_o(t)$ increases. This load current is limited through the coil L, which is of special interest if U_G is indicated to be greater than U_o. If the CSS is opened, then if $I_B > 0$, the voltage $u_o(t)$ will decrease.

Naturally, the current through L may not be interrupted suddenly. The diode D takes care of a closed current circuit if the CSS is opened.

$u_o(t)$ must be kept constant as much as possible at the value U_o. For this purpose, $u_o(t)$ is compared with a reference voltage e_r. If $e_r - u_o(t) = +\varepsilon$ (with $0 < \varepsilon \ll e_r$), then the regulator takes care of the CSS being closed, so that $u_o(t)$ increases. /16
As soon as $e_r - u_o(t)$ actually equals $-\varepsilon$, the CSS is again opened at the command of the regulator.

Fig. 10 gives an example of $u_o(t)$ for specific values of U_G and I_B.

AC → DC Converter /17

The converter transistors connect the points U, V, and W, varying with plus and minus for the stabilized supply voltage. If this happens as given in Fig. 11a, then the symmetric, 3-phase block voltages given in Fig. 11b exist between the points U, V, and W. If T_o is the period (20 msec for a voltage of 50 Hz) and T_{on} the time per period during which a transistor is conducting, then it must hold true that T_{on} is the same for all six transistors.

Moreover, the three pictures which Fig. 11a shows for the connection for the transistors in the three different phases must always be 1/3 T_o to be [unknown] relative to each other.

In Fig. 11a, it is deduced that T_{on} is equal to $\frac{1}{2}T_o$, so that in connection with the danger of a shortcircuit in the supply source via the two transistors in one phase can naturally never be completely realized.

If we reduce T_{on} (Fig. 11c), then we obtain voltages between U, V, and W.

The Course of Fig. 11d /19

If we load the converter with a star connection of three like resistances, then they will assume these currents, as given in Fig. 11e (at 11b) and in Fig. 11f (at 11d). At the same time, the current I_B taken up by the converter is drawn in these figures. From this, it is seen that by adjusting T_{on} (pulse width modulation), the size of I_B can be controlled.

If I_B is large, the frequency at which the condenser C must be loaded is high, while the CSS must be closed during a relatively long connection period.

At a smaller I_B, a lower connection frequency and a relatively shorter load time per period holds. This means a smaller effective value for the generator current.

So it is to adjust the generator current with the converter, as has already been assumed in the text at Fig. 8.

We are starting here from an ohmic load. If the load also comprises an inductive component, then the diodes delineated take care that the following current can keep flowing if the current through a conducting transistor is interrupted.

Finally, a filter is still necessary for removing the higher harmonics in the output current. This is placed between the converter and the network.

Naturally a large number of variants are possible with this method. Study and development of it are certainly necessary, if one is to know how far the requirements of Section 1.b.1. are satisfied.

Typical of all the variants of this cascade system is that the entire electrical power is always adapted in order to satisfy the requirements set.

The voltage regulation, the converter, and the filter therefore always deal with the entire power delivered and must consequently all be calculated at the (apparent) full power of the generator.

Because it operates here at high power (on the order of megawatts), the execution will meet up with very technical problems.

Method 2 /20

Fig. 12 gives a sketch of an entirely different approach. The generator (double-feed synchronous) driven by the mill is now directly coupled to the network. The converter supplying at the rotor provides for the requirements set in Sect. 1.b.1. being satisfied.

The most important advantage of this method is that here much cheaper power can be developed through power electronics (converter) for the price, but the good comes especially in the practical feasibility.

Because the higher harmonics of the already cheaper converter power can, moreover, scarcely occur here again via the generator at the output terminals, the voltages between U, V, and W will much better approximate a sinewave shape than the comparable voltages in Fig. 9.

The second part of this report is devoted to this method.

Because nothing can be found in the literature on this method, a fundamental analysis and a practical test of the principle were first required.

II. Method Investigated /21

2.a. Theoretical Considerations

2.a.1. Description of the Method Investigated

The generator usually used for the generation of electricity for a public three-phase current network, the 3-phase synchronous generator (SG), is naturally not suitable to satisfy requirement 1 in Sect. 1.b.1. ("to set that revolution for the windmill whereby $C_p = C_{po}$"), at least not when it is directly coupled to the network. There is then always only one generator revolution possible whereby the required network frequency can be delivered.

This is explained as follows. The operation of this generator is based on two magnetic fields being "elastically" coupled to one another, which turn at a constant revolution in the machine.

One filed, the stator rotary field, exists because in the rotary current winding of the stator at the connected network, the rotary current flows at the network frequency f_1.

The other field, the rotor rotary field, exists because an adjustable electromagnet rated with direct current (or a ring of electromagnets, the pole wheel) is being turned around.

At the speed of the stator rotary field n_1, it can be shown that:

$$n_1 = \frac{f_1}{p} \qquad (8)$$

Here, p is the number of coils per phase of the rotary current winding at the stator, or also, which is the same thing: the number of pole pairs in the pole wheel.

It will be clear that, as long as the connection between these magnetic fields exists, the pole wheel (the rotor) turns round with a constant (synchronous) revolution n_1, at which the stator rotary field also turns.

NB: If the stator rotary field thus draws the rotor rotary field with it, then the machine operates as a motor. If, on the other hand, the rotor rotary field draws the stator rotary field with it (by driving the rotor), then we have made a generator.

We now hypothesize just one generator with the same stator, but where the rotor does not consist of an electromagnet with

rated direct current, but a direct current winding (network as the stator), which is supplied with direct current at a frequency f_2. /22

Entirely analogous to what occurs at the stator (eq. 8), a rotary field will exist at the rotor such that this rotor winding (thus relative to the rotor) has a revolution of n_2 r/sec where $n_2 = f_2/p$ (p must also be equal here for stator and rotor).

If we let the rotor turn now with a revolution n_r r/sec, the rotary field thus generated for a stationary observer (thus relative to the stator) turns around with a rveolution $n_2 + n_r$.

If:

$$n_2 + n_r = n_1 \qquad (9)$$

the machine can turn synchronously with the network with a frequency $f_1 = p \times n_1$. The "elastic" connection between the magnetic fields therefore provides for the required relation between the revolutions to remain as according to eq. (9). If we have at out disposal a voltage source with an adjustable frequency f_2, so that we can control n_2, it follows from eq. (9) that we can let the machine turn synchronously at the network for any desired revolution. In other words, we can set any desired revolution for the machine by adjusting f_2. n_1 ($= p \cdot f_1$) is always fixed. If we control n_2 with f_2, then n_r follows from eq. (9).

If, however, we load the machine too severely, the connection between the (magnetic) rotary field is broken. The machine falls out of phase and eq. (9) is not longer true.

If we indeed have a voltage source at our disposal which under all the aforementioned circumstances can provide for a rotor supply with the required frequency f_2 (power electronics), this generator is very suitable for being driven by a windmill.

Because a high ratio exists between generator revolution and mill revolution, we can always set the required revolution with such a generator by adjusting f_2 (thus by controlling the revolution of the generator) for the mill (requirement 1, Sect. 1.b.1.), while the given frequency remains constant, so that the machine can be directly linked to the network.

The fact that the generator at any revolution can turn synchronously with the network implies that it also satisfies requirement 2 as far as the voltage is concerned (amplitude and frequency). /23

Equally, for the synchronous generator with rated direct current, we can also control the rotor current here. For this purpose, the voltage source which "f_2" delivers must also be adjustable in amplitude.

We shall further show that then (network as for a normal SG) the idle power delivered by the generator can be controlled with rating (requirement 3, Sect. 1.b.1).

With this, all the set requirements in Sect. 1.b.1 are satisfied.

In Fig. 13, the principle is sketched. The voltage source adjustable in U and f is a converter which is supplied from the stator.

If we neglect the losses at the generator, then:

$$P_1 = P_a + P_2 \tag{10}$$

If we neglect losses at the converter, then: $Pc = P_2$. Furthermore, P_{net} always $= P_1 - P_c$.

From these three equations, it then follows that: $P_{net} = P_a$, which naturally is logical, for P_a is the (mill) power that is supplied from outside the system and P_{net} is the power that is delivered. If we suppose that the system is loss-free, these powers must naturally be equal to each other.

P_c is, as it were, power which is pumped around by the machine. The amount of the power and the output at which this "pumping around" occurs determine the extra losses in this system, which ultimately are measured for applicability.

Fig. 13a is a combination of Fig. 13 and Fig. 6a and gives a diagram of the principle of the whole system.

It will be noted that the machine in build-up reminds one /26
of an asynchronous slip-ring armature motor (ASM). There are differences, of course.

The ASM generally has a rotor winding which is made for high current at low voltage (much lower than the network voltage). This is unfavorable for the semiconductor component of the converter.

The brush arrangement of the ASM is usually not calculated at continuous operation via the brushes.

The ASM has a short-circuit ring for nominal operation; it is superfluous here.

Building up a lesser known double-feed (a) synchronous motor is better suited for our application (ref. [4]).

Because in this machine stator and rotor are fed from the network, the rotor windings are calculated at high (network) voltage and low current, while the brush arrangement is well suited for continuous operation. By analogy with this machine, we will designate the generator we used by the name of Double-feed Synchronous Generator (DSG).

2.a.2. Power Balance as a Function of Wind Velocity /27

We have already noted that the size of the power P_2 that must be supplied to the rotor, and that must be delivered by the converter, is determined to a significant extent by the application of the system.

Therefore, we shall now give, with the help of eq. (10), the power balance ($P_1 = P_a + P_2$) and the path of P_a, drawn in Fig. 7 on page 103, , as a function of v_w (hereunder once more portrayed), a first approximation given for the course of P_2 as a function of v_w. From the power balance used, it follows that this approximation holds for an entriely loss-free machine.

Once again, it is shown that Fig. 7 for $v_{min} \leq v_w \leq v_k$ gives the most favorable path for P_a, which is only obtained if requirement 1 in Sect. 1.b.1. is satisfied. If we use Fig. 7 as the starting point for the calculation of P_1 and P_2, it is implied that here we assume that f_2 for $v_{min} \leq v_w \leq v_k$ is adjusted so that this requirement is always satisfied.

We begin with working out eq. (9), $n_2 + n_r = n_1$. With $n_2 = f_2/p$ /28
$n_1 = f_1/p$, we have: $f_2/p + n_r = f_1/p$. If we multiply the whole equation by 2π, and define $\omega_1 = 2\pi f_1$, $\omega_2 = 2\pi f_2$, and $\omega_r = 2\pi n_r$, all three in rad/sec, then we can write:

$$\frac{\omega_1}{p} = \frac{\omega_2}{p} + \omega_r \qquad (11)$$

Multiplying eq. (11) by the shaft couple T_a yields:

$$\frac{\omega_1}{p} T_a = \frac{\omega_2}{p} T_a + \omega_r T_a \qquad (12)$$

By multiplying

$$P_a = \omega_r T_a \qquad (7) \quad ,$$

$$P_1 = P_2 + P_a \qquad (10) \quad ,$$

and the already proven assumption: $P_1 : P_2 = \omega_1 : \omega_2$
we can solve eq. (12):

$$P_1 = \frac{\omega_1}{p} T_a \qquad (13)$$

$$P_2 = \frac{\omega_2}{p} T_a \qquad (14)$$

From Fig. 13, it is concluded that $P_a > 0$ and $P_1 > 0$ must hold. Otherwise, no power is ever delivered.

We deduce from this that the converter is so set up that $P_2 \geqslant 0$[1] also holds.

From the power balance, it follows that: $P_1 \geqslant P_a$, or with eq. (7) and (13) $\omega_1/p \geqslant \omega_r$. That is, ω_1/p is the highest velocity at which the generator can turn

In the area, $v_{min} \leq v_w \leq v_k$, $\omega_r \sim v_w$ must hold. If we choose $\omega_r = \omega_1/p$ (the maximum angular velocity allowed) /29
at v_k (the highest wind velocity at which $\omega_r \sim v_w$, then in this area:

$$\omega_r = \frac{v_w}{v_k} \cdot \frac{\omega_1}{p} \qquad (15)$$

holds true.

---

[1] $P_2 < 0$ means that the converter is operating (for the supply network). The damping effect of the generator at the higher harmonics then disappears. Therefore, we start here with $P_2 \geqslant 0$.

From the fact that all losses are neglected, it follows, moreover, that $v_{min} = 0$, so that eq. (15) holds for $0 \leq v_w \leq v_k$.

In Fig. 7, we say that for $v_{min} \leq v_w \leq v_k$ (under the set conditions) $P_a \sim V_w^3$. With c as a proportionality constant, we obtain:

$$P_a = c\,\omega_r^3 \tag{16}$$

and with $T_a = P_a / \omega_r$; $T_a = c\,\omega_r^2$, while the latter, substituted in eq. (13) and (14) yields:

$$P_1 = c\,\frac{\omega_1}{p}\,\omega_r^2 \tag{17}$$

$$P_2 = c\,\frac{\omega_2}{p}\,\omega_r^2 \tag{18}$$

From eq. (16) and (17), it now follows that: $P_1(\omega_r) = P_a(\omega_r)$ for $\omega_r = 0$ and for $\omega_r = \omega_1/p$.

If we set $P_{max} = P_1(\omega_1/p) = P_a(\omega_1/p) = c\{\omega_1/p\}^3$, then we can indicate $\frac{P_a}{P_{max}}(\omega_r)$ and $\frac{P_1}{P_{max}}(\omega_r)$ for $0 \leq \omega_r \leq \omega_1/p$ while $\frac{P_2}{P_{max}}(\omega_r)$ can be constructed from this using the power balance.

Because $\omega_r \sim v_w$ holds in the area designated $(0 \leq \omega_r \leq \omega_1/p)$ $\omega_r \sim v_w$, we can also set v_w along the abscissa from 0 to v_k.

$$P_a = c\frac{\omega_r}{p}\omega_r^2 \qquad P_1 = c\frac{\omega_1}{p}\omega_r^2 \qquad P_2 = P_1 - P_a \quad .$$ /30

We shall further look at P_2 (ω_r). For this we write:

$$P_2(\omega_r) = P_1(\omega_r) - P_a(\omega_r) = c\frac{\omega_1}{p}\omega_r^2 - c\,\omega_r^3 \; .$$

$P = 0$ for $\omega_r = 0$ and for $\omega_r = \omega_1/p$. In this last case, $\omega_2 = 0$ (eq. (11). The rotor is powered by direct current; the rotor rotary field stands still relative to the rotor. The machine operates like a normal SG.

P_2 is maximum for $\omega_r = 2/3\ \omega_1/p$ ($v_w = 2/3\ v_k$). This follows from $\frac{dP_2(\omega_r)}{d\,\omega_r} = 0$. After substituting, we find /31

$P_2\ (2/3\ \omega_1/p) = 4/27\ c\ (\omega_1/p)^3$ as the maximum value of P_2.

We assume that for $v_k < v_w \leq v_{max}$, P_a is drawn as in Fig. 7; it is no longer increasing, while ω_r is kept constant at ; direct current power; normal SG), then the situation which occurs for a wind velocity greater than v_k will remain equal for the electrical part at $v_w = v_k$. The stator power occurring then

$$P_1(v_k) = P_1\left(\frac{\omega_1}{p}\right) = P_a\left(\frac{\omega_1}{p}\right) = P_{max} = c\left(\frac{\omega_1}{p}\right)^3$$

is then considered as the full power of the generator.

Expressed in percentage of the full power, the maximum value of P_2 thus amounts to

$$\frac{P_2\left(\frac{2}{3}\frac{\omega_1}{p}\right)}{P_{max}} \times 100\% = \frac{\frac{4}{27}\, c\, \left(\frac{\omega_1}{p}\right)^3}{c\, \left(\frac{\omega_1}{p}\right)^3} \times 100\% = 14{,}8\%$$

We can thus conclude that the maximum power that can be "pumped around" via the converter and rotor amount to not quite 15% of the full power of the generator, mind you, when neglecting all losses. For electrical generator losses, P_2 is somewhat greater than is indicated in Fig. 14, while P_c for converter losses is again somewhat larger than the real P_2.

The value of v_w at which P_a can just cover these losses plus the frictional losses of the generator is defined as v_{min}.

Below v_{min}, the installation must be connected up in order for the converter power to be received out of the network.

Finally, we can, by setting the second derivative to zero, find that P_2 (ω_r) at $\omega_r = 1/3\ \omega_1/p$ has an inflection point.

2.a.3. Derivation of the Machine Equations /32

Because there is no literature on the way heretofore considered in which an ASM operates as a synchronous generator, we shall ourselves derive the machine equations with which to prove the assertion presented.

The voltage equations:

In Fig. 15 are given first of all the names and sketch arrangements used for voltages and currents at the stator and rotor.

We shall, for convenience, in setting up the equations start with a machine for which p = 1.

For the equations obtained with this, it is easy to show that they also hold for p = 2, 3, 4 and so on.

The spatial angle at which the winding of the rotor phase u (relative to v, w) at a certain moment is twisted relative to the winding of the stator phase U (relative to V, W), we call the position angle δ (see Fig. 16). With ω_r as the mechanical angular velocity of the rotor and δ_0 as the value of δ at moment t = 0, for $\delta(t)$ we can write: /33

$$\delta(t) = \omega_r t + \delta_o \tag{19}$$

In Fig. 16, it is even seen that for phase order uvw at the stator and rotor, ω_1, ω_2, and ω_r in eq. (11) are positive.

NB: For p = 1, according to eq. (11):

It is plain to see that the mutual influence of the stator and rotor currents at a certain moment is dependent on the position angle δ. From Fig. 16, it is derived that the effect (for p = 1) of a current in rotor phase u, v, w at stator phase U is proportional to $\cos\delta$; $\cos(\delta + 2/3\,\pi)$; $\cos(\delta + 4/3\,\pi)$, pole wheel respectively; while the effect of a current in stator phase U, V, W at rotor phase u is proportional to $\cos(-\delta)$; $\cos(2/3\,\pi - \delta)$; $\cos(4/3\,\pi - \delta)$, pole wheel respectively.

We start with a symmetrical machine which is always unsatisfied and then define the machine constants: /34

R_1 = ohmic resistance of a stator phase
L_{11} = selfinduction coefficient of a stator phase
M_{11} = coefficient of mutual induction between two stator phases
M_{21} = coefficient of selfinduction between a rotor phase and a stator phase, at the moment when $\delta = 0$ (Fig. 16)
R_2 = ohmic resistance of a rotor phase
L_{22} = selfinduction coefficient of a rotor phase
M_{22} = coefficient of mutual induction between two rotor phases
M_{12} = coefficient of mutual induction between a stator phase and a rotor phase, when $\delta = 0$.

We can now express the voltage equations as they hold for arbitrary voltages and currents.

Stator phase U:

$$u_{1u} = R_1 i_{1u} + L_{11} \frac{d}{dt} i_{1u} + M_{11} \frac{d}{dt} i_{1v} + M_{11} \frac{d}{dt} i_{1w} +$$

$$+ \frac{d}{dt} \left\{ M_{21} \cos(\delta)\ i_{2u} + M_{21} \cos(\delta + \tfrac{2}{3}\pi)\ i_{2v} + M_{21} \cos(\delta + \tfrac{4}{3}\pi)\ i_{2w} \right\}.$$

Rotor phase u:

$$u_{2u} = R_2 i_{2u} + L_{22} \frac{d}{dt} i_{2u} + M_{22} \frac{d}{dt} i_{2v} + M_{22} \frac{d}{dt} i_{2w} +$$

$$+ \frac{d}{dt} \left\{ M_{12} \cos(-\delta)\ i_{1u} + M_{12} \cos(\tfrac{2}{3}\pi - \delta)\ i_{1v} + M_{12} \cos(\tfrac{4}{3}\pi - \delta)\ i_{1w} \right\}.$$

a. When no zero conductor is present, or when the current in the neutral wire switchboard during symmetry is equal to zero, then:

$$i_{1u} + i_{1v} + i_{1w} = 0 \quad \text{and} \quad i_{2u} + i_{2v} + i_{2w} = 0 .$$

With this, we can write, for the second through the fourth term of the right member:

$$(L_{11} - M_{11}) \frac{d}{dt} i_{1u}$$

and

$$(L_{22} - M_{22}) \frac{d}{dt} i_{2u} .$$

b. In the case of symmetrical, sinusoidal three-phase voltages and currents, we can make use of the following notation: /35

Stator:

$$u_{1u} = U_1 \, e^{j(\omega_1 t + \alpha_1)} \qquad i_{1u} = I_1 \, e^{j(\omega_1 t + \alpha_1 - \phi_1)}$$

$$u_{1v} = U_1 \, e^{j(\omega_1 t + \alpha_1 - \frac{2}{3}\pi)} \qquad i_{1v} = I_1 \, e^{j(\omega_1 t + \alpha_1 - \phi_1 - \frac{2}{3}\pi)}$$

$$u_{1w} = U_1 \, e^{j(\omega_1 t + \alpha_1 - \frac{4}{3}\pi)} \qquad i_{1w} = I_1 \, e^{j(\omega_1 t + \alpha_1 - \phi_1 - \frac{4}{3}\pi)}$$

Rotor:

$$u_{2u} = U_2 \, e^{j(\omega_2 t + \alpha_2)} \qquad i_{2u} = I_2 \, e^{j(\omega_2 t + \alpha_2 - \phi_2)}$$

$$u_{2v} = U_2 \, e^{j(\omega_2 t + \alpha_2 - \frac{2}{3}\pi)} \qquad i_{2v} = I_2 \, e^{j(\omega_2 t + \alpha_2 - \phi_2 - \frac{2}{3}\pi)}$$

$$u_{2w} = U_2 \, e^{j(\omega_2 t + \alpha_2 - \frac{4}{3}\pi)} \qquad i_{2w} = I_2 \, e^{j(\omega_2 t + \alpha_2 - \phi_2 - \frac{4}{3}\pi)}$$

This sets indices for revolution with angular velocities ω_1 and ω_2 in the index diagram (complex surface).

The projection of these indices onto the vertical axis of the diagram gives the instantaneous values of the voltages and currents.

φ_1 is the angle between the voltage index and the current index of a stator phase (phase angle).

φ_2 gives the phase angle of the rotor.

With α_1 and α_2, we set the values of U_1 and U_2 fixed at time $t = 0$.

c. We find as a condition for synchronous operation:

Substituting in eq. (19), this yields: $\delta = (\omega_1 - \omega_2)t + \delta_0$.

With regard to what has been stated under a, b, c, we can write the voltage equations in complex form as follows:

/36

$$U_1 e^{j(\omega_1 t+\alpha_1)} = R_1 I_1 e^{j(\omega_1 t+\alpha_1-\phi_1)} + L_1 \frac{d}{dt}\{I_1 e^{j(\omega_1 t+\alpha_1-\phi_1)}\} +$$

$$M_{21}\frac{d}{dt}\Big[I_2 e^{j(\omega_2 t+\alpha_2-\phi_2)}\cdot\tfrac{1}{2}\{e^{j(\omega_1 t-\omega_2 t+\delta_o)} + e^{-j(\omega_1 t-\omega_2 t+\delta_o)}\} +$$

$$I_2 e^{j(\omega_2 t+\alpha_2-\phi_2-\frac{2}{3}\pi)}\cdot\tfrac{1}{2}\{e^{j(\omega_1 t-\omega_2 t+\delta_o+\frac{2}{3}\pi)} + e^{-j(\omega_1 t-\omega_2 t+\delta_o+\frac{2}{3}\pi)}\} +$$

$$I_2 e^{j(\omega_2 t+\alpha_2-\phi_2-\frac{4}{3}\pi)}\cdot\tfrac{1}{2}\{e^{j(\omega_1 t-\omega_2 t+\delta_o+\frac{4}{3}\pi)} + e^{-j(\omega_1 t-\omega_2 t+\delta_o+\frac{4}{3}\pi)}\}\Big].$$

After multiplying by the e-power, we find, for the terms between the large brackets:

$$\tfrac{1}{2}I_2\{e^{j(\omega_1 t+\alpha_2-\phi_2+\delta_o)} + e^{-j(\omega_1 t-2\omega_2 t+\alpha_2-\phi_2+\delta_o)} +$$

$$+ e^{j(\omega_1 t+\alpha_2-\phi_2+\delta_o)} + e^{-j(\omega_1 t-2\omega_2 t+\alpha_2-\phi_2+\delta_o+\frac{4}{3}\pi)} +$$

$$+ e^{j(\omega_1 t+\alpha_2-\phi_2+\delta_o)} + e^{-j(\omega_1 t-2\omega_2 t+\alpha_2-\phi_2+\delta_o+\frac{8}{3}\pi)}\}$$

The second, fourth, and sixth terms offered herein add up precisely to zero.

For the voltage equation of the stator, we then obtain:

$$U_1 e^{j(\omega_1 t+\alpha_1)} = R_1 I_1 e^{j(\omega_1 t+\alpha_1-\phi_1)} + L_1 \frac{d}{dt}\{I_1 e^{j(\omega_1 t+\alpha_1-\phi_1)}\} +$$

$$+ M_{21}\frac{d}{dt}\left[\tfrac{1}{2}I_2\{3e^{j(\omega_1 t+\alpha_2-\phi_2+\delta_o)}\}\right] .$$

Performing the differentiation yields the following:

$$U_1 e^{j(\omega_1 t + \alpha_1)} = R_1 I_1 e^{j(\omega_1 t + \alpha_1 - \phi_1)} + j\omega_1 L_1 I_1 e^{j(\omega_1 t + \alpha_1 - \phi_1)} + $$

$$+ j\omega_1 M I_2 e^{j(\omega_1 t + \alpha_2 - \phi_2 + \delta_o)} \qquad (20)$$

where $M = \frac{3}{2} M_{12} = \frac{3}{2} M_{21}$ is defined. ($M_{12} = M_{21}$ follows from the definition on page 21).

It is important that the ω_2's in these equations no longer occur. If this is not the case, it will be shown that the voltages (and, consequently, the currents) at the stator are non-sinusoidal and non-periodic. The sum of the two sinusoidal, periodic voltages of the different frequencies is in general always non-sinusoidal and non-periodic. /37

It is not difficult to see that, during the symmetry, from eq. (20), the stator equations for phases V and W can be found by multiplying all the terms by

Solving the voltage equation for rotor phase u takes place in the same manner as is given for stator phase U.

We thus give only the result:

$e^{-j\frac{2}{3}\pi}$ en $e^{-j\frac{4}{3}\pi}$

$$U_2 e^{j(\omega_2 t + \alpha_2)} = R_2 I_2 e^{j(\omega_2 t + \alpha_2 - \phi_2)} + j\omega_2 L_2 I_2 e^{j(\omega_2 t + \alpha_2 - \phi_2)}$$

$$+ j\omega_2 M\, I_1 e^{j(\omega_2 t + \alpha_1 - \phi_1 - \delta_o)}$$

We see that here the ω_1 no longer appear, so that at the rotor as well the voltages and currents are sinusoidal and periodic.

The equations also follow here for phases v and w by multiplying respectively by $e^{-j\frac{2}{3}\pi}$ en $e^{-j\frac{4}{3}\pi}$.

We can divide equations (20) and (21) by $e^{j\omega_1 t}$ and $e^{j\omega_2 t}$, respectively. What then remains are the equations from which we can get the moduli (independent of t) of, and phase shifts between, different quantities. In fact, it happens we are looking at the situation t = 0 $(e^{j\omega t} = 1)$.

The choice of the time t = 0 is, however, perfectly free, in view of the independence of t in the equations.

A clever choice is to so choose t = 0 that δ_0 ($\delta(t)$ at t = 0) is zero. Equations (20) and (21) change, relative to the above, into:

/38

$$U_1 e^{j\alpha_1} = R_1 I_1 e^{j(\alpha_1-\phi_1)} + j\omega_1 L_1 I_1 e^{j(\alpha_1-\phi_1)} + j\omega_1 M\, I_2 e^{j(\alpha_2-\phi_2)} .$$

$$U_2 e^{j\alpha_2} = R_2 I_2 e^{j(\alpha_2-\phi_2)} + j\omega_2 L_2 I_2 e^{j(\alpha_2-\phi_2)} + j\omega_2 M\, I_1 e^{j(\alpha_1-\phi_1)} .$$

We now define the complex quantities:

$$\underline{U}_s = U_1 e^{j\alpha_1} \quad , \quad \underline{I}_s = I_1 e^{j(\alpha_1-\phi_1)} \quad , \quad \underline{U}_r = U_2 e^{j\alpha_2}$$ and

$$\underline{I}_r = I_2 e^{j(\alpha_2-\phi_2)} \quad ,$$

Then we can write the equations in complex form:

$$\underline{U}_s = R_1\underline{I}_s + j\omega_1 L_1\underline{I}_s + j\omega_1 M\,\underline{I}_r \qquad (22)$$

$$\underline{U}_r = R_2\underline{I}_r + j\omega_2 L_2\underline{I}_r + j\omega_2 M\,\underline{I}_s \qquad (23)$$

We shall now show that equations (22) and (23) also hold for p = 2, 3, 4 and so on. For this, we return to Fig. 16 on page 119.

The angle δ through which the rotor must be turned to obtain again from $\delta = 0$ a stator phase U and a rotor phase u opposite to one another is 360° in the figure.

If, however, we do not have one, but p, coils per phase, then we again have even after 360/p° "U opposite u". There is thus no effect of the different phases as given on page 21, proportional to $\cos\delta$; $\cos(\delta + 2/3\,\pi)$ and so on, but to $\cos p(p\delta)$; $\cos p(\delta + 2/3\,\pi)$ and so on.

For p δ, we find, with $\delta = \omega_r t + \delta_0$ and $p\omega_r = \omega_1 - \omega_2$:

$$p\delta = (\omega_1 - \omega_2)t + p\delta_0 .$$

In setting up eq. (22) and (23), we have assumed $\delta_0 = 0$. The effect is then proportional to $\cos(p\delta) = \cos\{(\omega_1 - \omega_2)t\}$; $\cos\{p(\delta + 2/3\,\pi)\} = \cos\{(\omega_1 - \omega_2)t + 2/3\,\pi\}$ etc.

Because p is no longer here, eq. (22) and (23) will thus hold true generally.

Power Balance; the Electromagnetic Couple /39

For the simplified power balance of eq. (10), $P_1 = P_2 + P_a$, we must now indicate three points.

1) P_a must be replaced by P_{mech}. This is the mechanical power which is useful to use, which is obtained by subtracting the friction losses of the generator from the axle power P_a. As for P_a, we shall consider P_{mech} positive if it is supplied to the machine. We define T_{el} as the electromagnetic couple of the generator, then:

$$P_{mech} = \omega_r T_{el} \tag{24}$$

2) From choosing a positive current direction and voltage polarity in Fig. 15, it follows that the electrical power is also considered to be positive when it is supplied to the machine. In the generator operation being discussed here, P_1 is thus negative (instead of positive, such as is assumed for simplicity in Fig. 13 on page 114, while P_2 is clearly positive, as in eq. (10).

3) Because we have introduced R_1 and R_2, the copper loss of the stator (P_{Cu1}) and rotor (P_{Cu2}) is taken into consideration. In the power balance, we must subtract this from the supplied power.

With this, we obtain for the power balance:

$$P_1 + P_2 + P_{mech} - P_{Cu1} - P_{Cu2} = 0 \tag{25}$$

With the voltage equations (22) and (23), we can find expressions for P_1 and P_2. P_1 always equals $3\,Re\{\underline{U}_s \cdot \underline{I}_s^*\}$ and P_2 always equals $3\,Re\{\underline{U}_r \cdot \underline{I}_r^*\}$ (* means "supplied complex"). Multiplying eq. (22) by $3\underline{I}_s^*$ and eq. (23) by $3\underline{I}_r^*$ yields:

$$3\,\underline{U}_s \cdot \underline{I}_s^* = 3\,R_1\,\underline{I}_s \cdot \underline{I}_s^* + 3j\omega_1 L_1 \underline{I}_s \cdot \underline{I}_s^* + 3j\omega_1 M\,\underline{I}_r \cdot \underline{I}_s^*$$

$$3\,\underline{U}_r \cdot \underline{I}_r = 3\,R_2\,\underline{I}_r \cdot \underline{I}_r^* + 3j\omega_2 L_2\,\underline{I}_r \cdot \underline{I}_r^* + 3j\omega_2 M\,\underline{I}_s \cdot \underline{I}_r^*$$

We take the real part of these equations and we consider, moreover, that $\underline{I} \cdot \underline{I}^* = |\underline{I}|^2$ (thus real) and $|\underline{I}_s|^2 = I_1^2$, $\underline{I}_r^2 = I_2^2$, then we find: /40

$$P_1 = 3\ \mathrm{Re}\ \{\underline{U}_s \cdot \underline{I}_s^*\} = 3R_1\ I_1^2 + 3\ \mathrm{Re}\ \{j\omega_1 M\ \underline{I}_r \cdot \underline{I}_s^*\}$$

$$P_2 = 3\ \mathrm{Re}\ \{\underline{U}_r \cdot \underline{I}_r^*\} = 3R_2\ I_2^2 + 3\ \mathrm{Re}\ \{j\omega_2 M\ \underline{I}_s \cdot \underline{I}_r^*\}$$

Solution for the term $3\ \mathrm{Re}\ \{j\omega_1 M\ \underline{I}_r \cdot \underline{I}_s^*\} = 3\omega_1 M\ \mathrm{Re}\ \{j\underline{I}_r\ \underline{I}_s^*\}$ occurs with the definitions for $\underline{I}_s$ and $\underline{I}_r$ given on page 27.

We obtain:

$$\mathrm{Re}\ \{j\underline{I}_r \cdot \underline{I}_s^*\} = \mathrm{Re}\ \{jI_1 I_2 e^{j(\alpha_2-\phi_2)} \cdot e^{-j(\alpha_1-\phi_1)}\} =$$

$$= I_1 I_2\ \mathrm{Re}\ \{je^{j(\alpha_2-\alpha_1-\phi_2+\phi_1)}\} =$$

$$= I_1 I_2\ \mathrm{Re}\left[j\{\cos(\alpha_2-\alpha_1-\phi_2+\phi_1) + j\sin(\alpha_2-\alpha_1-\phi_2+\phi_1)\}\right].$$

With this we find:

$$\mathrm{Re}\ \{j\underline{I}_r \cdot \underline{I}_s^*\} = -I_1 I_2 \sin(\alpha_2-\alpha_1-\phi_2+\phi_1).$$

According to the same specification, we can calculate:

$$\boxed{\mathrm{Re}\,\{j\underline{I}_r \cdot \underline{I}_s^*\} = -I_1 I_2 \sin(\alpha_2-\alpha_1-\phi_2+\phi_1)\ .}$$

The equations are then changed to:

$$\boxed{\begin{aligned} P_1 &= 3\ \mathrm{Re}\ \{\underline{U}_s \cdot \underline{I}_s^*\} = 3R_1 I_1^2 - 3\omega_1 M\, I_1 I_2 \sin(\alpha_2-\alpha_1-\phi_2+\phi_1) \\ P_2 &= 3\ \mathrm{Re}\ \{\underline{U}_r \cdot \underline{I}_r^*\} = 3R_2 I_2^2 - 3\omega_2 M\, I_1 I_2 \sin(\alpha_2-\alpha_1-\phi_2+\phi_1) \end{aligned}}$$

In these equations, we can already recognize the terms $3R_1\ I_1^2$ and $3R_2\ I_2^2$ as P_{cu1} and P_{cu2}.

NB: If we have, as in Sect. 2.a.2, neglected the copper losses ($R_1 = R_2 = 0$), we then still have to prove here the assertion found in that section: $P_1 : P_2 = \omega_1 : \omega_2$ (the minus sign follows from the definition used here for P_1.)

When we add up the power equations for P_1 and P_2, we find: /41

$$P_1 + P_2 + 3(\omega_1-\omega_2)\, M\, I_1 I_2 \sin(\alpha_2-\alpha_1-\phi_2+\phi_1) - 3R_1 I_1^2 - 3R_2 I_2^2 = 0 .$$

Equating with $P_1 + P_2 + P_{mech} - P_{Cu1} - P_{Cu2} = 0$ (25)
yields:

$$P_{mech} = 3(\omega_1-\omega_2)\, M\, I_1 I_2 \sin(\alpha_2-\alpha_1-\phi_2+\phi_1) \quad \text{en met} \quad \omega_1 = \omega_2 + p\omega_r :$$

$$P_{mech} = 3\, p\, \omega_r\, M\, I_1 I_2 \sin(\alpha_2 - \alpha_1 - \phi_2 + \phi_1) \qquad (26)$$

For the electromagnetic couple, with $T_{el} = P_{mech} / \omega_r$, we find:

$$T_{el} = 3\, p\, M\, I_1 I_2 \sin(\alpha_2 - \alpha_1 - \phi_2 + \phi_1) \qquad (27)$$

Equation (27), together with the voltage equations (22) and (23), forms the machine equations.

Similarity to a Normal, Synchronous Generator

We shall now demonstrate that the couple equation (27) and the voltage equation for the stator (22) can be recast according to the equations usually used in the literature (and also the most clear) for a normal, synchronous generator.

For the voltage equation of a (normal) SG, we can write:

$$\boxed{\underline{U}_1 = R_1\underline{I}_1 + j\omega_1 L_1\underline{I}_1 + j\omega_1 M\frac{\underline{I}_r}{\sqrt{2}}}\ ,$$ (5 with the notation used here).

in which

$$\boxed{\underline{U}_1 = U_1 \quad \text{en} \quad \underline{I}_1 = I_1 e^{-j\phi_1} \qquad (\text{n.b. } \underline{U}_s = U_1 e^{j\alpha_1}\ ,\ \underline{I}_s = I_1 e^{j(\alpha_1-\phi_1)})}$$

$\underline{I}_r$ is the rotor (direct) current, as is "seen" from the stator; thus as an alternating current with angular frequency ω_1 and effective value $I_r/\sqrt{2}$.

We write here in the voltage equation for the DSG stator /42
$\underline{U}_s = R_1\underline{I}_s + j\omega_1 L_1\underline{I}_s + j\omega_1 M\underline{I}_r$, and if we recall that the difference between $\underline{U}_1$ and $\underline{U}_s$ and between $\underline{I}_1$ and $\underline{I}_s$ fit only in another choice for time t = 0, then the similarity is all the more clear.

For a normal SG, it is usual to transform the term $j\omega_1 M\underline{I}_r/\sqrt{2}$ through $-\underline{\mathcal{E}}_p \cdot E_p$ $(=|\mathcal{E}_p|)$ called the pole wheel voltage. It is the voltage generated by the rotor in the stator, which in the unloaded state ($I_1 = 0$) is equal to the phase voltage U_1.

The angle between $\underline{U}_1$ and $-\mathcal{E}_p$ is the load angle (usually) called θ.

The voltage equation for the SG changes with this to the known form:

$$\boxed{\underline{U}_1 = R_1\underline{I}_1 + j\omega_1 L_1\underline{I}_1 - \underline{E}_p \, .}$$

We will now do the same with eq. (22). For this purpose, we first multiply these equations by $e^{-j\omega_1}$. Then from the equation obtained:

$$\boxed{U_1 = R_1 I_1 e^{-j\phi_1} + j\omega_1 L_1 I_1 e^{-j\phi_1} + j\omega_1 M\, I_2 e^{j(\alpha_2-\alpha_1-\phi_2)}}$$

we see that we must define:

$$\boxed{\begin{aligned} -\underline{E}_p = E_p e^{j\theta} &= j\omega_1 M\, I_2 e^{j(\alpha_2-\alpha_1-\phi_2)} = \\ &= \omega_1\, M\, I_2\, e^{j(\alpha_2-\alpha_1-\phi_2+\frac{\pi}{2})} \, , \end{aligned}}$$

so that

$$\boxed{E_p = \omega_1\, M\, I_2} \quad \textit{and} \quad \boxed{\theta = (\alpha_2 - \alpha_1 - \phi_2 + \tfrac{\pi}{2}) \, .}$$

If we change to the notation here $\underline{U}_1 = U_1$ and $\underline{I}_1 = I_1 e^{-j\varphi_1}$, we find the same equation for the voltage equation for the DSG stator:

$$\underline{U}_1 = R_1 \underline{I}_1 + j\omega_1 L_1 \underline{I}_1 - \underline{E}_p \qquad (28)$$

With eq. (28), we can now also set the couple equation in a known form: /43

$$T_{el} = 3 \frac{p}{\omega_1} U_1 I_k \sin\theta = 3 \frac{p}{\omega_1} U_1 \frac{E_p}{\omega_1 L_1} \sin\theta$$

From $Re\{3\underline{U}_1 \cdot \underline{I}_1^*\}$, we find, in the same way as on page 29 as follows:

$$P_1 = 3 R_1 I_1^2 + 3 \, Re \{- \underline{E}_p \cdot \underline{I}_1^*\}$$

For $P_1 - 3R_1 I_1^2 = P_1 - P_{Cu\,1}$, we find on page 30:

$$- 3 \omega_1 M I_1 I_2 \sin(\alpha_2 - \alpha_1 - \phi_2 + \phi_1).$$

From eq. (26), it then follows:

$$\frac{P_1 - P_{cu1}}{P_{mech}} = - \frac{\omega_1}{p\omega_r}$$

If we now substitute that in here, we obtain:

$$P_1 - P_{cu1} = 3 \, \mathrm{Re} \{ - \underline{E}_p \cdot \underline{I}_1^* \} = - \frac{\omega_1}{p\omega_r} P_{mech} = - \frac{\omega_1}{p} T_{el} \, .$$

We calculate, using eq. (28)

$$\underline{I}_1 = \frac{\underline{U}_1 + \underline{E}_p}{j\omega_1 L_1} =$$

$$= -j \frac{U_1 - E_p e^{j\theta}}{\omega_1 L_1} = \frac{U_1 e^{-j\pi/2} - E_p e^{j(\theta - \pi/2)}}{\omega_1 L_1} \, .$$

Thus

$$\underline{I}_1^* = \frac{U_1 e^{j\pi/2} - E_p e^{-j(\theta-\pi/2)}}{\omega_1 L_1} .$$

With this, we write:

$$3 \operatorname{Re}\{-\underline{E}_p \cdot \underline{I}_1^*\} = 3 \operatorname{Re}\{E_p e^{j\theta}(\frac{U_1 e^{j\frac{\pi}{2}} - E_p e^{-j(\theta-\frac{\pi}{2})}}{\omega_1 L_1})\} =$$

$$= 3 \frac{E_p}{\omega_1 L_1} \operatorname{Re}\{U_1 e^{j(\frac{\pi}{2}+\theta)} - E_p e^{j(\frac{\pi}{2})}\} =$$

$$= 3 \frac{E_p}{\omega_1 L_1} \{U_1 \cos(\frac{\pi}{2}+\theta) - E_p \cos\frac{\pi}{2}\} = - \frac{3U_1 E_p}{\omega_1 L_1} \sin\theta .$$

With

/44

$$3 \operatorname{Re}\{-\underline{E}_p \cdot \underline{I}_1^*\} = - \frac{\omega_1}{p\omega_r} P_{mech} = - \frac{\omega_1}{p} T_{el}$$

we find:

$$T_{el} = \frac{3p}{\omega_1^2 L_1} U_1 E_p \sin \theta \qquad (29)$$

The advantage of equations (28) and (29) is that (especially in neglecting the small term $R_1 \underline{I}_1$), it leads to a very clear index disgram of the stator voltages and currents.

In particular, the effect of the size of I_2 ($\mathcal{E}_p$) and of T_a ($\simeq T_{el}$) is simple to review.

Fig. 17 gives the index of stator voltage and at the same time the network voltage ($|\underline{U}_1| = U_1$ is constant).

$\mathcal{E}_p \sin\theta$ is a measure of T_{el}; in the stationary state, $T_{el} \simeq T_a$. $-\underline{\mathcal{E}}_p$ is the index for pole wheel voltage. The modulus $-\underline{\mathcal{E}}_p$ (E_p) is proportional to I_2.

If the point $-\underline{\mathcal{E}}_p$ for a particular value of I_2 (U_2) comes precisely at the point P, then $j\omega_1 L_1 \underline{I}_1 \perp \underline{U}_1$ exists such that $\underline{I}_1$ lies exactly at the length of $\underline{U}_1$. φ_1 is then 180°, thus $I_1 \sin \varphi_1 = 0$ and $\cos \varphi_1 = 1$ (not idle power).

With an increase in I_2, the point $-\underline{\mathcal{E}}_p$ comes out above P on the dotted line (as drawn in Fig. 17). Angle φ_1 is then greater than 180°; the generator delivers idle power.

With a decrease in I_2, the point $-\underline{\mathcal{E}}_p$ will fall below point P on the dotted line (still at constant $T_{el} \simeq T_a$); the generator then assumes idle power from the network ($\varphi_1 < 180°$).

The voltage equation for the DSG rotor (eq. 23) naturally cannot be rewritten according to the (direct) voltage equation of the normal SG rotor ($U_r = R_r I_r$).

NB: For $\omega_2 = 0$, for eq. (23) for $\underline{U}_r = R_2 \underline{I}_r$, it seems we must then still consider that this equation does not hold for the entrie rotor circuit, but only for a phase of the rotary current winding.

Still, the advantage of eq. (23) is in recasting in another form. We do this as follows. With the complex numbers /46

written out, we find, for eq. (23) after multiplying by

$$e^{-j(\alpha_2 - \phi_2)} :$$

$$U_2 e^{j\phi_2} = R_2 I_2 + j\omega_2 L_2 I_2 + j\omega_2 M\, I_1 e^{-j(\alpha_2 - \alpha_1 + \phi_1 - \phi_2)}$$

The last term herein yields, after multiplying by

$$j e^{-j\frac{\pi}{2}} \quad (=1) \quad :$$

$$-\omega_2 M\, I_1 e^{-j(\alpha_2 - \alpha_1 + \phi_1 - \phi_2 + \frac{\pi}{2})} .$$

If we assume that $\theta = \alpha_2 - \alpha_1 - \varphi_2 + \frac{\pi}{2}$, then we find:

$$U_2\, e^{j\phi_2} = R_2 I_2 + j\omega_2 L_2 I_2 - \omega_2 M\, I_1\, e^{-j(\theta + \phi_1)} \qquad (30)$$

In the following section, we shall repeatedly make use of the rotor equation in this form.

Similarity to a Transformer

The machine eqaations (22) and (23) are, for $\omega_1 = \omega_2$, equal to those for a voltage transformer.

We shall develop this analogy further, because in the following section we can make use of it successfully.

It will appear that the DSG is conceived of as a voltage and frequency transformer.

On page 28, , we find, for the voltage equation of the DSG:

$$\underline{U}_s = R_1 \underline{I}_s + j\omega_1 L_1 \underline{I}_s + j\omega_1 M \underline{I}_r \qquad (22)$$

$$\underline{U}_r = R_2 \underline{I}_r + j\omega_2 L_2 \underline{I}_r + j\omega_2 M \underline{I}_s \qquad (23)$$

We now split L_1 and L_2 so that at the transformer and for for an asynchronous machine, it is usually:

$$L_1 = L_{1h} + L_{1s}$$

and

$$L_2 = L_{2h} + L_{2s}.$$

L_{1h} and L_{2h} are called the main inductivities, L_{1s} and L_{2s} the current inductivities. L_{1h} and L_{2h} are defined so that:

$$L_{1h} : L_{2h} : M = w_1^2 : w_2^2 : w_1 w_2$$

(and thus $\overline{L_{1h} L_{2h}} = M^2$).

[Text missing from original] /47

with w_1 and w_2 as the number of coils for a stator phase and a rotor phase, respectively.

Equations (22) and (23) change herewith to:

$$\underline{U}_s = R_1\underline{I}_s + j\omega_1 L_{1s}\underline{I}_s + j\omega_1 L_{1h}\underline{I}_s + j\omega_1 M\,\underline{I}_r \qquad (22a)$$

$$\underline{U}_r = R_2\underline{I}_r + j\omega_2 L_{2s}\underline{I}_r + j\omega_2 L_{2h}\underline{I}_r + j\omega_2 M\,\underline{I}_s \qquad (23a)$$

In both equations, the first term and the second term of the right member give the voltage loss the ohmic loss [sic] resistance of the windings and the distribution (flux not coupled).

We define the remaining term as

$$\underline{E}_s = j\omega_1 L_{1h}\underline{I}_s + j\omega_1 M\,\underline{I}_r$$

and

$$\underline{E}_r = j\omega_2 L_{2h}\underline{I}_r + j\omega_2 M\,\underline{I}_s$$

then eq. (22) and (23) herewith change into:

$$\underline{U}_s = R_1\underline{I}_s + j\omega_1 L_{1s}\underline{I}_s + \underline{E}_s \qquad (22b)$$

$$\underline{U}_r = R_2\underline{I}_r + j\omega_2 L_{2s}\underline{I}_r + \underline{E}_r \qquad (23b)$$

When we write out $\underline{E}_s$ and $\underline{E}_r$, making use of:

$$\underline{I}_s = I_1 e^{j(\alpha_1-\phi_1)} = I_1 \{\cos(\alpha_1-\phi_1) + j \sin(\alpha_1-\phi_1)\}$$

$$\underline{I}_r = I_2 e^{j(\alpha_2-\phi_2)} = I_2 \{\cos(\alpha_2-\phi_2) + j \sin(\alpha_2-\phi_2)\}$$

and $M^2 = L_{1h} L_{2h}$, then we find:

$$\frac{|\underline{E}_s|}{|\underline{E}_r|} = \frac{\omega_1}{\omega_2} \sqrt{\frac{L_{1h}}{L_{2h}}} \quad \text{and} \quad \frac{\mathrm{Im}\,\{\underline{E}_s\}}{\mathrm{Re}\,\{\underline{E}_s\}} = \frac{\mathrm{Im}\,\{\underline{E}_r\}}{\mathrm{Re}\,\{\underline{E}_r\}}$$

From this last, it follows that the arguments of $\underline{E}_s$ and $\underline{E}_r$ are equal, so that these indicators coincide in spite of the value of ω_2.

If we get $L_{1h} : L_{2h} = w_1^2 : w_2^2$ so that $\sqrt{L_{1h} / L_{2h}} = w_1/w_2$, then it follows herewith:

$$\frac{\underline{E}_s}{\underline{E}_r} = \frac{\underline{E}_s}{\underline{E}_r} = \frac{\omega_1}{\omega_2} \cdot \frac{w_1}{w_2} .$$

If we define: $|\underline{E}_s| = E_s$, $|\underline{E}_r| = E_r$ and $\nu = \frac{\omega_1}{\omega_2} \cdot \frac{w_1}{w_2}$ /48
we find: $E_r = \nu E_s$ and $\underline{E}_r = \nu \underline{E}_s$.

Fig. 18a gives the substitution diagram for eq. (23b) and Fig. 18b for ν X eq. (22b).

Because $\underline{E}_r = \nu \underline{E}_s$, we can also draw Figs. 18a and 18b for each with one voltage source "$\underline{E}_r$". Then we must consider that such substitution diagrams (complex) are calculated quantities and not voltages and currents with physical meaning.

The actual rotor and stator quantities always have completely different frequencies and thus may need be broken down into one diagram.

Neglecting the distribution and ohmic resistance ($L_{1s} = L_{2s} = 0$, $R_1 = R_2 = 0$), eq. (22b) and (23b) change into $\underline{U}_s = \underline{E}_s$ and $\underline{U}_r = \underline{E}_r$. Because the neglected terms are usually small, relative to $\underline{E}_s$ and $\underline{E}_r$, the following usually holds (with $\underline{E}_r = \nu \underline{E}_s$ and $E_r = \nu E_s$):

/49

$$\boxed{U_2 \simeq \nu U_1} \quad \text{and} \quad \boxed{\underline{U}_r \simeq \nu \underline{U}_s .}$$

From this, we write as follows:

$$\boxed{\frac{U_2}{\omega_2} : \frac{U_1}{\omega_1} \simeq w_2 : w_1}$$

which shows what we have done with a voltage-frequency transformation.

From eq. (23a), it follows that these approximations do not hold true for very small values of ω_2 (ν), because the term $R_2 \underline{I}_r$ in the right-hand member predominates instead of $\underline{E}_r$, (that is the single term in eq. 23a does not consist of ω_2).

With reference to the above, we define: $\Delta u_2 = u_2 - \nu u_1$, where ΔU_2 is consequently very small.

For $\Delta u_2 = u_2 - \nu u_1$, we can also write, with $E_r = \nu E_s$:

$$\boxed{\Delta U_2 = (U_2 - E_r) + \nu(E_s - U_1).}$$

We define:

$$\Delta U_{22} = U_2 - E_r \quad \text{and} \quad \Delta U_{21} = \nu(E_s - U_1),$$

so that $\Delta U_2 = \Delta U_{21} + \Delta U_{22}$.

If $|\underline{U}_r|$ and $|\underline{E}_r| >> |R_2\underline{I}_r + j\omega_2 L_{2s}\underline{I}_r|$, then

$$|\underline{U}_r| - |\underline{E}_r| = U_2 - E_r = \Delta U_{22} \simeq R_2 I_2 \cos\phi_2 + \omega_2 L_{2s} I_2 \sin\phi_2 .$$

If $|\underline{U}_s|$ and $|\underline{E}_s| >> |R_1\underline{I}_s + j\omega_1 L_{1s}\underline{I}_s|$, then

$$\nu\,|\underline{E}_s| - \nu\,|\underline{U}_s| = \nu(E_s - U_1) = \Delta U_{21} \simeq -\nu(R_1 I_1 \cos\phi_1 + \omega_1 L_{1s} I_1 \sin\phi_1).$$

Under the set conditions, it then holds as an approximation for ΔU_2, that:

$$\Delta U_2 \simeq R_2 I_2 \cos\phi_2 + \omega_2 L_{2s} I_2 \sin\phi_2 - \nu(R_1 I_1 \cos\phi_1 + \omega_1 L_{1s} I_1 \sin\phi_1).$$

If the machine delivers watt and idle power to the network ($\cos\varphi_1 < 0$; $\sin\varphi_1 < 0$), then all the terms herein are positive. If the machine delivers only watt power to the network and takes its idle power from the network ($\cos\varphi_1 < 0$; $\sin\varphi_1 > 0$, then the last term is negative.

In the expression found for ΔU_2, only the term $R_2 I_2 \cos\varphi_2$ is not dependent on ω_2 (NB: $\nu = w_2/w_1 \times \omega_2/\omega_1$). For small values of $_2$, these terms predominate. Because U_2 and E_r are also smaller with decreased ω_2, for small values of /50
ω_2 when U_2 and E_r in the large order comes from $R_2 I_2$, the

approximation for ΔU_{22} and consequently for ΔU_2 can no longer be used (see stipulation, p. 43).). For $\omega_2 = 0$, the approximation fits very well. For $\nu = 0$: $U_2 = \Delta U_2 = R_2 I_2$.

We can now make use of the following formulae:

For the voltage equation for the stator:

$$\underline{U}_s = R_1 \underline{I}_s + j\omega_1 L_1 \underline{I}_s + j\omega_1 M \underline{I}_r . \tag{22}$$

$$\underline{U}_s = R_1 \underline{I}_s + j\omega_1 L_{1s} \underline{I}_s + j\omega_1 L_{1h} \underline{I}_s + j\omega_1 M \underline{I}_r \tag{22a}$$

$$\underline{U}_s = R_1 \underline{I}_s + j\omega_1 L_{1s} \underline{I}_s + \underline{E}_s \tag{22b}$$

with

$$\underline{U}_s = U_1 e^{j\alpha_1} \text{ and } \underline{I}_s = I_1 e^{j(\alpha_1 - \phi_1)}$$

$$\underline{U}_1 = R_1 \underline{I}_1 + j\omega_1 L_1 I_1 - \underline{E}_p \tag{28}$$

with

$$\underline{U}_1 = U_1 \ , \ \underline{I}_1 = I_1 e^{-j\phi_1} \ , \ -\underline{E}_p = E_p e^{j\theta} \text{ and } E_p = \omega_1 M I_2 \ ;$$

For the rotor voltage equation:

$$\underline{U}_r = R_2\underline{I}_r + j\omega_2 L_2\underline{I}_r + j\omega_2 M\,\underline{I}_s \tag{23}$$

$$\underline{U}_r = R_2\underline{I}_r + j\omega_2 L_{2s}\underline{I}_r + j\omega_2 L_{2h}\underline{I}_r + j\omega_2 M\cdot\underline{I}_s \tag{23a}$$

$$\underline{U}_r = R_2\underline{I}_r + j\omega_2 L_{2s}\underline{I}_r + \underline{E}_r \tag{23b}$$

with

$$\underline{U}_r = U_2 e^{j\alpha_2} \text{ and } \underline{I}_r = I_2 e^{j(\alpha_2-\phi_2)}$$

$$U_2 e^{j\phi_2} = R_2 I_2 + j\omega_2 L_2 I_2 - \omega_2 M\, I_1 e^{-j(0+\phi_1)} \tag{30}$$

Furthermore, we find: $\underline{E}_r = \nu \underline{E}_s$ and $E_r = \nu E_s$ with

$$\nu = \frac{w_2}{w_1}\cdot\frac{\omega_2}{\omega_1}.$$

For the couple equation, we use only:

$$T_{el} = \frac{3p}{\omega_1^2 L_1} U_1 E_p \sin\theta \tag{29}$$

Resuming, we find in the section on the DSG, the following features. /51

On the side of the stator, the DSG displays in all respects the behavior of a normal synchronous generator.

None of the stator quantities depend on the synchronous operation $(\omega_1 = \omega_2 + p\,\omega_r)$ of the number of generator revolutions.

The required rotor voltage U_2, which must be delivered by the converter, is practically entirely determined by the number of generator revolutions.

2.a.4. Special Properties of a Combination Windmill - DSG /52

Using what was set forth in the preceding section for the DSG, a theoretical study can be carried out for the properties of electricity generation with a DSG which is driven by a windmill.

We begin by refining the requirements of Sect. 1.b.1. in the machine equations (28), (29), and (30).

NB: In these equations, we consider the machine constants (R_1, R_2, L_1, L_2, and M) as known.

The voltage at the stator is the network voltage. For phase U_1 for which eq. (28) is set up, $u_1 \sin(\omega_1 t + \alpha_1) = u_{net}(t)$ thus must hold, in which u_{net} (t) is the voltage of an arbitrary phase of the network, as a function of t. The quantities U_1, ω_1, and α_1, which enter into the machine equations, are consequently fixed.

The power coefficient C_p must be kept at the value C_{po} by letting the number of mill revolutions n_m vary proportionally to v_w, such that $\mu = \mu_0$ always holds. It is possible to do this because the number of generator revolutions $\omega_r / 2\pi$ can be controlled with the converter frequency ω_2 according to $\omega_r = \omega_1/p - \omega_2/p$, while the number of mill revolutions is directly obtained from the number of generator revolutions, because the mill shaft and generator shaft are coupled to one another via a rigid transmission. At a specific wind velocity, ω_2 must consequently have a certain value, so that ω_2 in eq. (30) is then fixed.

T_{el} is also fixed in a stationary condition for a specific v_w, because the electromagnetic couple then makes a balance with the shaft couple presented. In neglecting losses of the friction couple of the generator, $T_a = T_{el}$.

In equations (28), (29), and (30), we then keep I_1, φ, I_2, θ, U_2, and φ_2 as unknowns (not fixed quantities), while we can only solve for 5 of these 6 unknowns from the equations (5, because two of the equations are complex). (We do not consider E_p as unknown, because it follows directly from I_2.) /53

Because we have five equations in six unknowns, we can set another quantity to a known value with one of the non-fixed quantities (unknowns).

Naturally, we take this liberty to set the cos φ_1 to a known value with U_2.

The things mentioned agree with what has already been set down on p. 14: "The voltage of the converter must be controlled in frequency and amplitude, in order to be able to adjust for C_{po} the requirement n_m (ω_r) and the known cos φ_1. [sic]

For this purpose, two control signals must be supplied for the converter, which define the values of the voltage and the frequency. We shall go further into this here.

Control of the Maximum Power Point by Controlling the Converter Frequency ω_2

From the fact that we are concerned with a synchronous generator, it follows that we cannot change ω_2 abruptly, and the machine is then always falling out of phase. In synchronous operation, $\omega_1/p = \omega_2/p + \omega_r$ must at least hold for those values of ω averaged over time. Only small deviations in the instantaneous values of the angular velocity are permitted. This is because the stator rotary field (angular velocity ω_1/p) and the rotor rotary field (angular velocity $\omega_2/2 + \omega_r$) are bound elastically, as it were, to one another.

For such small deviations, the load angle θ is altered such that the thus developed change in T_{el} (eq. 29) provides for restoration of the balance so that the relation $\omega_1/p = \omega_2/p + \omega_r$ remains true. Any adjustment of ω_2 thus must be such that ω_r can adapt, moreover, so that the machine stays in phase.

The control signal with which the converter frequency ω_2 is set can be obtained in two different ways, namely by using a forward control at which the required ω_2 is set from v_w or by using an adjustment with feedback, at which ω_2 is determined exactly from the value of P_{net} (Fig. 13, p. 114).

The forward control makes use of a known property, namely that ω_r must be kept proportional to V_w at $\mu = \mu_0$ and thus keeping $C_p = C_{po}$. The herein required proportionality constant can be determined beforehand. /54

Fig. 19 shows the block diagram for such a control. The wind velocity v_w is measured. The peaks in v_w (t) during high inertias will not lead to comparable peaks in $P_a(t)$. By always integrating V_w (t) over a certain time Δt, we obtain a function v_{meas} (t) which for the correct choice of Δt, such that thence the path of $P_a(t)$ can be easily derived. The value of Δt must be determined from the time which passes before an increase in v_w is followed by an increase in T_a.

For $v_{min} \leq v_w \leq v_k$, the function generator delivers a control voltage which is proportional to the required value of $p\omega_r$ for

For $v_k \leq v_w \leq v_{max}$, the control voltage no longer increases, ($p\omega_r = \omega_1$ and $\omega_2 = 0$).

If $v_{meas} < v_{min}$ or $v_{meas} > v_{max}$, the equipment must be taken out of operation.

The control voltage for the converter is finally obtained by subtracting the output voltage of the function generator from the voltage which is proportional to ω_1 (naturally, with the same proportionality constant as for the function generator). /55

The converter must then naturally be so set up that it delivers the known ω_2 through this control, while changes in ω_2 occur sufficiently slowly that the synchronous operation remains guaranteed.

In general, a forward control works less accurately than control with feedback. There is no control for the set purpose. In this case, "under given (weather) conditions which encounter adjustment, whereby as large an electrical power as possible is generated to deliver (P_{net}) to the network", it is also indeed achieved. The control is good when P_{net} is measured and ω_2 is always controlled for the value at which P_{net} is greatest.

With such control (with feedback), the correct value of ω_2 is thus found, without letting v_w, C_p, μ, etc. rise.

Control of ω_2 is, then, a search procedure; the greatest dP_{net} / dt must always be determined for each change in ω_2. In the direction in which ω_2 is changed a little, one must be careful that the machine does not fall out of phase. Secondly, it is again "observed" for dP_{net} / dt and again fixed how ω_2 must change, and so on.

Such control is more complicated in construction than forward control.

Control of cos φ_{net} with the Converter Voltage

We have already stated that cos φ_1 [1] is set at a known value by controlling the voltage U_2 delivered by the converter over a rotor phase.

---

[1] We assume here that the converter gets no idle power from [words missing in original document].

We actually find also that the required rotor voltage in the first approximation is defined by the rotor frequency ω_2, according to $U_2 \simeq \nu U_1$.

It is the small deviation ΔU_2 of this value of U_2 determined by ω_2 which defines cos φ_1 (we define: $\Delta U_2 = U_2 - \nu U_1$).

Therefore U_2 can be very accurately controlled.

When we allow the converter voltage U_2 to be determined by a control voltage which is derived from the difference between the known phase angle $_1$ and the actual phase angle φ_1, then this means that the information in this control voltage must also be over the value of ω_2. U_2 is always determined for the most part by ω_2 (νU_1) and only for a small part (ΔU_2) by the load conditions and the known cos φ_1. Therefore, it is better to let the converter voltage depend on the set ω_2, as far as the part ΔU_1 is concerned. /56

For this, a coupled frequency-voltage control is necessary which the output voltage of the converter provides at a definite frequency ω_2 at approximately the correct value ($U_2 = \nu U_1$).

In addition, a special voltage control must then be present which the required rotor voltage sets exactly (ΔU_2) for a specific cos φ_1. This voltage control must get its information from the difference between the (set) known phase angle φ_1 and the measured phase angle.

From the substitution diagram of Fig. 18 (and from the approximation derived for ΔU_2), we see that the requirement for ΔU_2 for a specific cos φ_1, is determined for relatively small ohmic resistances and distribution inductivities. (R_1, R_2, L_{1s}, L_{2s}) of the generator.

With regard to the design of the DSG, we can therefore conclude that besides the known advantages of a relatively large air slit width in the SG, there is an extra advantage here that the accuracy with which cos φ_1 can be set increases with the size of the air slit width. A large air slit width always means greater distribution and thus larger L_{1s} and L_{2s}, while L_{1h}, L_{2h}, and M are correct by decreasing. The ΔU_2 required for a certain load condition will therefore decrease, while νU_1, is not altered.

The value of $\frac{\Delta U_2}{U_2} = \frac{\Delta U_2}{\nu U_1 + U_2}$ will consequently be greater, which is a known clarification for the requirement, relative to the control accuracy of U_2. Naturally, larger R_1

and R_2 have this same advantage, but an increase herewith means an increase in copper loss.

The increase in the required rated power, which involves an increase in the air slit width, will lead to very small losses.

Overload Capacity of the Generator /57

Introduction

We shall now look at how much danger exists that the generator will be drawn out of phase by a sudden increase in wind velocity. Of interest here is the value of the overload capacity O.

We define:

$$O = \frac{T_{el,k}}{T_{el,\,0}}.$$

With $T_{el,k}$ as the (unknown) couple, that is the electromagnetic couple for which the generator falls out of phase, assume that the converter voltage and frequency are not controlled (U_2 and ω_2 constant).

$T_{el,k}$ is thus T_{el} at $\theta = \pi/2$:

$$T_{el,k} = \frac{3p}{\omega_1^2 L_1} U_1 E_p \sin\frac{\pi}{2}.$$

And with $T_{el,0}$ as the electromagnetic couple for the condition $\mu = \mu_0$ (maximum power point) at a specific ω_r, $(0 < p\omega_r \leq \omega_1)$. If we use the index 0 for the appropriate quantity at $T_{el,0}$ and the index k for the appropriate quantity at $T_{el,k}$, then it follows from the couple equation (29):

$$O = \frac{T_{el,k}}{T_{el,o}} = \frac{E_{p,k}}{E_{p,o} \sin \theta_o} \qquad (31)$$

The greater O is, the less the danger of falling out of phase.

NB: In neglecting friction losses for the generator, $T_a \approx T_{el}$ under stationary conditions, so that $T_{el,0} = c\,\omega_r$ (eq. 16, p. 18).

For $p\,\omega_r = \omega_1$ and $v_w > v_k$ $(\mu \neq \mu_0)$, $T_{el,o}$ and thus O are not defined. We shall in this case define O as the ratio between the (unknown) couple and the full-load couple.

In Fig. 20 is the index diagram for the stator equations for a given specific load condition. The resistance R_1 is neglected here, because it is very much smaller than $\omega_1 L_{1s}$, especially for a machine with a somewhat larger air slit width.

It can be concluded that L_{1h} is inversely proportional to the (effective) air slit width. Although L_{1s} increases with increasing air slit width, the increase in L_{1h} will predominate. /58

For a given I_1, the value of $\omega_1 (L_{1h} + L_{1s}) I_1$ will consequently decrease for increasing air slit width, so that the angle θ also decreases (Fig. 20).

The value of O (eq. 31) thereby decreases and the danger of falling out of phase decreases. (We say that a large air air slit is also favorable for the controllability of cos φ_1.

For a given T_{el}, the value of $\mathcal{E}_p \sin$ is fixed for a specific machine (Fig. 20). When idle power is delivered to the network $(\varphi_1 > \pi)$, the angle θ is smaller than when idle power id taken up from the network /59

Because a certain ratio will exist between $E_{p,k}$ and $E_{p,0}$, the value of O at $\varphi_1 > \pi$ is thus greater than at $\varphi_1 < \pi$ (eq. 31).

We assume that $\varphi_1 < \pi$ is not known as a stationary condition, and further that it originates from $\varphi_1 = \pi$ $(\cos \varphi_1 = -1)$ as a stationary condition with the greatest danger of the machine falling out of phase.

$E_{p,0}$ and θ in eq. (31) are then the values E_p and θ, which go with $T_{el} = T_{el,0}$ and $\cos \varphi_1 = -1$.

With this definition of O, we start with an uncontrolled converter. In actuality, the converter control reacts well for a change in T_{el}. φ_1 always decreases for an increase in the angle θ. The voltage control of the converter reacts to this with an increase in U_2. I_2 and E_p will thereby also increase, such that φ_1 is again 180°.

The value of O is then also designed to give the impression of the required control velocity for the voltage of the converter.

<u>O at Full Load and $\varphi_1 = \pi$</u>

We shall begin with the overload capacity to select for full load. The angle θ is then the greatest. We have seen full load in Sect. 2.a.2. as it occurred for $v_k \leq v_w \leq v_{max}$. In that

case $p\omega_r = \omega_1$ and $\omega_2 = 0$. The rotor equation (30) changes herewith into $U_2 = R_2 I_2$.

As the converter voltage is not controlled (U_2 constant), I_2 and thus E_p are constant. If we define $T_{el,v}$, $E_{p,v}$, θ_v, and O_v as the values T_{el}, E_p, θ, and O under stationary conditions for full load and $\varphi_1 = \pi$, then:

$$O_v = \frac{T_{el,k}}{T_{el,v}} = \frac{E_{p,k}}{E_{p,v} \sin \theta_v}$$

and with $E_{p,k} = E_{p,v}$ constant:

$$O_v = \frac{1}{\sin \theta_v} .$$

This is, as was expected, the expression for the normal synchronous generator. For a generator with a somewhat larger air slit width, $\theta_v = 30^o$ is a normal value. Substituting, this yields: $O_v = 2$. /60

When in this case $(v_k \leq v_w \leq v_{max})$, an increase in v_w provides an increase in T_a, the cos φ_1 control may only temporarily provide for a greater converter voltage (generator E_p). In order to anticipate generator overload, it must be provided for that T_a again reaches the maximum existing value (for stationary conditions).

O for Partial Load and $\varphi_1 = \pi$

For $v_{min} \leq v_w \leq v_k$, the generator is less severely loaded, and $p\omega_r < \omega_1$ and $\theta < \omega_2 < \omega_1$.

If we again start with an uncontrolled converter, then there are two important differences from the full load conditions with $\omega_2 = 0$.

For a smaller load, I_1 and thus $\omega_1 (L_{1h} + L_{1s}) I_1$ are smaller, so that the angle θ is smaller than for full load,

If, as holds for $\omega_2 = 0$, E_p is constant ($E_{p,k} = E_{p,0}$), then a larger O is delivered (eq. 31), so that the danger of falling out of phase is smaller than with full load.

However, because the rotor equation contains no more terms, E_p will not stay the same for constant U_2 and changing T_{el}, so that here $E_{p,k} \neq E_{p,0}$.

In order to know for sure that overload capacity for partial load is greater than for full load, we must thus show that $E_{p,k} \geqslant E_{p,0}$ always holds for partial load, irrespective of the value of θ_0, provided that $\theta \leq \theta_0 \leq \theta_v$ and irrespective of the value of ω_2.

If we derive the relation between E_p and θ from the voltage equations, then it results that this indicates not such a clear expression as above.

This is no more possible at the hand of a construction in the index diagram, starting with constant U_2 and ω_2.

Only by using an artifice (I_2 contains a constant instead of U_2) can we show the above for not too low values of ω_2.

For the artifice mentioned, we need an index diagram, in which in addition to the stator quantities, rotor quantities can also be indicated. /61

Fig. 21 gives such an index diagram for a specified θ_0 and $\varphi_1 = -\pi$. It is obtained by using the voltage equations on p. 45.

In Fig. 22, a part of it is indicated once more (thick). In the same figure, starting with this diagram at $\theta = \theta_0$, the diagram is constructed for $\theta = \pi/2$ and $E_{p,k} = E_{p,0}$ (thus assume that I_2 is constant, (thin).

We see that the required U_2 ($|U_r|$) for $\theta = \pi/2$ is smaller than the required U_2 at $\theta = \theta_o$. /62

From this, we can (for the case shown here) draw the following conclusions.

When we hold U_2 and ω_2 constant (instead of I_2, and thus E_p), as the definition of 0 requires, then U_2 at $\theta = \pi/2$ is greater than necessary for $E_{p,k} = E_{p,0}$.

From the substitution diagram in Fig. 18, we see that as a result, I_2 is greater at $\theta = \pi/2$, so that $E_{p,k} > E_{p,0}$.

From eq. (31), it then follows that the overload capacity here is greater than at full load.

In order to come to general conclusions from this special (indicated) case, we must show that the cause of the decrease in the required U_2 for increasing θ (which we use in the proof) a general [words missing in original].

We can write, for U_2: $U_2 = \nu U_1 + \Delta U_2$ and for $\Delta U_2 = \Delta U_{21} + \Delta U_{22}$: $U_2 = \nu U_1 + \Delta U_{21} + \Delta U_{22}$. /63

Because νU_1 is constant (at constant ω_2 which we always start with), we must thus show that:

$$\Delta U_{21} + \Delta U_{22} \text{ at } \theta = \theta_o > \Delta U_{21} + \Delta U_{22} \text{ at } \theta = \frac{\pi}{2} \text{ and } E_{p,k} = E_{p,o}.$$

However, we cannot show that it always holds.

We see in Fig. 21 and 22 that, starting from $\varphi_1 = -\pi$ at $\theta = \theta_o$, it always holds that ΔU_{21} ($= U_1 - E_s$) for increasing angle θ, and constant E_p decreases. For ΔU_{22}, we can only show that this changes so little for values of ω_2 for which $(\omega_2 L_{2s})^2 \gg R_2^2$, for increasing angle θ, that the decrease in ΔU_{21} will certainly predominate.

Only for this case (not too small values of ω_2) can we thus directly conclude that the overload capacity is certainly greater than in zero load.

We can indicate the above as follows.

We find the smallest possible value of ΔU_{22} for a at zero load ($\theta_o = \theta$; $I_1 = 0$). In the index diagram $\underline{E}_r$ and $\underline{I}_r$ then are practically perpendicular to each other, so that $\Delta U_{22} \simeq \omega_2 L_{2s} I_2$ (Fig. 21).

When the slanting side of the triangle "$R_2 \underline{I}_r$ --- $j\omega_2 L_{2s} \underline{I}_r$" at $\theta = \pi/2$ lies exactly on the length of the index $\underline{E}_r$, ΔU_{22} has the maximum value at $\theta = \pi/2$:

$$I_2 \sqrt{R_2^2 + (\omega_2 L_{2s})^2} \quad .$$

For $\omega_2 L_{2s} I_2 \simeq I_2 \sqrt{R_2^2 + (\omega_2 L_{2s})^2}$, and thus for $(\omega_2 L_{2s})^2 \gg R_2^2$, even in the most unfavorable case in which ΔU_{22} is maximum at , the decrease in ΔU_{22}, predominates, as mentioned above.

When ω_2 has a smaller value than that at which $(\omega_2 L_{2s})^2 \gg R_2^2$, then it requires O smaller than O_v not be maintained long. First, θ_0 will be greater than zero in the stationary output state, so that ΔU_{22} there is greater than $\omega_2 L_{2s}$, while there is no probability that ΔU_{22} is exactly maximum at /64

Secondly, a small increase in ΔU_{22} still does not directly mean an increase in ΔU_2, because ΔU_{21} decreases for increasing angle [sic].

Thirdly, when ΔU_2 finally nevertheless increases with increasing angle θ, this also does not directly imply that O is smaller than O_v, because for this small a load $(v_{min} \leq v_w < v_k)$ sin θ_0 is till smaller than sin θ_v (eq. 31).

We can conclude that the most critical situation occurs for very small values of ω_2. The machine then turns at about full load, so that sin θ_0 is not much smaller than sin θ_v, w while U_{21} $(\simeq \nu\omega_1 L_{1s} I_1)$ is so small that its favorable effect on O practically disappears.

In Fig. 23, the (small) part of the index diagram in which $\underline{U}_r$ occurs is shown for a small value of ω_2 $(R_2^2 \gg (\omega_2 L_{2s})^2)$ and $\theta_0 \simeq \theta_v$

$\underline{E}_r$ will hardly change for changing angle θ, because ν is very small.

At constant U_2 the point of the index $\underline{U}_r$ is on the dotted arc.

If $\theta = \pi/2$, $\underline{I}_r$ has the same direction as $\underline{U}_s$ ($R_2 \underline{I}_r$ vertical).

The index $R_2 \underline{I}_r$ is then much smaller than at $\theta = \theta_0$ $(\underline{U}_r \simeq \underline{E}_r + R_2 \underline{I}_r)$, so that I_2 (E_p) is smaller for $\theta = \pi/2$.

$E_{p,k}$ is in this case consequently smaller than $E_{p,k}$. [sic].

If we set $\theta_0 = 30^\circ$, we neglect $\omega_2 L_{2s}$ and $\omega_1 L_{1s}$ relative to R_2, and we approximate the arc by a horizontal dotted line, then: "$R_2 I_r$ at $\theta = \theta_0$" = 2 X "$R_2 I_r$ at $\theta = \pi/2$", so that $E_{p,0} = 2\ E_{p,k}$ and $0 = 1$ (eq. 31).

This means that stable operation under these conditions is impossible.

The larger $R_2 I_2$ is relative to E_r for these small values of ω_2, the farther out the dotted line of the arc lies and the less thick is 0 in the most critical situation at one.

It can be shown that for not too small values of L_{2s} / L_{2h} /65
(i.e. for a somewhat larger air slit width), the situation "$\omega_2 L_{2s} \ll R_2$ and $E_r \gg R_2 I_2$ will not occur [sic].

We must not conclude that for the required wind velocity for the converter voltage, the situation in this area ($\omega_2 \ll \omega_1$; $\theta_0 \simeq \theta_v$ is defined.

Finally, when ω_2 is so small that E_r is much smaller than $R_2 I_2$, the situation approaches rapidly at which $\omega_2 = 0$ and $U_2 = R_2 I_2$.

It is possible, with a free large approximation, to /66
record an entirely simple relation between the ratio $v_{w,k} / v_{w,0}$ (index k for $\theta = \pi/2$; index o for $\theta = \theta_0$) and the overload capacity 0. $V_{w,k}$ and $V_{w,0}$ then must be interpreted as the wind velocities as follows from T_a and thus not defined instantaneous values of v_w (although they can also naturally be at constant wind speeds).

From $0 = \frac{T_{el,k}}{T_{el,0}}$ and $T_{el} \simeq T_a$, it follows that:

$$0 = \frac{T_{a,k}}{T_{a,0}}$$

From constant ω_2 (definition of 0), it follows that ω_2 is constant, so that:

$$0 = \frac{\omega_r T_{a,k}}{\omega_r T_{a,o}} = \frac{P_{a,k}}{P_{a,o}} .$$

From $P_a = C_p \eta_m P_w$ (eq. 6, p. 7), it then follows that:

$$0 = \frac{C_{p,k}\ \eta_{m,k}\ P_{w,k}}{C_{p,o}\ \eta_{m,o}\ P_{w,o}} .$$

NB: $T_{el,0}$ ($\simeq T_{a,0}$) is defined as the electromagnetic couple at $\mu = \mu_0$ ($C_p = C_{po}$) for a specific ω_r ($0 < \omega_r < \omega_1$).

If we assume that η_m (the mechanical output of the mill remains constant, ($\eta_{m,k} = \eta_{m,0}$)), then we find further with $P_w \sim v_w^3$:

$$0 = \frac{C_{p,k}}{C_{p,o}} \left(\frac{v_{w,k}}{v_{w,o}} \right)^3$$

Because ω_r is constant and $v_{w,k} > v_{w,0}$, $\mu_k < \mu_0$ and $C_{p,k} < C_{p,0}$ ($\mu = \pi n_m D / v_w$, with $n_m \sim \omega_r$ and constant ω_r, it follows that: $\mu \sim 1/v_w$).

Now the value of $C_{p,k} / C_{p,0}$ at given $v_{w,k} / v_{w,0}$ is not so simple to give.

In the first place, this value depends on the type of mill (Fig. 4, p. 100), and in the second place no simple relation is given between C_p and μ for a given mill type.

In order to nevertheless get some idea of the increase in T_a for an increase in v_w and constant ω_r, we shall use, for $\mu = \mu_0$ the free large approximation /67

$$\frac{C_p}{C_{po}} = \frac{\mu}{\mu_o}$$

With this and with $\mu \sim 1/v_w$, we find for O:

$$O = \frac{\mu_k}{\mu_o} \left(\frac{v_{w,k}}{v_{w,o}} \right)^3 = \frac{v_{w,o}}{v_{w,k}} \left(\frac{v_{w,k}}{v_{w,o}} \right)^3 = \left(\frac{v_{w,k}}{v_{w,o}} \right)^2 .$$

So that

$$\frac{v_{w,k}}{v_{w,o}} = \sqrt{O} .$$

It is easy to see that in the same way

$$\frac{v_{w,k}}{v_{w,v}} = \sqrt{O_v} ,$$

with $v_{w,v}$ as the wind velocity at which $T_{el} = T_{el,v}$

<u>Temporary Control with ω_2</u>

We always start from the fact that $T_a \simeq T_{el}$ and that to an increase in T_a (v_w) there must correspond an increase in E_p (increase in converter voltage) to provide for the generator remaining in phase and cos φ_1 having a known value.

Changes in ω_2 (the frequency of the converter) will have no effect on this. The stator quantities which play an important role in this are always completely independent of ω_2.

There is, however, a conceivable situation in which there can occur decreases, although temporary, in ω_2 (so long as there can, thus long $p\omega_r < \omega_1$, so that the machine falls out of phase.

This situation occurs whe, for increasing v_w , the difference between T_a and $T_{el,0}$ is used to accelerate at the rotor. T_{el} then initially remains equal to $T_{el,0}$.

Naturally, this cannot be imposed as ω_2 . Only when the possibility exists of deriving the converter frequency for an increase in v_w (T_a) from the number of rotor revolutions (instead of letting ω_r follow from ω_1 and ω_2 as usual) is this realizable.

Through $T_a - T_{el,0}$, ω_r will then increase, whereby ω_2 decreases. When, however, ω_2 has reached a value at which $\mu = \mu_0$ ($C_p = C_{p0}$) ω_2 must, in order to have the optimal situation, be again imposed (held fixed at this value). /68

Then voltage control of the converter still provides for the correct rating (E_p).

Copper and Iron Losses in a DSG

For the copper loss in the stator and rotor, we find, respectively $P_{Cu1} = 3R_1I_1^2$ and $P_{Cu2} = 3R_2I_2^2$.

The relation between I_1 and I_2, and thus between P_{Cu1} and P_{Cu2} depends, among other things, on the angles φ_1 and θ.

For illustration, we choose the case in which $\theta_v = 30^\circ$ and $\varphi_1 = 180^\circ$. Fig. 24 gives the part of the index diagram which is of interest here (compare Fig. 21).

If we choose index v for the quantity at full load, then here: /69

$$E_{p,v} = 2\,\omega_1 L_1 I_{1,v} \xrightarrow{\text{fig.}} \omega_1 M\, I_{2,v} = 2\,\omega_1 l_1 I_{1,v}$$

so that

$$\frac{I_{1,v}}{I_{2,v}} = \frac{1}{2}\,\frac{M}{L_1} \simeq \frac{1}{2}\,\frac{M}{L_{1h}} = \frac{w_2}{2w_1} .$$

If we want P_{cu1} and P_{cu2} to be equal to each other at full load,

$$P_{cu1,v} = P_{cu2,v} \rightarrow R_1 I_{1,v}^2 = R_2 I_{2,v}^2 .$$

then $R_1 : R_2 = 4w_1^2 : w_2^2$.

We can sketch the path of P_{cu1} and P_{cu2} as a function of P_1. For P_{cu1} , it clearly follows that $P_{cu1} \sim I_1^2$ and $P_1 \sim I_1$: $P_{cu1} \sim P_1^2$. P_{cu2} as a function of P_1 we derive as follows:

From Fig. 24, it follows in this case that $U_1 = \sqrt{3}\,\omega_1 L_1 I_{1,v}$ and $E_{p,v} = 2\omega_1 L_1 I_{1,v}$. If $\theta < \theta_v$ while $\varphi_1 = 180°$, then $E_p^2 = (\omega_1 L_1 I_1)^2 + U_1^2$.

From

$$\frac{E_p^2}{E_{p,v}^2} = \frac{(\omega_1 L_1 I_1)^2 + U_1^2}{E_{p,v}^2}$$

it follows, after substituting the expression found for U_1 and $E_{p,v}$ in the right-hand member:

$$\frac{E_p^2}{E_{p,v}^2} = \frac{(\omega_1 L_1 I_1)^2 + (\sqrt{3}\,\omega_1 L_1 I_{1,v})^2}{(2\,\omega_1 L_1 I_{1,v})^2} = \frac{1}{4}\left(\frac{I_1}{I_{1,v}}\right)^2 + \frac{3}{4} .$$

thus:

$$\frac{I_2^2}{I_{2,v}^2} = \frac{P_{cu2}}{P_{cu2,v}} = \frac{1}{4}\left(\frac{P_1}{P_{1,v}}\right)^2 + \frac{3}{4} .$$

In Fig. 25, P_{cu1} , P_{cu2} , and P_{cu} (normalized at $P_{cu,v} = 2P_{cu1,v} = 2P_{cu2,v}$) are sketched as functions of P_1 (normalized at $P_{1,v}$).

We can still calculate that in this case, P_{cu} / P_1 has a minimum at /70

$$\frac{P_1}{P_{1,v}} = \frac{I_1}{I_{1,v}} \approx 0,77 ,$$

while

$$\left(\frac{P_{cu}}{P_1}\right)_{min} = 0,97 \frac{P_{cu,v}}{P_{1,v}} .$$

At $P_1 / P_{1,v} = 0.6$, P_{cu} / P_1 is again equal to $P_{cu,v} / P_{1,v}$.

The iron losses (P_{Fe}) are divided into hysteresis losses ($P_{Fe,h}$) and cyclone losses ($P_{Fe,w}$). /71

The iron losses in the stator (P_{Fe1}) are practically constant because U_1 and ω_1 are constant, while for the voltage induced at the stator (E_s), E_s always $\approx U_1$.

The iron losses at the rotor are not constant. It follows from the practically constant E_r/ω_2 ($E_r/\omega_2 = \nu E_s/\omega_2 \simeq \nu U_1/\omega_2 = w_2 U_1/w_1\omega_1$) that the rotor flux is nearly constant, but because

ω_2 is not constant, $P_{Fe2,h} \sim \omega_2$ and $P_{Fe2,w} \sim \omega_2^2$ will hold.

The rotor iron losses are greatest at $\omega_2 = \omega_1$ ($\omega_r = 0$; the machine then operates purely as a transformer). At $\omega_2 = 0$ ($p\omega_r = \omega_1$), there are no iron losses.

In order to limit losses, the rotor must naturally be laminated.

In Fig. 26, the iron losses are sketched as a function of $p\omega_2$ (and ω_2) for the case in which, for $\omega_2 = \omega_1$: $P_{Fe1} = P_{Fe2}$ and $P_{Fe2,h} = P_{Fe2,w}$. It is normalized at ω_1 and at the total iron losses for

If we start from the fact that P_1 as a function of ω_r has a path as given in Fig. 14, p. 117, ($P_1 = c\,\omega_1\,\omega_r^2$), then for that case, the iron losses can be shown as a function of P_1. Using:

$$\frac{P_1}{P_{1,v}} = \left(\frac{p\omega_r}{\omega_1}\right)^2 = \frac{(\omega_1-\omega_2)^2}{\omega_1^2} = \left(1-\frac{\omega_2}{\omega_1}\right)^2 \qquad \frac{\omega_2}{\omega_1} = 1 - \sqrt{\frac{P_1}{P_{1,v}}} \;;$$

$$\frac{P_{Fe2,h}(\omega_2)}{P_{Fe2,h}(\omega_2=\omega_1)} = \frac{\omega_2}{\omega_1}$$

and

$$\frac{P_{Fe2,w}(\omega_2)}{P_{Fe2,w}(\omega_2=\omega_1)} = \left(\frac{\omega_2}{\omega_1}\right)^2$$

this is done in Fig. 27, in which P_1 is normalized again at $P_{1,v}$ and P_{Fe} at $P_{Fe,n}$.

Combining Figs. 25 and 26 finally yields Fig. 28, in which copper losses as well as iron losses are recorded. Here is set, next to the conditions mentioned, $P_{Cu,v} = P_{Fe,n} = P_{norm}$. /73

It is certainly not said that the assumptions used here are the most suitable ones for the DSG.

It operates here only as an example, that nevertheless provides provides some insight.

2.a.5. The Converter /75

Up to now we have considered the converter as an ideal voltage source, which yields a sinusoidal voltage, controllable in amplitude and frequency.

Without going into a specific design for a converter, we shall here bring forward a general view which we have to make for every converter and which surely affects the whole design of the DSG and converter.

For the working mechanism of the DSG, it is necessary that a specific power P_2 is supplied to a rotary current winding at the rotor. This power is only defined through the shaft power presented and the ratio between the number of generator revolutions ω_r and the network frequency ω_1. It is not of essential importance either that the power delivered is at a low voltage and high current or, inversely, at high voltage and low current. This does have, however, an effect on the losses in the DSG. Using machine theory, it follows that for a generator, an optimal design is found at a free large rotor current, in other words, for a relatively small number of rotor windings.

For a converter which must deliver that power P_2, we can show, however, that this will correctly have a high yield for a much higher voltage and lower current (NB: if no impedance adjustment takes place).

Fig. 9a (a part of Fig. 9, p. 106) shows this.

Because at least one connecting semiconductor component enters into each converter, what now follows, which is related to this, is generally valid.

The CSS contravenes, when this is conducting, at a (forward) voltage drop. This voltage drop consists of a constant part (intrinsic voltage drop) and a current-dependent part (resistive voltage drop).

For a high current, the current-dependent part is large, /76

while the total voltage loss is large relative to the output voltage of the converter, which for high current is low for a specific power to deliver (P_2). The loss that herewith exists will therefore be larger as the current through the semiconductor is larger, and thus as the converter voltage is lower. As far as the current is concerned, moreover, it clearly follows that the (inevitable) ohmic losses are small, the smaller the effective value of the current.

The things mentioned show that the yield of a converter is the highest for a load with a high input impedance (U / J), while the optimal design of the DSG ("a relatively small number of rotor windings ") correctly shows a low input impedance. /77

Thus an impedance adjustment is necessary. We can thereby consider a transformer between the converter and the DSG. When we take a relatively large number of rotor windings for the DSG (for example, on the order of the number of stator windings), we insert, as it were, the transformer into the DSG. A third possibility, in which use is made of a new generation of converters which are still in the process of development, is that whereby the impedance adjustment takes place in the converter itself.

What has been treated so far likewise holds for a converter which delivers a pure sinusoidal voltage, as well as for a converter which delivers voltage in which only the envelope is a sine curve. However, in this last case, the problems occurring are greater.

The current-shape factor, $\rho_i = i_{eff} / i_{meas}$ is then larger. The active rotor current, which the magnetic field generates, is defined by i_{meas} , while the losses are determined through i_{eff} .

Another problem is that in such a case, moreover, the maximum value of the current is much greater than the averaged value, while this maximum value forms the limits both for the components and for the working mechanism of a converter.

The previously mentioned new generation of converters then also delivers a real sinusoidal output voltage.

Resuming, it can thus be stated that the optimum number of rotor windings in a DSG is determined through the converter design; naturally, such that all the herewith associated DSG and converter losses being considered, one arrives at an optimum design.

2.b. Practical Section /78

In this part of the report, results are given for a first attempt at a generator which operates as a Double-feed Synchronous Generator (DSG). The purpose of the experiment was to show that:

Synchronous generator operation at any revolution is possible in the manner presented in the preceding section.

In neglecting losses, the powers are in the ratio of $P_1 : P_2 : P_a = \omega_1 : \omega_2 : p\omega_r$, as is derived.

The experiment has a highly improvised character; use is made of available means which for this purpose are far from ideal.

The real interest in this experiment, however invalid, nevertheless goes far beyond the results mentioned in this part of the report. Much of the theory derived in the previous section finds its origin in questions which were evoked in "playing" with the experimental set-up.

2.b.1. Description of the Experimental Set-up

A synchronous slip-ring armature motor is used as a DSG, in which the brush direction is intensified in order to make possible permanent rotor supply (see further, p. 68).

The three-phase, direct-voltage / alternating-voltage inverter (McMurray-type inverter) is used as a converter, which is described in J.A. Wiersma's graduation paper (see further, p. 69).

To drive the generator (in fact, the simulation of the windmill), use is made of a pole-changeover, asynchronous motor. With this drive-motor, the generator can be driven with full=load revolution and with 1/3, 1/2, and 2/3 load. Control of the couple on the drive-motor (T_a of the generator) was possible in two ways: 1) by controlling the motor voltage, which is made possible because the motor is supplied from a controllable /79
transformer, and 2) by controlling the slip of the drive-motor. Because in synchronous generator operation, the relation $\omega_1 = \omega_2 + p\omega_r$ holds, the value for ω_r (and thus for the slip of the drive-motor) follows from this equation when ω_1 (network frequency) and ω_2 (converter frequency) are imposed. By controlling the converter frequency, the slip, and consequently the couple, of the asynchronous drive-motor can be controlled, while as a result of the steep slope of the couple-revolution curve, the number of motor and generator revolutions are only

changed a little. This is sketched in Fig. 31. From point 1, for example, point 2 is reached through an increase in voltage (control transformer), for which ω_r is not changed, while point 3 is reached by increasing the converter frequency.

Fig. 32 gives the construction of the experimental set-up with which the measurements are made at $p\omega_r = \frac{1}{3}\omega_1, \frac{1}{2}\omega_1$ and $\frac{2}{3}\omega_1$. /80
The converter is here supplied from a direct-voltage network. This is in contrast to the design sketched on p. 114 , Fig. 13, in which the converter is supplied from the stator of the DSG.

With the experimental set-up of Fig. 13, measuring is done at $p\omega_r = \omega_1$. The rotary-current winding of the rotor must then be rated with direct current $(\omega_2 = \omega_1 - p\omega_r = 0)$.

NB: Here the current in the windings of different rotor phases is not the same.

Especially in machines with a small number of coils per phase (p = 1 or 2), this leads to an uncontrollable heating up of the rotor. Therefore it is better to take a very low value of ω_2 instead of $\omega_2 = 0$. It appears that it is possible to achieve this with the inverter used here.

The Generators Used /83

In Sect. 2.a.1. on p. 14, it has already been noted that an asynchronous slip-ring armature motor can be used as a DSG.

Generally, an ASM has a relatively small number of rotor windings (w_2) in relation to the number of stator windings (w_1), with the result that the nominal rotor current is much greater than the nominal stator current. If such a machine ($w_2 / w_1 \ll 1$) is used as a DSG, then the converter (which delivers the rotor current) must be suitable at low voltage (U_2 w_2/w_1) to give a very high current. This requires a converter with very sturdy semiconductor components, in proportion to the nominal converter power.

Therefore, what is sought after is an ASM with not too different numbers of rotor and stator windings in each one.

In the table below are presented a number of data for two machines suitable in the industry association which provide these requirements.

1 a.s.m.	2 schijnbaar vollast vermogen	U_1	U_{20}	3 I_1 vollast	I_{20}	4 p pool-paren	$\frac{w_2}{w_1}$
G_I	37,6 kVA	220 (380) V	70 (121) V	57 A	54 A	2	0,3
G_{II}	10,2 "	220 (380) "	127 (220) V	15,5 "	8,8 "	2	0,6

Key: 1. ASM
2. Apparent full-load power
3. I_1, full-load
4. p, pole pairs

The index I_{20} is the required effective value of the rotor voltage in order to induce nominal voltage in the stator at $\omega_2 = \omega_1, \omega_r = 0$. I_{20} [sic] is the corresponding value of the rotor current.

In the columns for U_1 and U_{20}, the couple voltages are given after the phase voltages.

From p = 2, it follows that the maximum generator revolution (at $\omega_r = \omega_1/p$) is 1500 rpm.

From the voltage equation of the stator, in which $I_1 = 0$ is substituted and with the definition of I_{20}, it follows that the value of I_{20} does not depend on the number of generator revolutions. /84

If we are not going to deliver watt power as well as idle power, using the generator, to the network, then the sinusoidal voltage induced in the stator from the rotor must have a higher effective value than the network voltage. Irrespective of the number of revolutions, a current is thus necessary there which is greater than I_{20}.

When, as is the case for the inverter used, the rotor voltage (and consequently the induced voltage) is not purely sinusoidal, then we can only use the given value of I_{20} to obtain an overall inducing of the required rotor current.

Another problem that exists through the use of an asynchronous slip-ring armature motor as a double-feed synchronous generator goes along with the fact that an asynchronous machine has as small an air slit as possible, while the air slit in a synchronous machine is much larger.

Because the main inductivity is inversely proportional to the (effective) air slit width, this will, consequently, be much larger for an asynchronous machine than for a synchronous one.

This has further consequences. An important consequence, which is easy to observe using the index diagram of Fig. 17 on p. 120, is that the load angle θ for an ASM used as a generator will be much larger than the load angle for a comparable synchronous generator under the same conditions. The danger of falling out of phase is thus much greater with an ASM.

The Converter Used

The three-phase converter which was used in the experiment was built in the past year by members of the industry association. There is a converter of this type in the literature, known as the McMurray inverter. The name "inverter" (instead of "converter") is used here because switching on the thyristors is provided through the apparatus itself (here using idle thyristors and a /86 resonance ring. In the following, therefore, we shall use the name "inverter" for this apparatus. Fig. 34 (from ref. [6]) gives the principal diagram for the inverter. The part with the supply source (± 110 v direct voltage), the main thyristors (6), and the three-phase load are indicated with heavy lines. A diode is included antiparallel to each main thyristor, among other things to make possible the delivery of an accelerating current (inductive load). Switching off the main thyristors takes place using two complementary idle thyristors and a resonance ring, together with the commutation circuit mentioned (see Fig. 34). The most important properties which the inverter makes available for our purposes are:

an output voltage which is adjustable over a wide range of sizes and frequencies,

a practically non-homopolar component in the output voltage,

and no harmonics with order number divisible by three.

A number of differences, which are observed in the experiment with the DSG in combination with this inverter, are associated with the fact that the output voltage of the inverter is not actually sinusoidal.

Fig. 35 gives the output voltages with their sinusoidal envelopes. Each half-voltage consists of four pulses. The size of the voltage (envelope) is controlled using the width of these pulses (pulses width modulation).

The number of pulses per half period (here, four) forms a compromise between the advantages of a large number of pulses which occurs with higher harmonics and the disadvantage of the (inevitable) extra energy loss through switching off the thyristors repeatedly during the period.

2.b.2. Findings in the Experiment /88

The first and without doubt the most important result of the experiment is that it was shown that the test generators (GI and GII) indeed operating synchronously can deliver power to a public network at an entirely different generator revolution than the normal synchronous revolution ($n_r = f_1 / p$ rpm / sec), provided the rotor is rated in the correct way with an angular frequency $\omega_2 = \omega_1 - p\omega_r$. The generators must be synchronized in the usual way for a synchronous generator, whereas the generators "normally" fall out of phase with too large a shaft couple.

The experiments were initially begun with a large 37.6 kVA machine (GI). A problem here was that even with a high inverter frequency ω_2, the impedance of the rotor circuit was still so low that even at minimum inverter voltage (minimum pulsewidth), the current was too high for the inverter. Therefore, forward couple resistances must always be included in the rotor circuit.

The rotor current which could be so obtained was not yet sufficient to induce a supply voltage in the stator, with the result that the generator always takes on idle power from the network.

Nevertheless, it seems possible with this machine to deliver a few kilowatts (watt power) to the network, both at about 1/3 and 1/2 of the normal synchronous revolution of the machine ($\omega_2 \simeq 2/3\, \omega_1$ and $\omega_2 \simeq 1/2\, \omega_1$).

This machine was clearly too large for further experiments, in view of the equipment available.

In using smaller generators (GII, 10.2 kVA) in the

experimental set-up in Fig. 32, p. 133 , the following was observed in the first instance.

1. For $\omega_r \simeq \frac{1}{3}\frac{\omega_1}{p}, \frac{1}{2}\frac{\omega_1}{p}$ and $\frac{2}{3}\,\omega_1/p$, the synchronous generator draws on the network, where: $p\omega_r = \omega_1 - \omega_2$.

2. By controlling the rotor current I_2, the rating can be found, for a given shaft couple, at which the stator current I_1 (= network current) is minimum.

In using the small generator with direct-current rating /89
($\omega_2 = 0;\ p\omega_r = \omega_1$; the set-up in Fig. 33, p. 135), the generator can also draw synchronously on the network, while for each shaft couple here, I_1 can also be brought to a minimum by adjusting the rating.

We shall now explain these findings further.

For 1: For operation at $\omega_r \simeq \frac{1}{3}\frac{\omega_1}{p}$, for which the highest rotor voltage is required ($U_2 = \gamma U_1$ with $\gamma = \frac{W_2}{W_1}\frac{\omega_2}{\omega_1}$), the maximum effective inverter voltage very clearly appears to be too low.

The result of this is that even with zero load (P_1=0), the network at this revolution must deliver idle power for the rating of the generator. At $\omega_r \simeq \frac{1}{2}\frac{\omega_1}{p}$ and $\omega_r \simeq \frac{2}{3}\frac{\omega_1}{p}$, the generator could be tested from zero load to full load. However, the commutator drive-motor offers further a fourth possibility, namely $\omega_r \simeq \frac{\omega_1}{p}$; no experimenting could be done using the set-up with the inverter (Fig. 32). In Sect. 1.b.2., it appears that with this inverter, no stable operation is expected for low values of ω_2 (f_2 on the order of a couple of Hz). Therefore, measuring with the set-up in Fig. 33 (direct-current rating) takes the place of this measurement.

For 2: From normal synchronous generator theory, it is known that for a given shaft couple, a minimum can be found for the delivered stator current I_1 by varying the rating current, while the delivered (watt) power P_1 remains practically constant for changing rating current.

Also what this involves, and the DSG thus shows, as expected, is the behavior of the normal synchronous generator.

With the experiments at these revolutions, it is now truly demonstrated that stable operation with a combination DSG and asynchronous drive-motor is possible, but up to now no consideration has been taken of the stabilizing influence which the drive-motor exercises with its steep couple-revolution curve over the whole. Because the couple-revolution curve of the

windmill is much less steep (Fig. 5a, p. 105), it is necessary to show that the DSG itself provides a sufficient stabilizing effect.

A first proof of this is, naturally, the mere fact that /90
revolution of the motor-generator combination through the DSG is defined by the relationship $\omega_r = \frac{\omega_1 - \omega_2}{p}$ in which we give ω_2 a known value), and not through the drive-motor.

As additional proof of the stabilizing effect of the DSG, we have allowed the asynchronous drive-motor operate at the unstable flank of its couple-revolution curve, so that it is irrefutably shown that the DSG can provide stability. This test was carried out as follows. For nominal voltage at the drive-motor, the generator was synchronized to the network at a revolution of 1000 rpm ($p\omega_r = \frac{2}{3}\omega_1$, $\omega_2 = \frac{1}{3}\omega_1$). By increasing the inverter frequency ω_2, a shaft couple was set up such that 1.5 kW is delivered to the network (point 1 in Fig. 36). By gradually decreasing the supply voltage of the drive-motor and increasing the inverter frequency (ω_2), the number of revolutions /91
($\omega_r = \frac{\omega_1 - \omega_2}{p}$) is lowered, while P_1 is held at 1.5 kW[1] (shaft-couple constant). The couple, moreover, initially changed rapidly (Fig. 36), so that the voltage continuing strongly must be lowered (point 2). From the fact that P_1 at a given moment is hardly changed at all with an increase in ω_2 and secondly would again go down, so that the motor voltage must be increased again to keep delivering 1.5 kW, it can be inferred that we have passed point 3 and are going in the direction of point 4. When the generator revolution came below 800 rpm (starting from 1000 rpm), it began to show the first indication of instability, and just above 750 rpm, it fell out of phase. We had then almost arrived at the following tested revolution ($\omega_r = \frac{1}{2}\omega_1/p$; $\omega_2 = \frac{1}{3}\omega_1$). When we consider that the drive-motor had with it a slip of fully 20%, while the manufacturer set 5% as the maximum permissible slip, then there is no doubt that we are concerned with the unstable flank of the couple-revolution curve.

Stable operation is thus possible without the stabilizing effect of the asynchronous drive-motor. Why the generator falls out of phase, however, is not entirely clear. Perhaps the unstable flank of the couple-revolution curve is much steeper at that point. Perhaps also it has to do with problems which exist through the strong asymmetry of the ASM used as a DSG, into which we shall enter further in Sect. 2.b.4.

---

[1] For loads much larger than 1.5 kW, this same experiment is not feasible, because the much more severe (unstable) drive-motor will then draw the generator out of phase. This the more so as we, using the small air slit of the DSG, however, operate at relatively large load angles (p. 143).

2.b.3. Measurement Results /92

The measurements were made in order to control the derived relationship $P_1 : P_2 : P_a = \omega_1 : \omega_2 : p\omega_r$. This relation holds true only while neglecting all losses. In actuality, this relationship holds for the share that the powers have in the air-slit power, while the actual input and output power measured must be decreased relative to the losses.

The power diagram in Fig. 37 shows this.

The measurements at $p\omega_r = \frac{2}{3}\omega_1$, $p\omega_r = \frac{1}{2}\omega_1$ and $p\omega_r = \frac{1}{3}\omega_1$ are /93
done with the experimental set-up as sketched in Fig. 32, p. 133 .

The measurement at $p\omega_r = \omega_1$ $(\omega_2 = 0)$ is done using the experimental set-up of Fig. 33, p. 135 .

The electrical powers P_1 and P_2 are measured using wattmeters, for which the Aaron couple is applied in the rotor circuit, because no neutral point is available.

The shaft power P_a is determined by measuring the power taken up by the drive-motor and multiplying it by the motor output. This last can always be determined quite accurately from the output curves given by the manufacturer. Because these curves are given at constant (network) voltage for the drive-motor, the shaft couple is always set by controlling the inverter frequency ω_2 (slip control). The result of this, however, is that the ratio between ω_1, ω_2, and ω_r at any measurement point is a bit different. For the drawing in Fig. 38, therefore, a small correction is applied to the measurement values.

In the diagrams of Figs. 38 a, b, c, and d, the lines drawn for the powers P_1, P_2, and P_a as a function of P_1 are given for the (loss-free) case $P_1 : P_2 : P_a = \omega_1 : \omega_2 : p\omega_r$.

The points presented in the diagrams give the measured values.

We see that the measured values of P_a and P_2 always come out above the lines drawn, which is in agreement with the power diagram sketched in Fig. 37.

In order to get an idea of the losses occurring in the generator, the values of $P_1 / (P_2 + P_a)$ are calculated for the different measurement points and are set forth in Fig. 39.

It is striking how small these values are at the same P_1 but they differ for different revolutions for each.

Each time this will occur because for increasing ω_r, and thus for decreasing ω_2, the friction losses increase, but the rotor iron-losses decrease.

However, in view of the fact that the highly improvised character of the experiments will have a great influence on the losses in the generator (voltages and currents not sinusoidal), we must here be very careful of drawing general conclusions for /96 the DSG. From half load to full load, we find a good 0.85 for the ratio $P_1 / (P_2 + P_a)$, while from the data for the machine used as a DSG, one concludes that it has an output of 85% as a motor.

The practical evidence that these powers furnish a measure for the validity of the relation $P_1 : P_2 : P_a = \omega_1 : \omega_2 : p\omega_r$ is of great interest because from it follows the applicability of the DSG as a generator for a windmill. In the set-up for Fig. 14 on p. 117 (see also Fig. 40), in determining the "maximum 14.8% of the full-load power which must be brought about for /97 this system through power electronics", use is always made of this relationship.

In Fig. 40, P_1, P_2, and P_a are given as functions of ω_r $(\omega_r \sim V_w)$ for $V_{min} \leq V_w \leq V_k$,

the lines drawn in neglecting all losses, as they follow from $P_1 : P_2 : P_a = \omega_1 : \omega_2 : p\omega_r$ (as in Fig. 14),

the dotted lines as they follow from the measurements at the generator.

We must consider well that here only the generator losses /98 are taken into account and not those of the converter, so that as far as that is concerned, the deviations will be greater. On the other hand, we must consider that a very small machine is involved here, which is, moreover, used in a manner for which it was not constructed. We may therefore expect that the deviations from the theoretical values will be smaller rather than larger.

2.b.4. Influence of Non-Perfect System Parts on the Behavior of the Machine /99

In Sect. 2.b.2., we specified individual findings in the experiments which correspond to expectations.

Here, we shall go into individual odd differences which are observed. These are not in general typical of a DSG with converter. They can be explained by the non-ideal behavior of the system parts used.

Observations

1. When no exchange of (watt) power takes place between the generator and the network ($P_1 = 0$), the minimum effective value of the stator current (which occurs for a specific rating) appears to be much greater than zero ($> 5A$).

2. In calculating $\cos \varphi_1$ from the measured values of the delivered power P_1, I_1, and the network voltage U_1, using $\cos \varphi_1 = P_1 / 3U_1 I_1$, it also appears that at minimum I_1 (correct rating) "$\cos \varphi_1 = 1$" does not fit in ~~in~~ all.

3. For very small values of slip in the drive-motor, when the ratio $\omega_2 : p\omega_r$ thus is very close to the values of 2:1, 1:1, or 1:2, the generator appears to oscillate around the revolution ω_r.

For 1 and 2: The fact that no rating is found at which I_1 is zero at zero load, and that under loaded conditions, the work factor has a value of one, forms an important deviation from the known behavior of the normal synchronous generator.

The cause of the deviations noted in 1 and 2 must be sought in the non-ideal behavior of the inverter. In setting up the theory in the preceding section, we always started from a sinusoidal rotor voltage (inverter voltage). The inverter voltages presented to the rotor (Fig. 35, p. 139, u_{rs}, u_{st}, and u_{tr}) are, however, far from sinusoidal. The voltages induced at the stator will therefore also not be sinusoidal. Photographs 1, 2, and 3 show this clearly.

If the effective value of the voltages photographed is 220 v, then the instantaneous value will be alternately larger and smaller than the instantaneous [words missing in the original] 220 v effective. If the stator is now connected to /101
the network, by so doing, current peaks will exist as shown in photographs 4, 5, and 6 (top image). If the induced voltage

was shown to be sinusoidal (and 220 v_{eff}), these current peaks naturally did not exist, and the effective value of the current was shown to be zero. The effective value of the currents photographed is, however, decidedly not zero, while the current still does not provide for delivered power P_1 (moreover, this also follows from measurements from accurate study of the photo images). The minimum attainable effective value of the zero-load current is smaller, the larger ω_2 is; 7.9 A for $\omega_2 = \frac{1}{3}\omega_1$, 6.5 A for $\omega_2 = \frac{1}{2}\omega_1$, and 5.8 A for $\omega_2 = \frac{2}{3}\omega_1$.

The deviation mentioned in point 1 from the predicted behavior is hereby explained.

It will be clear that it can, moreover, be explained herewith why the work factor is not equal to one at minimum I_1 (point 2). Also, when the generator current always delivers to the network, and thus when the induced stator voltage is higher than the network voltage, the voltage shape deviating from a sine curve provides extra peaks in the current. These peaks increase with the effective value of the current, but not the delivered power P_1. Calculating cos φ_1, from cos $\varphi_1 = P_1 / 3U_1 I_1$ then yields a value which is much smaller than one. We must then also consider that here the angle φ_1, which is defined as the phase angle between the sinusoidal stator voltage and current, has lost its significance, because the voltage and current occurring here are not sinusoidal.

The work factor, which we thus can no longer call "cos φ_1", is defined as:

$$\text{w.f.} = \frac{P_1}{U_{1\,eff} \quad I_{1\,eff}}$$

In the case mentioned in 1, this is equal to zero; in the case mentioned in 2, it is less than one.

The above-mentioned problems occur especially with the McMurray-type inverter used here, because the voltage is built up from a number of pulses. With the new generation of converters (Sect. 2.a.5.), the existing transformation of the current is very much less; comparable to the current transformation [words missing in original].

Photographs 7 through 9 show the current shape described. /103

Photographs 1, 2, and 3 are still worth further study. It is striking, for example, that as the width of the pulses from which the sine curve is built up differs, so also the number of

pulses per period differs for different revolutions (4, 6, and 8, respectively).

For an explanation of this, we refer again to Fig. 25. In this figure, it is shown that the voltages imposed at the rotor terminals u_{rs}, u_{st}, and u_{tr} are each built up from 8 pulses per period. Because two of these three voltages always coincide, the rotor "sees", per period of the rotor voltages and currents, $(T_2 = \frac{1}{f_2} = \frac{2\pi}{\omega_2})$, {3 (phases) X 8 (pulses)} /2 (which coincide) = 12 pulses per period. Of these 12 pulses, there are found, per period of the stator voltages and currents, $(T_1 = \frac{1}{f_1} = \frac{2\pi}{\omega_1})$, $12 \times T_1/T_2 = \frac{\omega_2}{\omega_1} \times 12$ in the induced voltages at the stator. For photos 1, 2, and 3, they are thus 1/3, 1/2, and 2/3 X 12, respectively, thus 4, 6, and 8.

Thereby the (absolute) pulse width naturally changes at different revolutions. That the relative pulse width (i.e., the ratio between the pulse length and period length) also differs is caused by the fact that the required rotor voltage is different at different values of ω_2 ($U_2 = \nu U_1$ with $\nu = \frac{\omega_2}{\omega_1} \frac{\omega_2}{\omega_1}$), in which U_2 is determined by the relative pulsewidth of the inverter.

From the foregoing, we can now conclude that the experiments are performed correctly at very particular revolutions, because the values of ω_2 concerned are such that $\frac{\omega_2}{\omega_1} \times 12$ is always a whole number, so that a whole number of peaks occurs in the stator voltage and current per stator period T_1. It hereby happens that the current in photos 4 through 9 display the same image for each period of stator voltage. At arbitrary values of ω_2, this is not the case, because the number of peaks per stator period is then not a whole number, whereby a shifting current image exists relative to voltage.

With accurate study of the example of photo 7, it then appears that the frequency with which the image of the current peaks is repeated is somewhat greater than 50 Hz. This fits, in view of the fact that, under loaded conditions, ω_2 must be somewhat greater than 1/3 ω_1, because the drive-motor reaches the required slip for the usual couple.

We shall now also look into why the inverter used /105
is but very restrictedly suitable.

First of all, the current peaks as shown in photos 7, 8, and 9 are naturally not allowed for current delivery to the public network.

When the number of peaks per stator period T_1 $(\frac{\omega_2}{\omega_1} \times 12)$ is much greater than one, they can be filtered out. If it is no longer the case that the peak frequency in the vicinity comes from the network frequency f_1, then filtering is practically impossible.

With this inverter, at $\frac{\omega_2}{\omega_1} = \frac{1}{12}$ ($f_2 \approx 4$ Hz), one "rotor peak" per stator period T_1 is "found again" in the stator current. Besides the fact that this naturally can never be filtered away, it is hard to doubt whether with such a severely transformed induced stator voltage, synchronous operation is even possible. Naturally, an improvement can be expected when a filter is placed on the exit from the inverter. An attendant problem in filtering, however, is stability. A more satisfactory result is expected for a converter with a much higher internal frequency (it comes down to this here that there are many more than 8 pulses per period in the coupled inverter voltage). On the one hand, the DSG hereby approximates much better the behavior of a normal synchronous generator (an assertion which, among other things, is justified by the statement that the minimum stator current under zero load is smallest when the number of peaks in the stator current is greatest; photo 6). On the other hand, for such a very much higher internal converter frequency, the peaks in the stator current I_1 to very low values of ω_2 can be filtered away with a relatively light filter.

For 3: As for the oscillation of the generator, what is initially observed as "oscillation for a small drive-couple (lightly loaded generator)" caused much suspicion in the beginning. The solution, however, was found when upon further inspection, it appeared that with open stator terminals ($I_1 = 0$) and a rated rotor, the effective value of the stator voltage varied strongly, if a very low frequency voltage is superposed. The phenomenon occurs in all three phases; however it always shifts 1/3 period. The more accurately satisfied is the ratio of 2:1, 1:1, and 1:2 respectively, the lower the frequency and the greater the amplitude of the swings. It is clear that the oscillation of the rotor, when the generator operates synchronously with the network, is a result of this. The current and consequently the /106
electromagnetic couple also always change with changing voltage. If the frequency of the swings is sufficiently low, the rotor oscillates by variations in the couple. We must then explain how the voltage can vary so. For this, the following theory is proposed.

The test generator has a rather high asymmetry (the current in rotor phase w, for example, is always about 10% greater than in the other two phases). The rotor rotary-current fields which exist through the combined operation of the currents in the three rotor phases, are thereby not always equally large. When, as is the case here, one current has a significantly greater effective value than the other two, the rotor rotary-current field is ellipsoidal instead of spherical. The ellipse "naturally lies still" relative to the rotor (Fig. 41).

A period of the stator voltage exists whereby the rotor is /107

operated over a certain angle ($\frac{p\omega_r}{\omega_1} \times \frac{360}{p}$ degrees), while at the same time the rotor rotary-current field relative to the rotor operates over such an angle ($\frac{\omega_2}{\omega_1} \times 360/p$ degrees) that the stator over "looks" the total operation $[(p\omega_r/\omega_1 + \frac{\omega_2}{\omega_1}) \times \frac{360}{p}$ degrees] = 360/p degrees.

If there is no particular ratio between $p\omega_r$ and ω_2, then after each period of the stator voltage, the rotor has another position relative to the stator.

The maxima and minima of the rotor rotary-current field are thereby always found again at a second stator plane, so that the effect herewith is averaged out. If one of the ratios mentioned, between $p\omega_r$ and ω_2 (2:1, 1:1, and 1:2, respectively) is held exact, it is easy to conclude that the maxima and minima of the rotor rotary-current field occur at the same rotor position relative to the stator. The phase voltages appearing will thereby no longer be the same for each. Through the small deviations in these exact ratios for these experiments, deviations which are the result of slip in the drive-motor, maxima and minima in the rotor rotary-current field will, as it were, "run around" slowly in the machine. This is especially true in a very lightly loaded generator in drive-motor slip so small that the variations in the current existing due to this phenomenon frequently lead to such low variations in the electromagenetic couple of the generator that the rotor oscillates violently. It cannot be explained exactly why the swings are worst at $\omega_2 = \frac{1}{3}\omega_1$. Presumably, an explanation for this is only just possible when the source of the asymmetry is known. Perhaps also the more severely transformed induced stator voltage at this low a value of ω_2 has something to do with it. In any case, this problem is not to be expected in a well-constructed generator, because it can be made sufficiently symmetrical.

The proof of the proposed theory on the oscillation at $\omega_2 = 1/3\,\omega_1$ (the situation with the worst oscillation) was tested twice with the same load conditions: once with as high a voltage as possible for the drive-motor for which the usual couple can thus be obtained with a small slip, and once with as low a voltage as possible and as large a slip as possible. In the first case, $p\omega_r = \omega_2$ was practically exactly 2:1 and the generator oscillated violently. In the second case, the ratio between $p\omega_r$ and ω_2 deviated so much already that oscillation no longer occurred. This behavior is consistent with the proposed theory.

Besides the powers P_1, P_2, and P_a (Fig. 38a, b, c, d), the values concerned for I_1, I_2, and U_2 are also measured. It is naturally nice when the values measured at the generator can be tested on the part of the calculations with the machine equations set up in Sect. 2.a.3. We must be careful here that the equations /108

hold for sinusoidal voltages and currents, while in actuality these are not absolute. Also, in order not to make the calculations too complex, use must be made of constant values for the coefficients L_1, L_2, and M occurring in the equations, while these are not the ones used here. When we consider all the deviations taking place here, it appears the bounds between which the measurements and the calculated values are the same must be so great that no single conclusion can be drawn for the results of such a test. It is therefore not worth the trouble to take up the results of the test in this report.

In this section, we shall go in detail into the non-sinusoidal nature of the rotor voltage and current. We shall still further go into the non-constant nature of the coefficients L_1, L_2, and M.

The prime source of the non-constant nature of L_1, L_2, and M is the saturation of the iron with which we are concerned, irrespective of the shape of the rotor voltage. As an example, Fig. 42 gives the measured values of M as a function of the induced stator voltage E_s, for the case in which the rotor is rated with a purely sinusoidal voltage. As the generator is more severely loaded, E_s is greater and thus (Fig) [sic] M is smaller. The same holds true for the coefficients L_1 and L_2. If in simple calculations it nevertheless works with an averaged (constant) value for the coefficients, calculation must be done with errors of a few percent. This last holds when all the voltages are sinusoidal. For a rotor voltage such as the inverter delivers, the matter is more complicated. Fig. 43 (in which Fig. 42 is again taken up) gives the values of M such that they are measured at different values of ω_2 using the inverter. It is striking that the curves which are measured using the inverter for different values of ω_2 have practically the same path, while they lie much higher than the curves measured with sinusoidal rotor voltage $(\omega_2 = \omega_1)$. This is easy to explain. The given values of E_s are always effective values, because these are used in the calculations.

The saturation of the iron, and with it the values of L_1, /110
L_2, and M, are however, connected with the averages values of the induced voltage. For the entirely different voltage shapes with which we are concerned here, the ratio between the averaged values and the effective values is, naturally, also different. For the same effective values (equal values of E_s in Fig. 43), therefore, the averaged values, and thus the saturation state and L_1, L_2, and M are different. The dependence of M (and also of L_1 and L_2) on the load state of the generator is now much greater even. E_s always equals E_p in measuring E_s with open stator terminals, so that the saturation state of the machine is entirely determined by the rotor volt-

age. If, however, the generator is closed at the network, then the resulting magnetic flux in the machine and thus the saturation state is determined by the (sinusoidal) stator voltage and the (non-sinusoidal) rotor voltage. The values of M involved in this case will, depending on the load, lie somewhere between the values with sinusoidal rotor voltage and those with the rotor voltage delivered with the inverter. The error which now exists when we work with an averaged value of M (and likewise L_1 and L_2) is thus even greater by far (here certainly greater than 10%).

Although, as a result of all these deviations from the ideal behavior, calculations are pointless as a control of the measured values, nevertheless the calculation method to use is given in the last section of the report, because this could also be useful in determinations for a suitable machine for possible further experiments.

2.b.5. Calculation Method /111

The machine equations found in Sect. 2.a.3.:

$$T_{el} = \frac{3p}{\omega_1^2 L_1} U_1 E_p \sin\theta \tag{29}$$

$$\underline{U}_1 = R_1 \underline{I}_1 + j\omega_1 L_1 \underline{I}_1 - \underline{E}_p \tag{28}$$

$$U_2 e^{j\phi_2} = R_2 I_2 + j\omega_2 L_2 I_2 - \omega_2 M I_1 e^{-j(\theta + \phi_1)} \tag{30}$$

with:

$$\underline{U}_1 = U_1;\ \underline{I}_1 = I_1 e^{-j\phi_1};\ -\underline{E}_p = E_p e^{-j\theta} \text{ and } E_p = \omega_1 M I_2$$

can be solved when sufficient data are known. In each case, the constants U_1, ω_1, p, R_1, and R_2 must be set for this purpose and, although not actually constant, L_1, L_2, and M. Of the remaining 9 variables, to know T_{el}, ω_2, I_1, φ_1, I_2, φ_2, E_p, θ, and U_2, one must still set 3, because the other 6 variables can be solved from the equations and the corresponding definitions. That solution must occur generally [word illegible in original]. The elimination of the unknowns is a practically endless task, especially also because the angles occur as sine and cosine. Only when the three variables ω_2, T_{el}, and φ_1 are taken as set, is direct solution possible. (Thereby, ω_2 can then be a chosen value, or by means of $\omega_2 = \omega_1 - p\omega_r$ a chosen value follows for ω_r.)

Because, in operating with a DSG with a windmill, ω_r and T_{el} follow from wind velocity for a given windmill, while the phase angle φ_1 is held at a specific (adjustable) value by control, precisely this case is meaningful for our application.

Using eq. (29) and eq. (28) split into a real and an imaginary part, according to: /112

$$U_1 = R_1 I_1 \cos\phi_1 + \omega_1 L_1 I_1 \sin\phi_1 + E_p \cos\theta \tag{28r}$$

$$0 = -R_1 I_1 \sin\phi_1 + \omega_1 L_1 I_1 \cos\phi_1 + E_p \sin\theta \tag{28i}$$

we can eliminate I_1, θ, and E_p as follows.

NB: In the right-hand member, we use knowns exclusively, or known quantities in the preceding.

From eq. (29), it follows that:

$$E_p \sin\theta = \frac{\omega_1^2 L_1}{3pU_1} T_{el}.$$

Substituted into eq. (28i), this yields, for the elimination of I_1:

$$I_1 = \frac{E_p \sin\theta}{R_1 \sin\phi_1 - \omega_1 L_1 \cos\phi_1}$$

Dividing eq. (28i) and (28r) by each other yields:

$$\frac{E_p \sin\theta}{E_p \cos\theta} = \mathrm{tg}\theta = \frac{E_p \sin\theta}{U_1 - R_1 I_1 \cos\phi_1 - \omega_1 L_1 I_1 \sin\phi_1}$$

and

$$\theta = \mathrm{arctg}|\mathrm{tg}\theta|$$

E_p can now be determined from the values of $E_p \sin\theta$ and θ according to $E_p = E_p \sin\theta / \sin\theta$. For zero load ($\sin\theta = 0$), difficulties exist here. We therefore use:

$$E_p = \frac{U_1 - R_1 I_1 \cos\phi_1 - \omega_1 L_1 I_1 \sin\phi_1}{\cos\theta}$$

$\cos\theta = 0$ does not occur under achievable operating conditions.

From $E_p = \omega_1 MI_2$, it then follows that: /113

$$I_2 = \frac{E_p}{\omega_1 M}$$

From eq. (30), written out in real and imaginary parts,

$$U_2 \cos\phi_2 = R_2 I_2 - \omega_2 M I_1 \cos(\theta + \phi_1) \tag{30r}$$

$$U_2 \sin\phi_2 = \omega_2 L_2 I_2 + \omega_2 M I_1 \sin(\theta + \phi_1) \tag{30i}$$

U_2 and φ_2 can finally be solved for. The terms $\cos(\theta+\varphi_1)$ and $\sin(\theta+\varphi_1)$ occurring in these equations we find by substituting $e^{j\varphi_1}$ in eq. (28) and then splitting it into real and imaginary parts. We find:

$$\cos(\theta + \phi_1) = \frac{U_1 \cos\phi_1 - R_1 I_1}{E_p}$$

$$\sin(\theta + \phi_1) = \frac{U_1 \sin\phi_1 - \omega_1 L_1 I_1}{E_p}$$

Dividing eq. (30r) by eq. (30i) yields:

$$\frac{U_2 \sin\phi_2}{U_2 \cos\phi_2} = tg\phi_2 = \frac{\omega_2 L_2 I_2 + \omega_2 M I_1 \sin(0 + \phi_1)}{R_2 I_2 - \omega_2 M I_1 \cos(0 + \phi_1)}$$

after which φ_2 is found from

$$\phi_2 = arctg|tg\phi_2|$$

and U_2 from

$$U_2 = \frac{R_2 I_2 - \omega_2 M I_1 \cos(\theta + \phi_1)}{\cos\phi_2}$$

From the constants needed for the calculations, the network voltage U_1, the network frequency ω_1, and the number of pole pairs p of the generator are known directly. R_1 and R_2 can be measured with a Wheatstone bridge. L_1, L_2, and M are measured for rating the rotor with open stator chain ($I_1 = 0$) and for rating the stator with open rotor chain ($I_2 = 0$). The things mentioned are simple to do from the machine equations. /114

From the formulae, it can be derived that the deviation which exists in the calculations the non-constant nature of L_1, L_2, and M, as is set forth on p. 80 apart, for normal values of cos φ_1.

has no effect on I_1;

causes a deviation in E_p, θ, and I_2, which is percentage-wise surely smaller than the product error in the values used for the coefficients;

causes deviations in U_2 and φ_2 which strongly depend on ω_2 and the load conditions.

It is necessary to be careful with this last deviation. The other calculated values are more reliable for sinusoidal voltages and currents.

Conclusions /115

Although the theory proposed for the Double-feed Synchronous Generator cannot yet be controlled at all points, the experiments carried out still give sufficient grounds for believing in the accuracy of this theory.

We therefore conclude that the system with the DSG and converter (as shown in Fig. 13a on p. 115) is very suitable for generating electrical energy for a public network using a windmill, because the revolutions to the mill can always force the maximum wind power to be used.

Because the generator in this system, irrespective of the mill (generator) revolution, always generates a voltage with constant amplitude and frequency, it can be directly coupled to the network.

As with the normal synchronous generator, control of the idle power ($\cos \varphi_{net}$) to deliver is possible with rating.

A very important advantage is that the properties above are achieved due to a method whereby only a portion of the mechanical power provided, maximum about 15% of the full-load power of the installation, must be effected through the converter. This has economical advantages and will also benefit practical feasibility.

Although this system is also most suited for wind energy, it still cannot be made up. In the first place, for this, further research is necessary on a set-up with system components specially developed for this application, and in the second place, comparable results in other systems are needed.

For supply for the rotor circuit of the DSG, a converter is needed which can be regulated in voltage and frequency.

The requiremnt is set, for this converter, that it be able to induce at the stator a good sinusoidal voltage, via the rotor circuit. This is needed because the network current delivered is otherwise not sinusoidal. It is implied that the converter voltage may contain no harmonics with a low order number. /116
Harmonics with a high order number (such as a wrinkle) provide no problems, because these are self-filtered away through the generator, so that they are not found again in the network.

The required rotor voltage for the DSG is in the first approximation proportional to the rotor frequency.

Therefore, it is usual for the converter to have a coupled

frequency-voltage control which brings the output voltage at a certain frequency to about the right value.

In addition, there must then be available a special voltage control which accurately sets the required rotor voltage for a specific cos φ_{net}.

If we consider the generator construction-wise as an asynchronous slip-ring armature machine, the greatest difference necessary in the construction is a much greater air-slit width. This must be comparable to the air-slit width of a synchronous generator of the same power. This is necessary because otherwise the load angle of the generator is much greater than is usual for a synchronous generator, for which the dange of falling out of phase is greater[1].

This greater air-slit width also benefits the controllability of cos φ_{net}.

The number of rotor windings can be freely chosen, in principle.

Within the limits of what is technically achievable, it must be so chosen that it comes to an optimum development, aside from all the losses associated with it (in DSG and converter).

To continue this research, the necessary things are: a generator which satisfies the set requirements, a therewith suitable converter, and a good simulator for the windmill.

Only then is it possible to control the maximum power point and cos φ_{net}, because these naturally are most clearly associated with the characteristics of the generator and converter used.

The results attained at present decidedly justify a continuation of this research.

---

[1] See Supplement.

REFERENCES

1. Golding, E.W., The Generator of Electricity by Wind Power, E&F.N. Spon Ltd., London, 1955. /117

2. Schwarz, F. C., "Power electronics, I," lecture.

3. Schwarz, F. C., "Power electronics, II," lecture.

4. El-Magrabi, M. G., Allgemeine Theorie der Doppelt Gespeisten Synchronmaschine [General Theory of the Double-Feed Synchronous Machine], Verslag Leemann, Zürich, 1950.

5. Taegen, F. G., Inleiding tot de Theorie van de Elektrische Machines [Introduction to the Theory of Electrical Machines], Pt. 2.a., Technische Hogeschool, Delft, 1969.

6. Wiersma, J. A., Een Driefasen Gelijkspanning-Wisselspanning Omzetter met in Grootte en Frequentie Regelbare Uitgangsspanning [A Three-Phase Direct/Alternating Voltage Converter with Output Voltage Adjustable in Size and Frequency], Dissertation, Technische Hogeschool, Delft, 1972.

List of Symbols Regularly Referred to /118

NB: For more extensive definitions, refer to the pertinent page in the report.

A	surface of the plane swept by the vanes	m^2
C_p	power coefficient, p. 4	-
C_{po}	maximum value of C_p for a given mill	-
D	diameter of the vane circle; $A = \pi(D/2)^2$	m
$-\underline{E}_p$	index which represents the pole wheel voltage; $\lvert -\underline{E}_p \rvert = E_p = \omega_1 M I_2$	V
$\underline{E}_r$	induced rotor voltage, p. 41	V
$\underline{E}_s$	induced stator voltage, p. 41	V
f_1	frequency at the stator	Hz
f_2	frequency at the rotor	Hz
$\underline{I}_r$ (I_2)	index of the rotor current	A
$\underline{I}_s$ (I_1)	index of the stator current	A
$\underline{I}_1$	index of the stator current	A
L_{11}	self-induction coefficient of a stator phase	H
L_{22}	self-induction coefficient of a rotor phase	H
L_1	$L_1 = L_{11} - M_{11}$	H
L_2	$L_2 = L_{22} - M_{22}$	H
L_{1h} / L_{1s}	L_1 splits into the main inductivity L_{1h} and the distributed inductivity L_{1s}	H / H
L_{2h} / L_{2s}	L_2 splits into main inductivity L_{2h} and distributed inductivity L_{2s}	H / H
M_{11}	coefficient of mutual induction between two stator phases	H
M_{12} / M_{21}	$M_{12} = M_{21}$; coefficient of mutual induction between a stator phase and a rotor phase	H / H

/119

M_{22}	coefficient of mutual induction between two rotor phases	H
M	$M = 3/2\ (M_{12}) = 3/2\ (M_{21})$	H
n_m	vane-shaft revolutions	rpm
n_r	generator revolutions	rpm
n_1	revolutions of stator rotary-current field relative to the stator	rpm
n_2	revolutions of the rotor rotary-current field relative to the rotor	rpm
p	number of pole pairs in the generator	-
P_a	shaft power provided to the generator	W
P_{Cu1}	copper loss in the stator	W
P_{Cu2}	copper loss in the rotor	W
P_{Fe1}	iron loss in the stator	W
P_{Fe2}	iron loss in the rotor	W
P_{mech}	mechanical power of the generator, according to $P_{mech} = \omega_r T_{el}$	W
P_W	power provided by the wind, p. 1	W
P_1	electrical power at the stator	W
P_2	electrical power at the rotor	W
R_1	ohmic resistance of a stator phase	ohm
R_2	ohmic resistance of a rotor phase	ohm
T_a	shaft couple provided to the generator	Nm
T_{el}	electromagnetic couple of the generator	Nm
$\underline{U}_r$ (U_2)	index of rotor voltage;	V
$\underline{U}_s$ (U_1)	index of stator voltage;	V
U_1	index of stator voltage $\underline{U}_1 = U_1$ voltage drops in the generator, p.	V

/120

v_w	wind velocity	m/sec
v_k, v_{max} v_{min}	p. 6	m/sec
w_1	number of windings for a stator phase	-
w_2	number of windings for a rotor phase	-
δ	position angle of the rotor; p. 21	rad
δ_0	δ at time t = 0	rad
η_m	mechanical output of the mill + transmission to the generator shaft	-
θ	load angle; angle; between $\underline{U}_1$ and $-\underline{E}_p$	deg
μ	acceleratability, p. 4	-
μ_0	value of μ at which $C_p = C_{po}$	-
ν	$\nu = \frac{w_2}{w_1} \frac{\omega_2}{\omega_1}$	-
φ_1	phase angle between stator voltage and current	deg
φ_2	phase angle between rotor voltage and current	deg
ω_m	angular velocity of the vane shaft	rad/sec
ω_r	angular velocity of the generator shaft	rad/sec
ω_1	angular velocity of the stator rotary-current field relative to the stator	rad/sec
ω_2	angular velocity of the rotor rotary-current field relative to the rotor	rad/sec

Beaufort Scale

/121

Wind Power	Wind Velocity Between "-" m/sec	Averaged in m/sec	Wind Velocity in km/h
0	0 - 0.5	0.28	1
1	0.6 - 1.7	1.11	4
2	1.8 - 3.3	2.50	9
3	3.4 - 5.2	4.45	16
4	5.3 - 7.4	6.4	23
5	7.5 - 9.8	8.6	31
6	9.9 - 12.4	11.1	40
7	12.5 - 15.2	13.9	50
8	15.3 - 18.2	16.6	60
9	18.3 - 21.5	20.0	72
10	21.6 - 25.1	23.3	84
11	25.2 - 29.0	27.2	98
12	29.0 m/s	104 km/h.	

Supplement

On p. 69 and in the conclusion, it is mentioned that the load angle θ will be large in using an asynchronous slip-ring armature motor as a double-feed synchronous generator, so that the danger of falling out of phase is greater (and the overload capacity is consequently smaller) than for a comparable normal synchronous generator.

This assertion, and the conclusion that this can be remedied by increasing the air-slit width, holds true without more, when the machine is oversaturated.

Because somewhat severe saturation always occurs in a machine, the effect of the air-slit width actually is small, however.

There are reasons for considering that the overload capacity of a DSG with an air-slit width as that for a usual ASM is still comparable to that of a normal synchronous generator.

/2

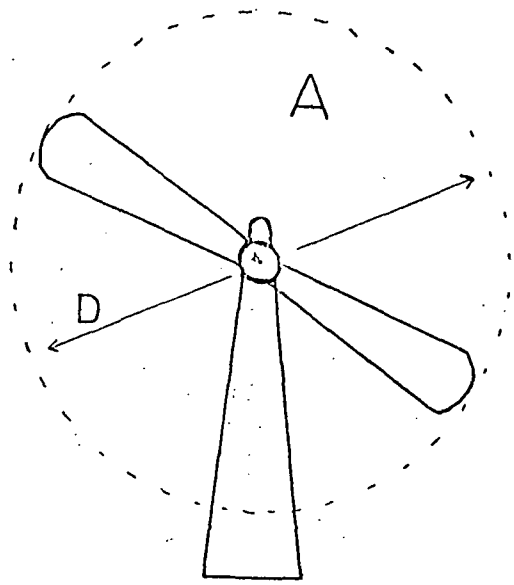

A wiekencirkel |m²|

D diameter |m|

Fig. 1
Key: 1. A vane circle |m²|

/3

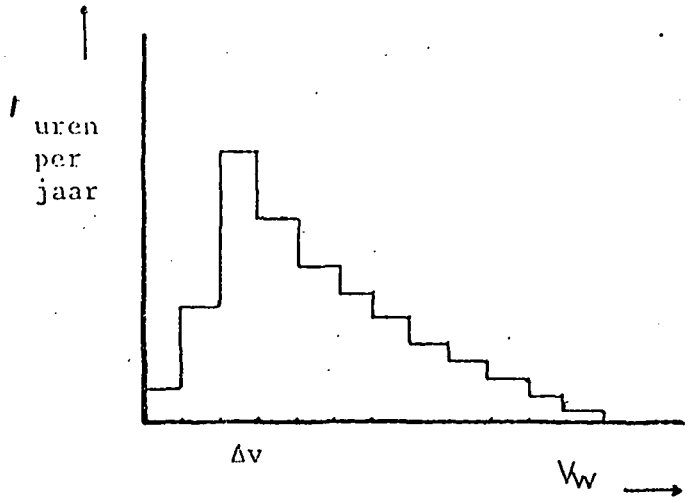

Fig. 2
Key: 1. Hours per year

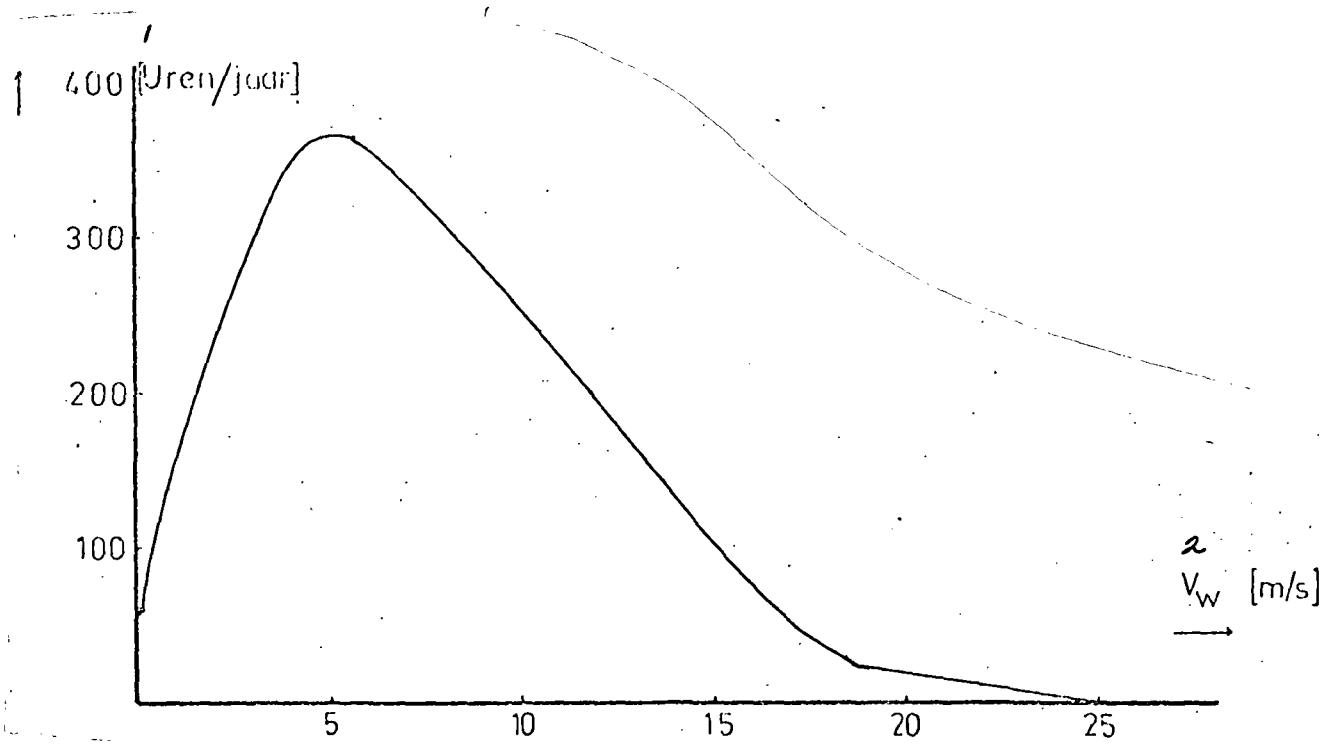

Fig. 3a

Key: 1. Hours/year
2. V_W [m/sec]

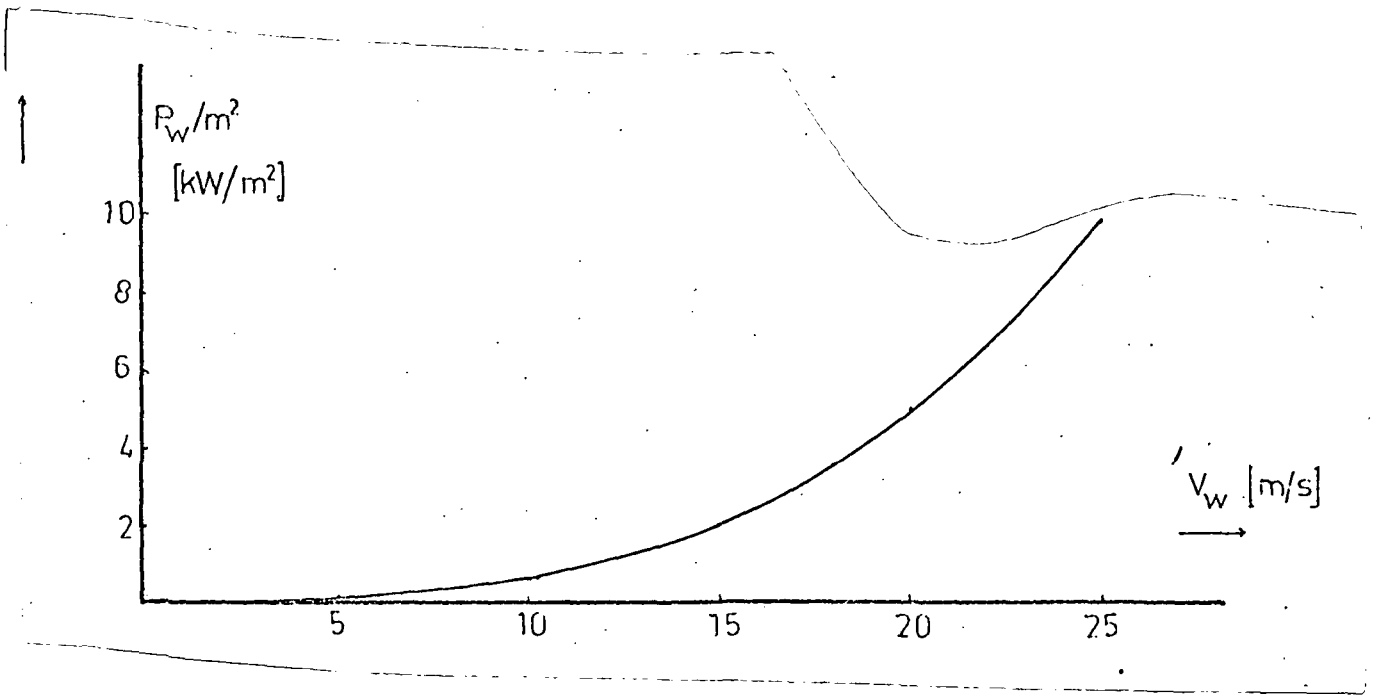

Fig. 3b

Key: 1. V_w [m/sec]

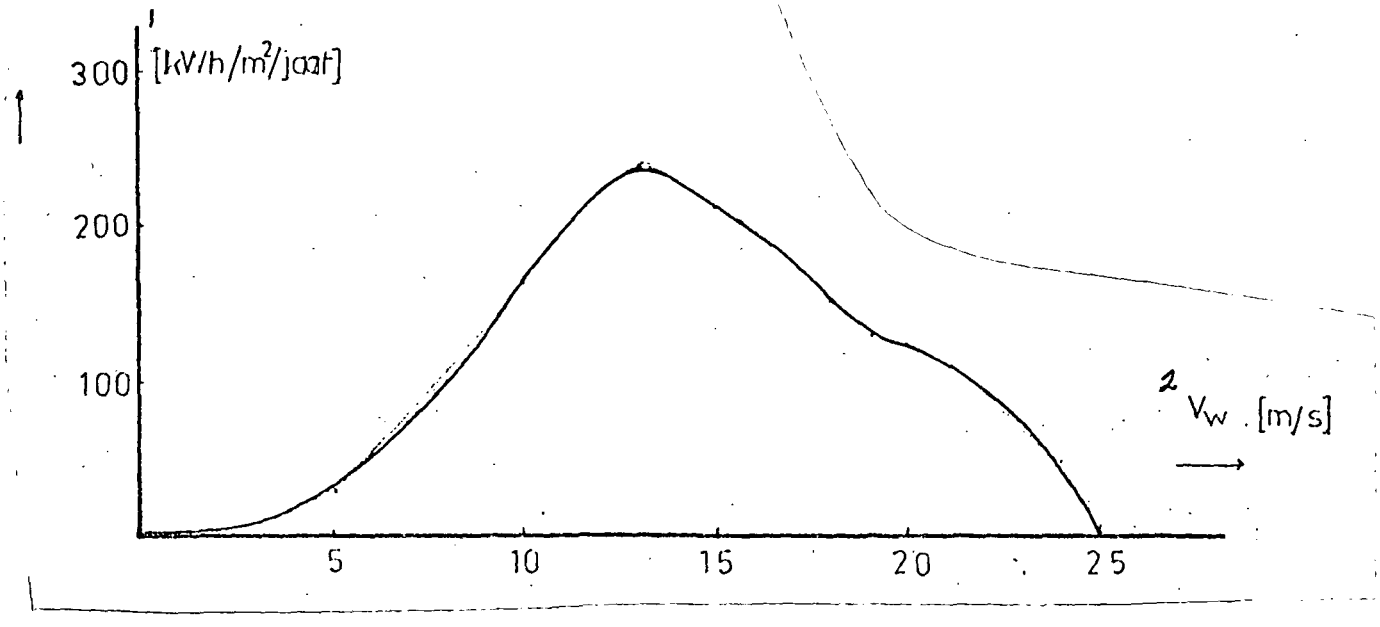

Fig. 3c

Key: 1. [kWh/m^2/year]
2. V_w [m/sec]

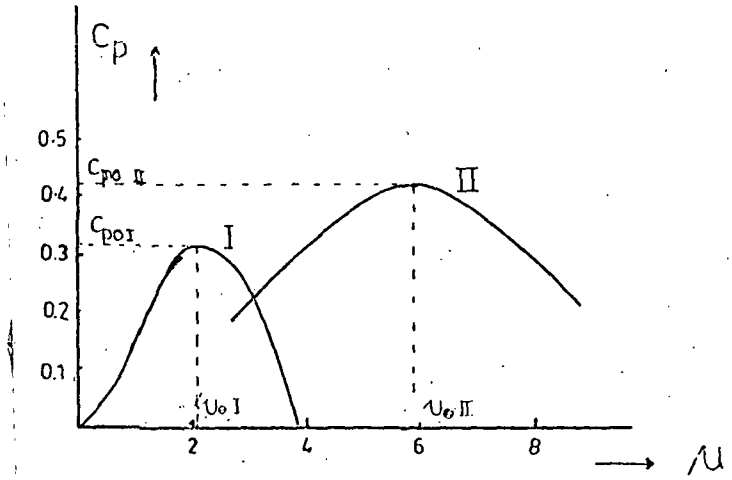

1 I. Hollandse molen

$\mu_o \approx 2$, $C_{po} \approx 0,32$

(langzaam loper)

2 II. Propellor type

$\mu_o \approx 6$, $C_{po} \approx 0,42$

(snel loper)

Fig. 4. Taken from ref. [1]
Key: 1. I. Holland mill
$\mu_o \simeq 2$, $C_{po} \simeq 0.32$
(slow runner)
2. II. Propellor type
$\mu_o \simeq 6$, $C_{po} \simeq 0.42$
(fast runner)

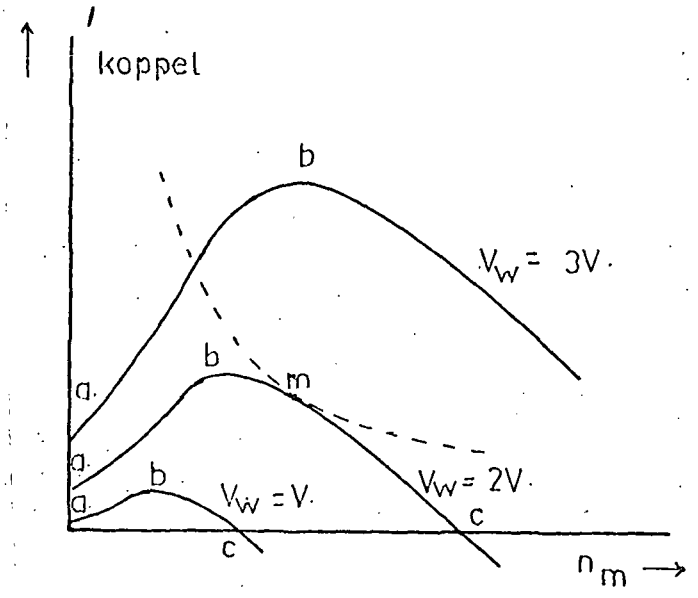

2 Enkele koppel-toerenkrommen van een windmolen. De hyperbool geeft de lijn met "koppel x n_m = konstant"

Fig. 5

Key: 1. Couple
2. Individual couple-drive curves for a windmill. The hyperbola gives the line for "couple X n_m = a constant".

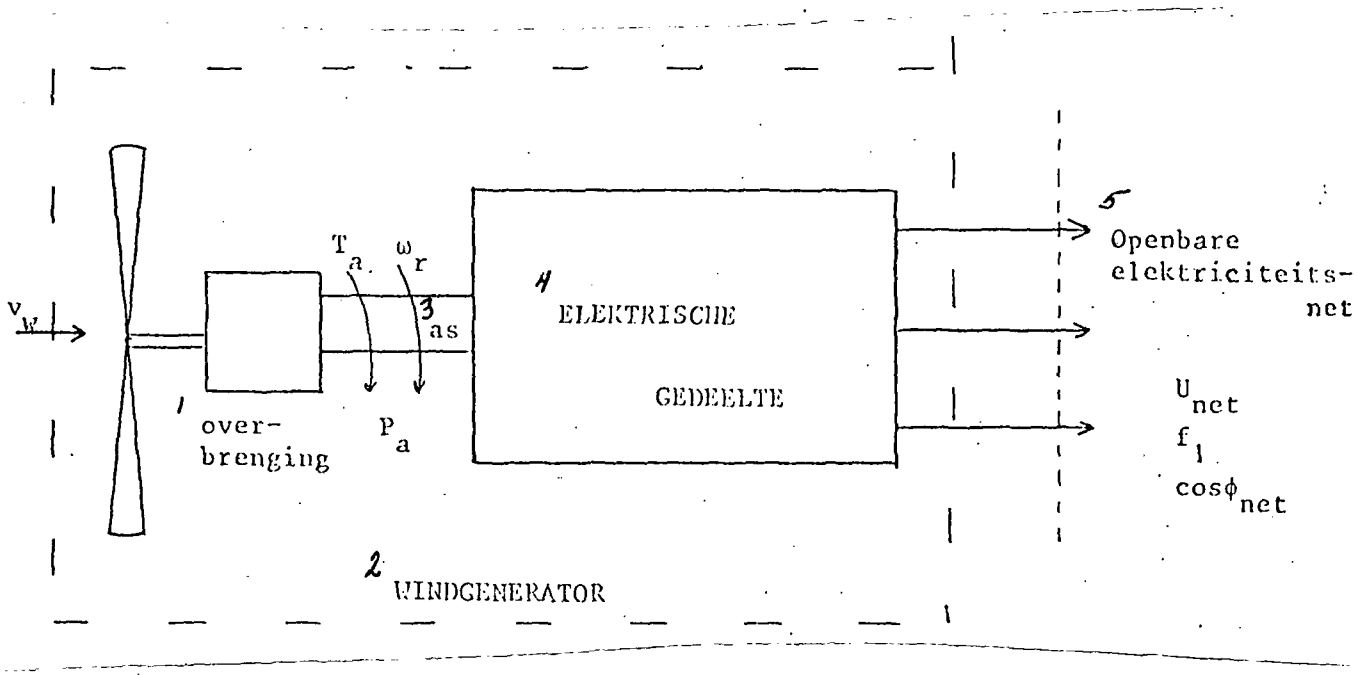

Fig. 6

Key:
1. Transmission
2. WIND GENERATOR
3. Shaft
4. ELECTRICAL PART
5. Public electricity network

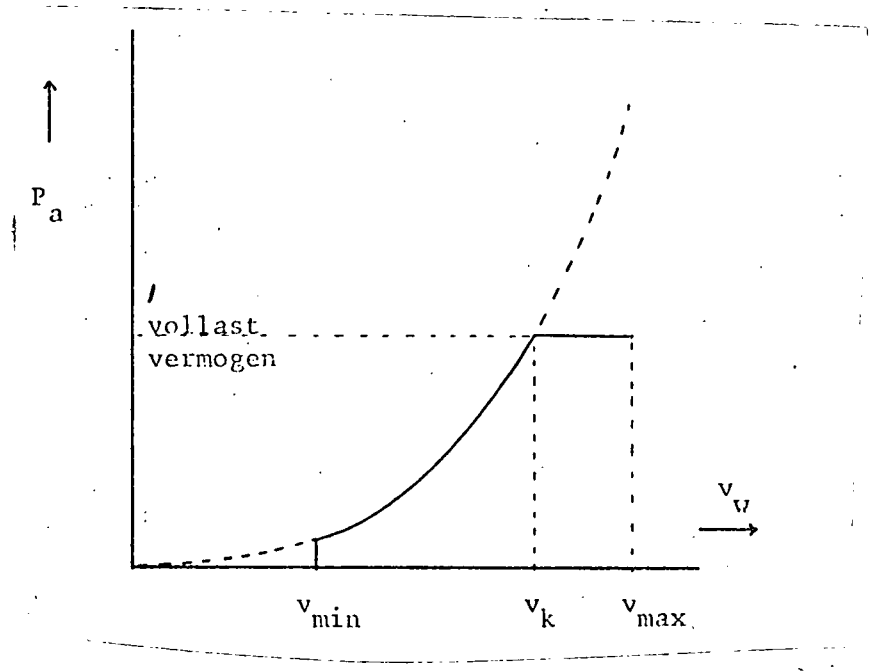

Fig. 7
Key: 1. Full power

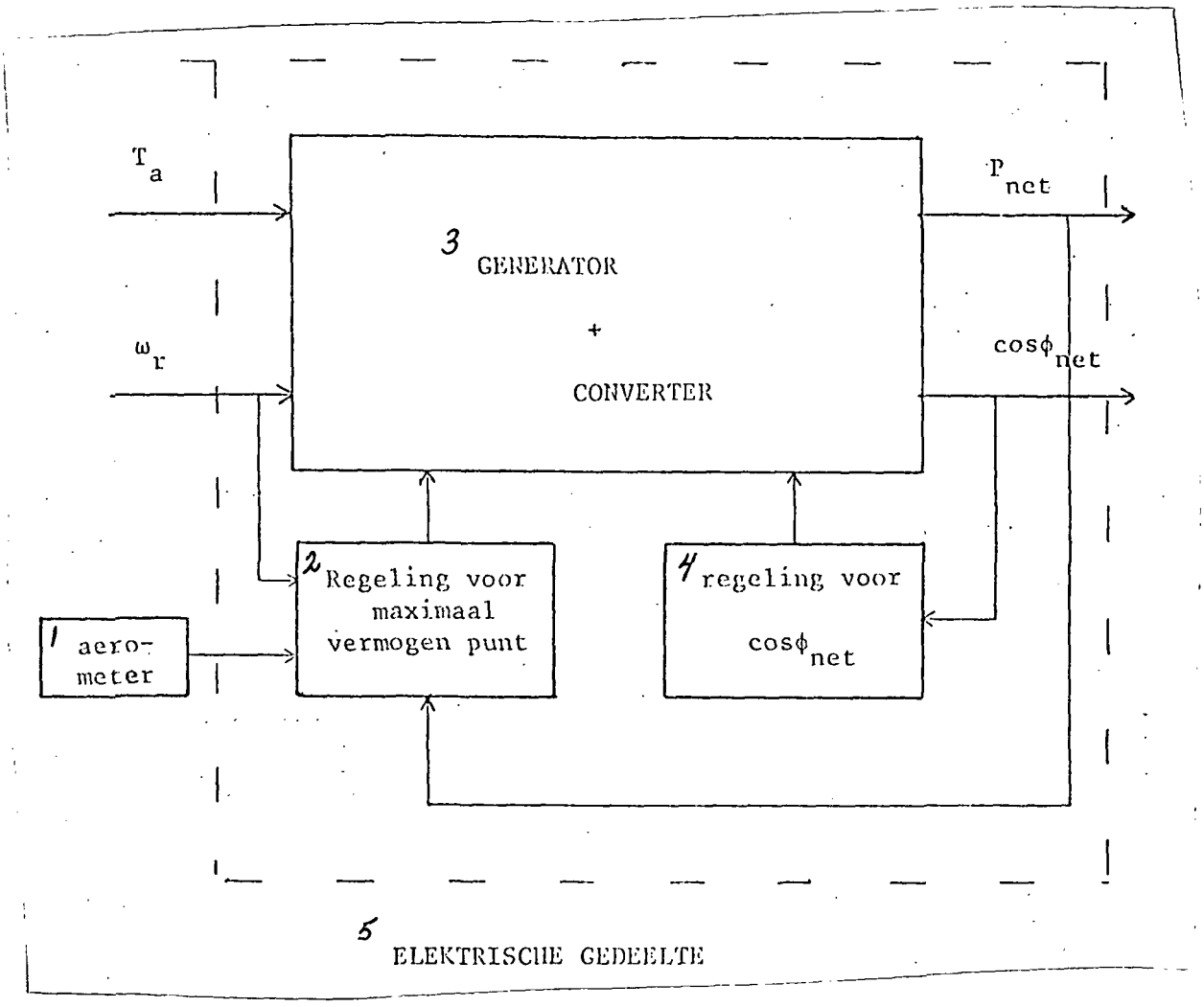

/13

Fig. 6a

Key:
1. Aerometer
2. Adjustment for maximum power point
3. GENERATOR + CONVERTER
4. Adjustment for cos φ_{net}
5. ELECTRICAL PART

/14

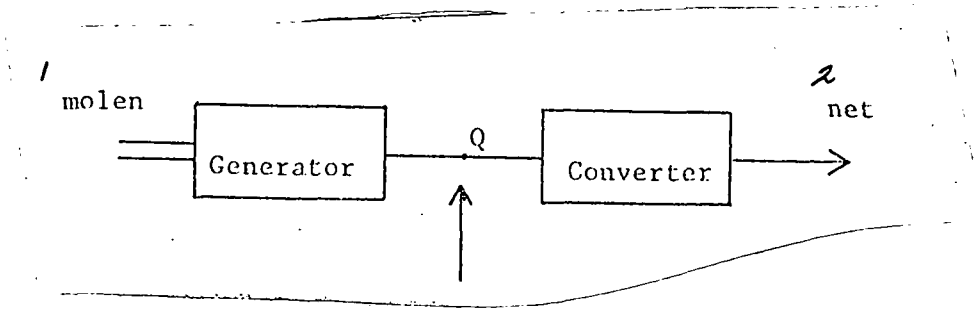

Fig. 8
Key: 1. Mill
2. Network

/15

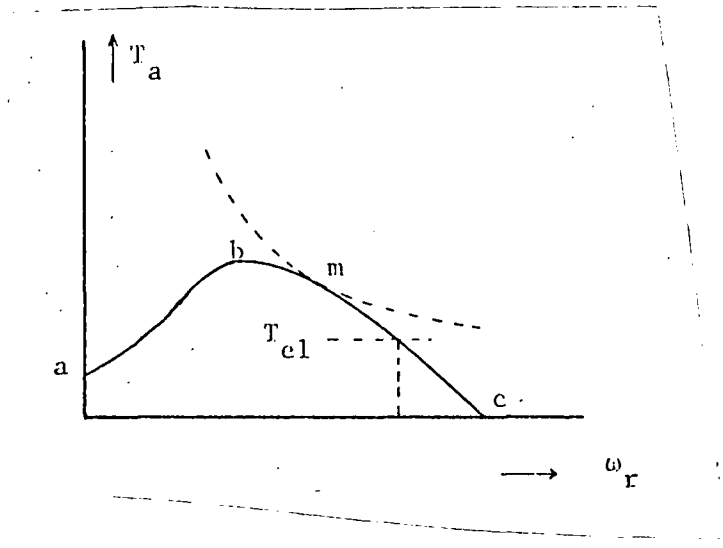

Fig. 5a. Couple-drive curve for a windmill, taken from Fig. 5. m is the maximum power point.

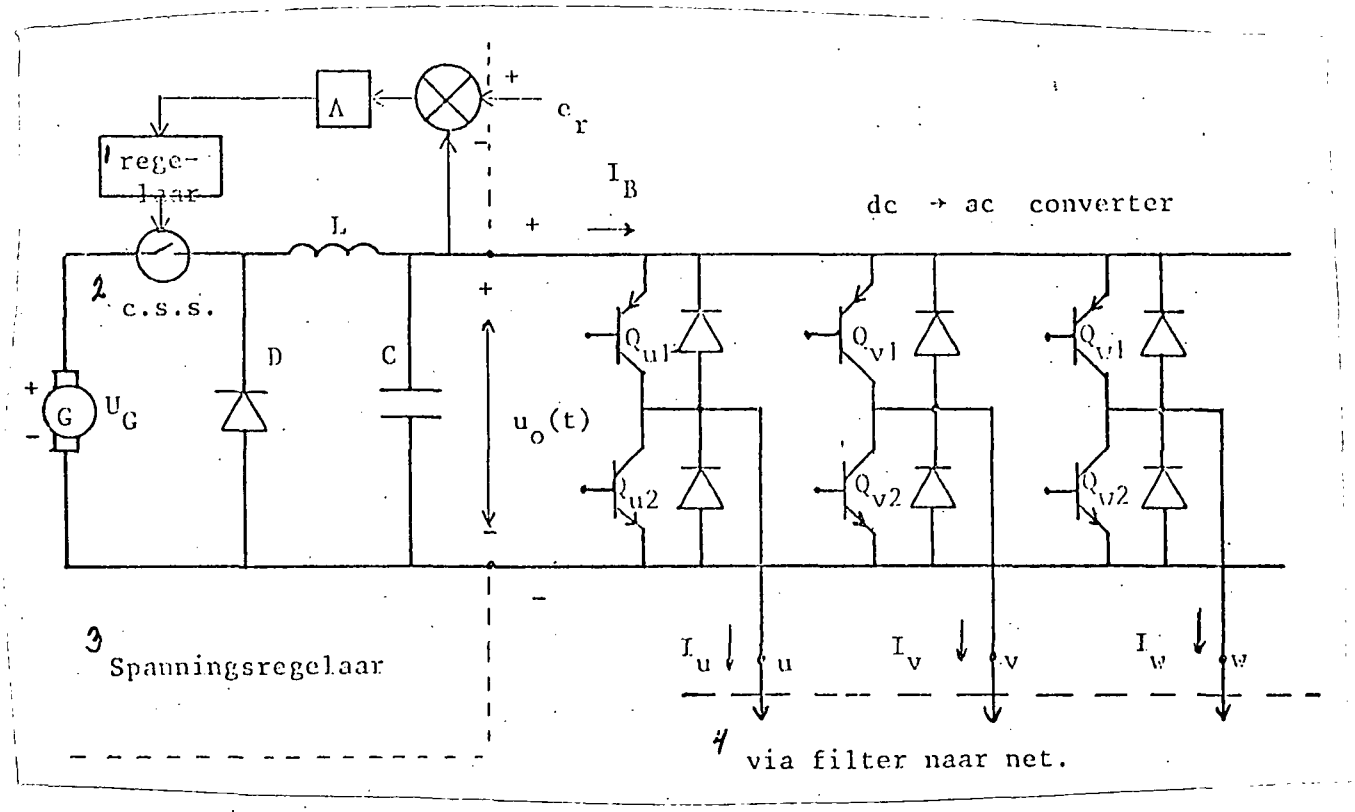

Fig. 9, free according to ref. [3].

U_G - terminal voltage of the direct current generator

$u_o(t)$ - direct current delivered to the 3-phase converter as a function of t

U_o - average value of $u_o(t)$; see Fig. 10.

I_B - current taken up by the 3-phase converter

Key:
1. Regulator
2. CSS
3. Voltage regulator
4. Via filter to network

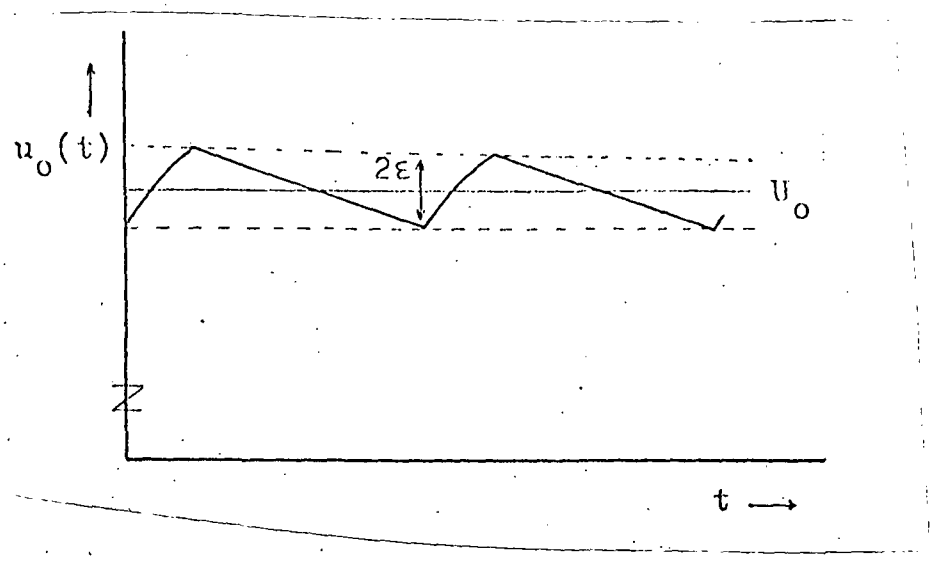

Fig. 10. U_G determined on the rising side, I_B the falling side. When the wrinkle (2ε top-top) is sufficiently small relative to U_o, I_B will not be affected.

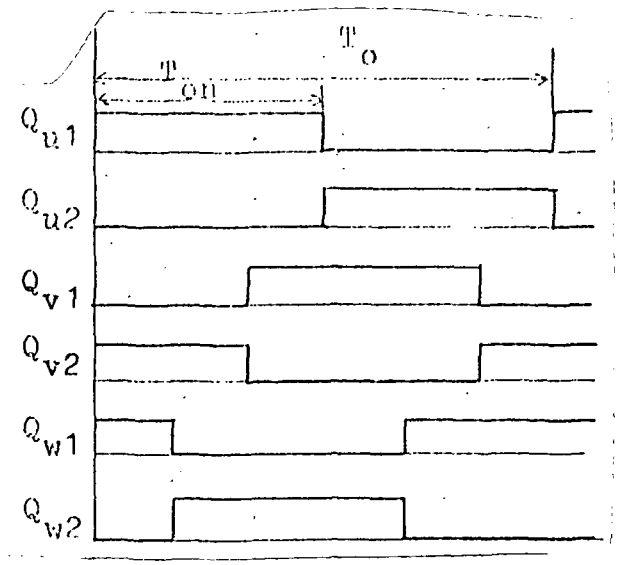

a)

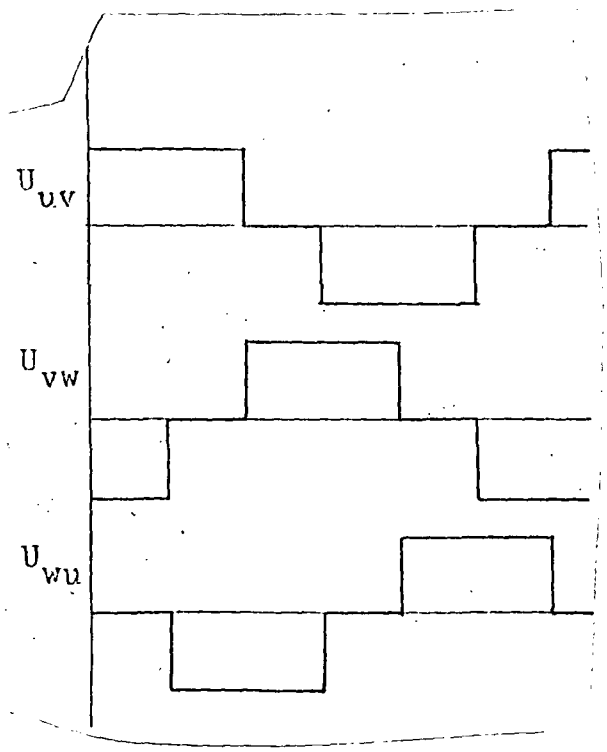

b)

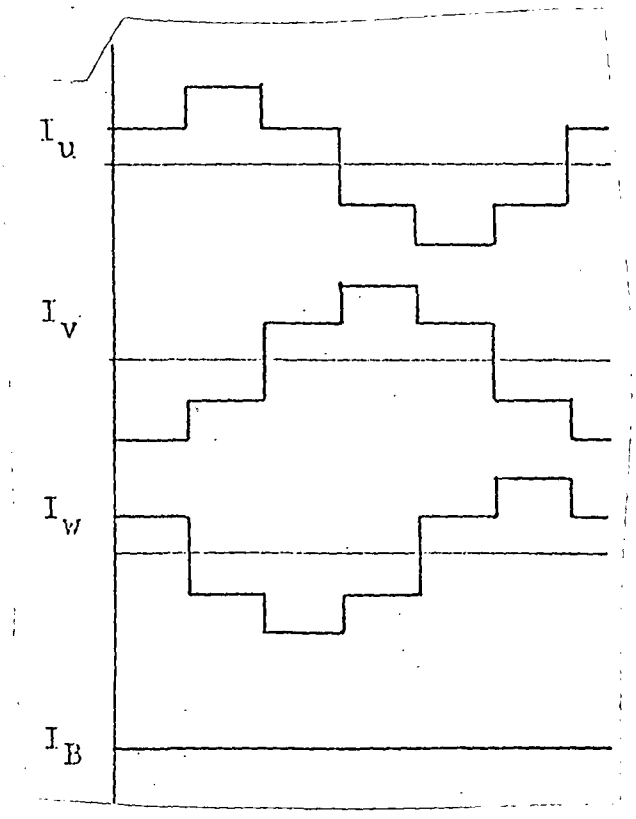

c)

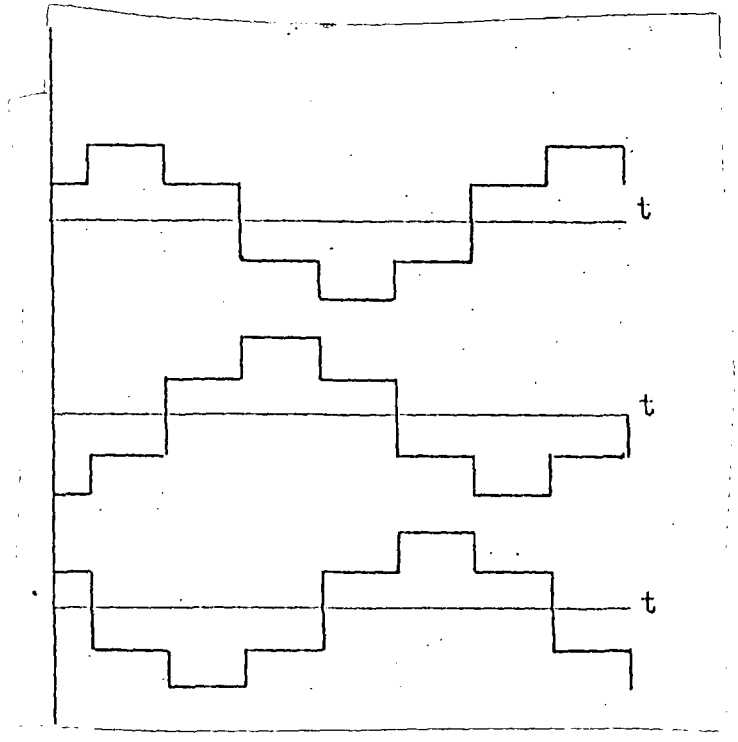

d)

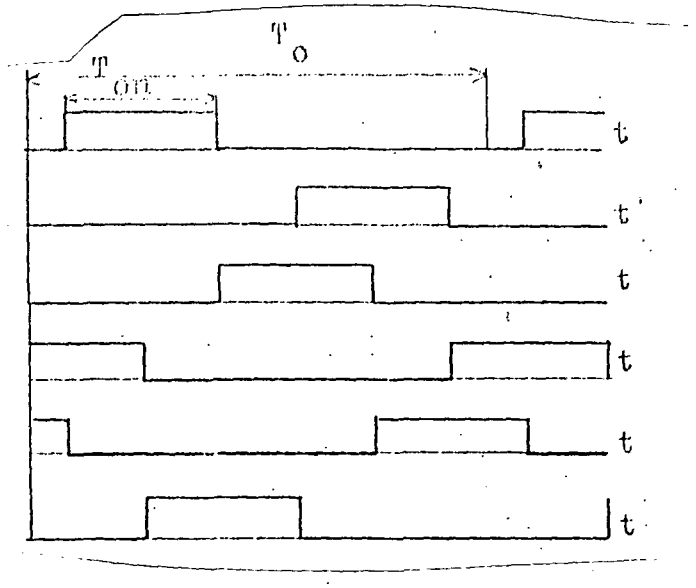

e)

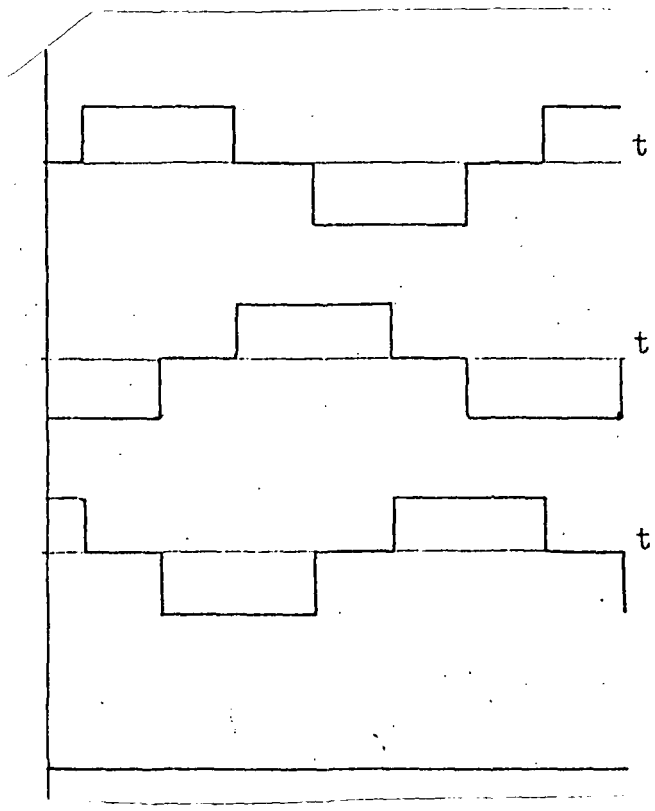

f)

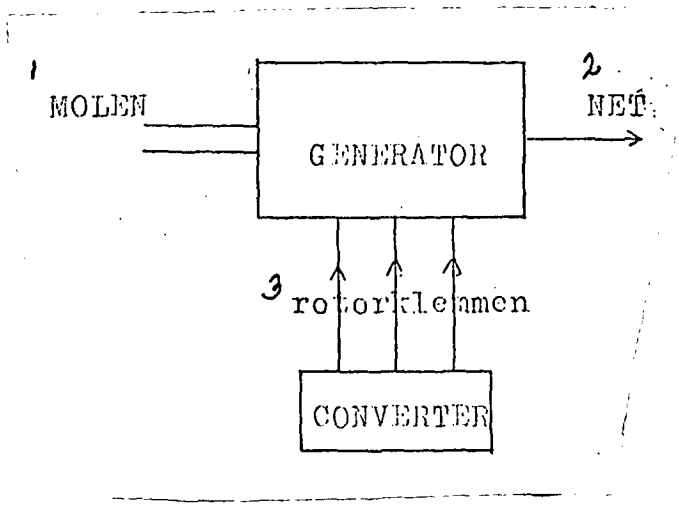

Fig. 12
Key: 1. MILL
2. NETWORK
3. Rotor terminals

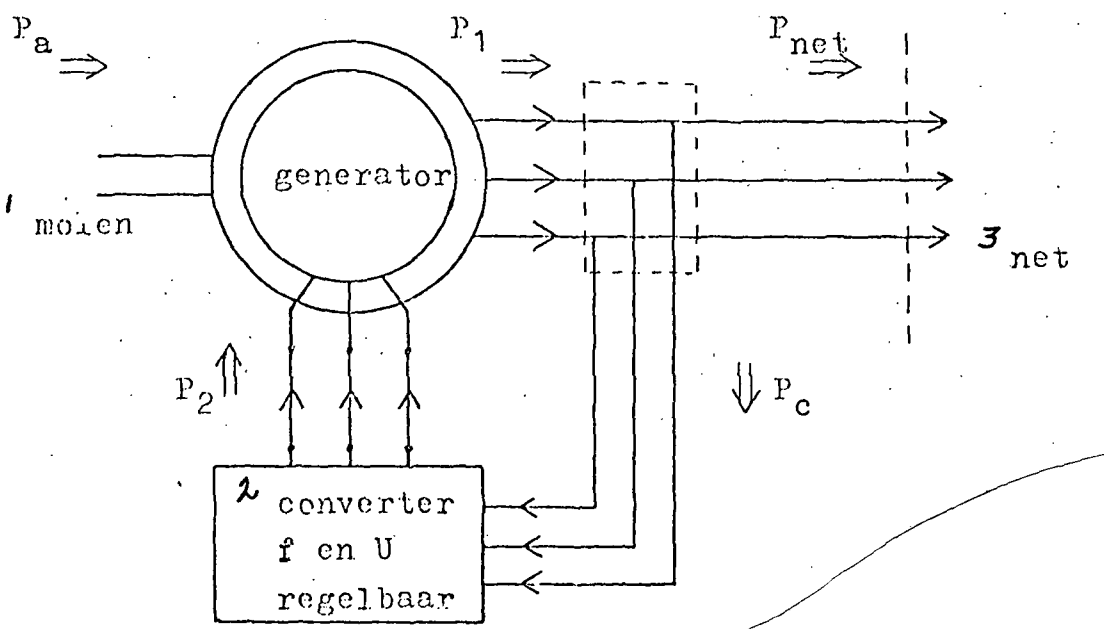

Fig. 13

Key:
1. Mill
2. Converter, f and U adjustable
   - P_a - via the axle-supplied mechanical power
   - P_2 - electrical power supplied to the rotor
   - P_1 - electrical power delivered to the stator
   - P_c - electrical power taken up by the converter
   - P_{net} - power delivered to the network
3. Network

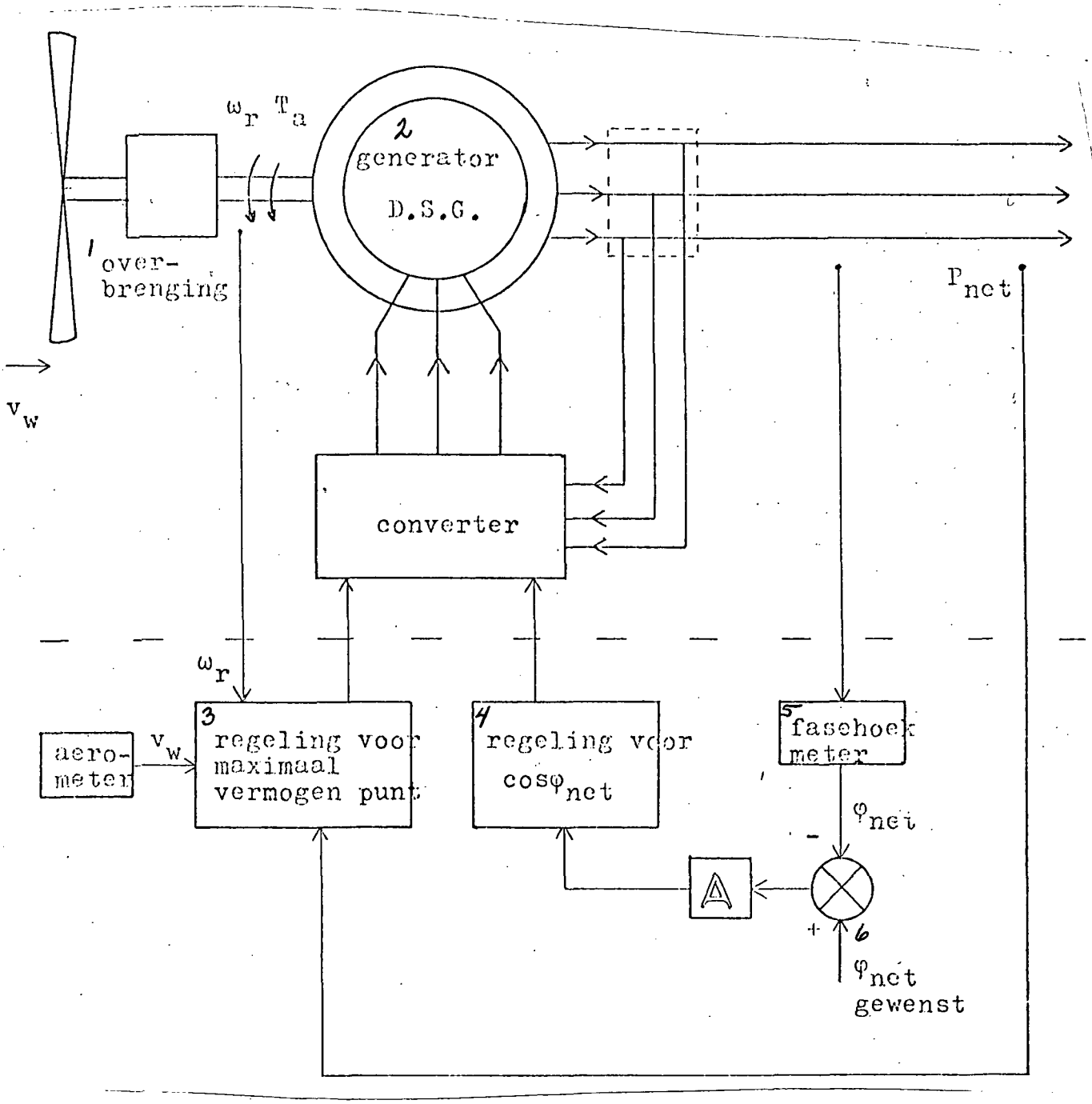
ω_r T_a
2
generator
D.S.G.
1
over-
brenging
P_{net}
v_w
converter
ω_r
3
regeling voor
maximaal
vermogen punt
4
regeling voor
$\cos\varphi_{net}$
5
fasehoek
meter
aero-
meter
v_w
φ_{net}
-
+
6
φ_{net}
gewenst

Fig. 13a

Key: 1. Transmission
2. DSG generator
3. Regulation for maximum power point
4. Regulation for cos φ_{net}
5. Phase angle meter
6. φ_{net} known

/27

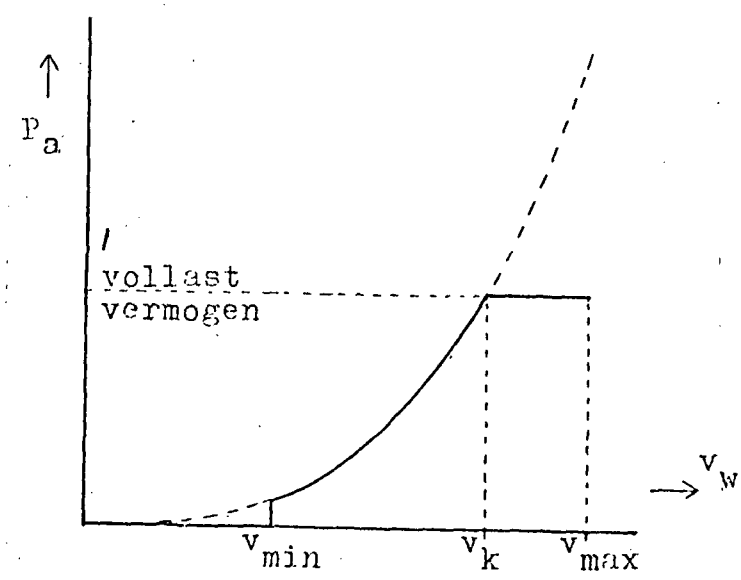

Fig. 7
Key: 1. Full power

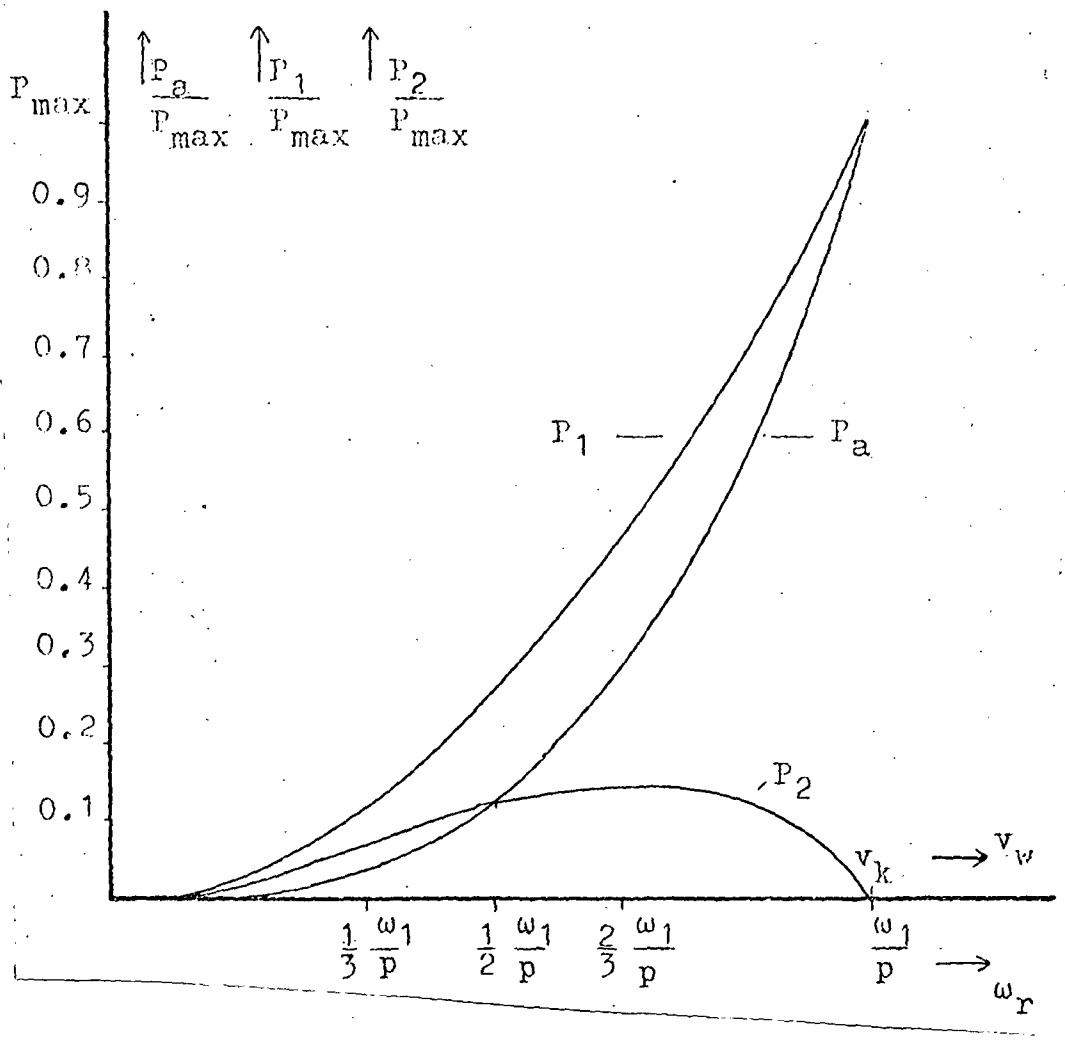
P_{max}
$\frac{P_a}{P_{max}}$
$\frac{P_1}{P_{max}}$
$\frac{P_2}{P_{max}}$
0.9
0.8
0.7
0.6
0.5
0.4
0.3
0.2
0.1
P_1
P_a
P_2
v_k
v_w
$\frac{1}{3}\frac{\omega_1}{p}$
$\frac{1}{2}\frac{\omega_1}{p}$
$\frac{2}{3}\frac{\omega_1}{p}$
$\frac{\omega_1}{p}$
ω_r

Fig. 14

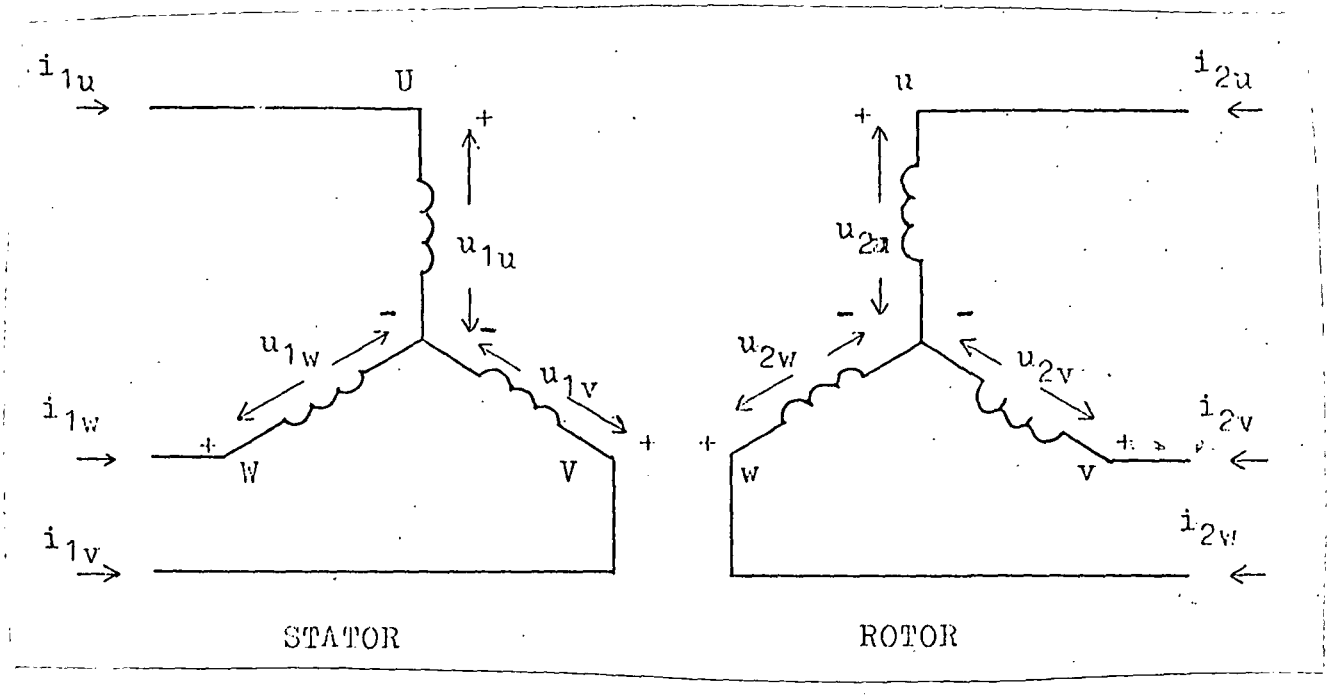
i1u
U
+
u1u
-
u1w
-
u1v
i1w
+
W
V
+
i1v
STATOR
u
i2u
+
u2u
-
-
u2w
u2v
i2v
+
w
v
i2w
ROTOR

Fig. 15

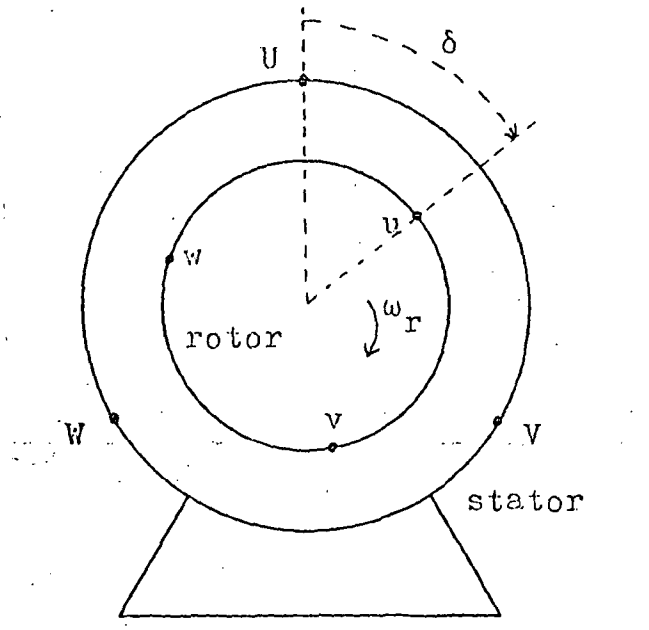

p = 1

Fig. 16

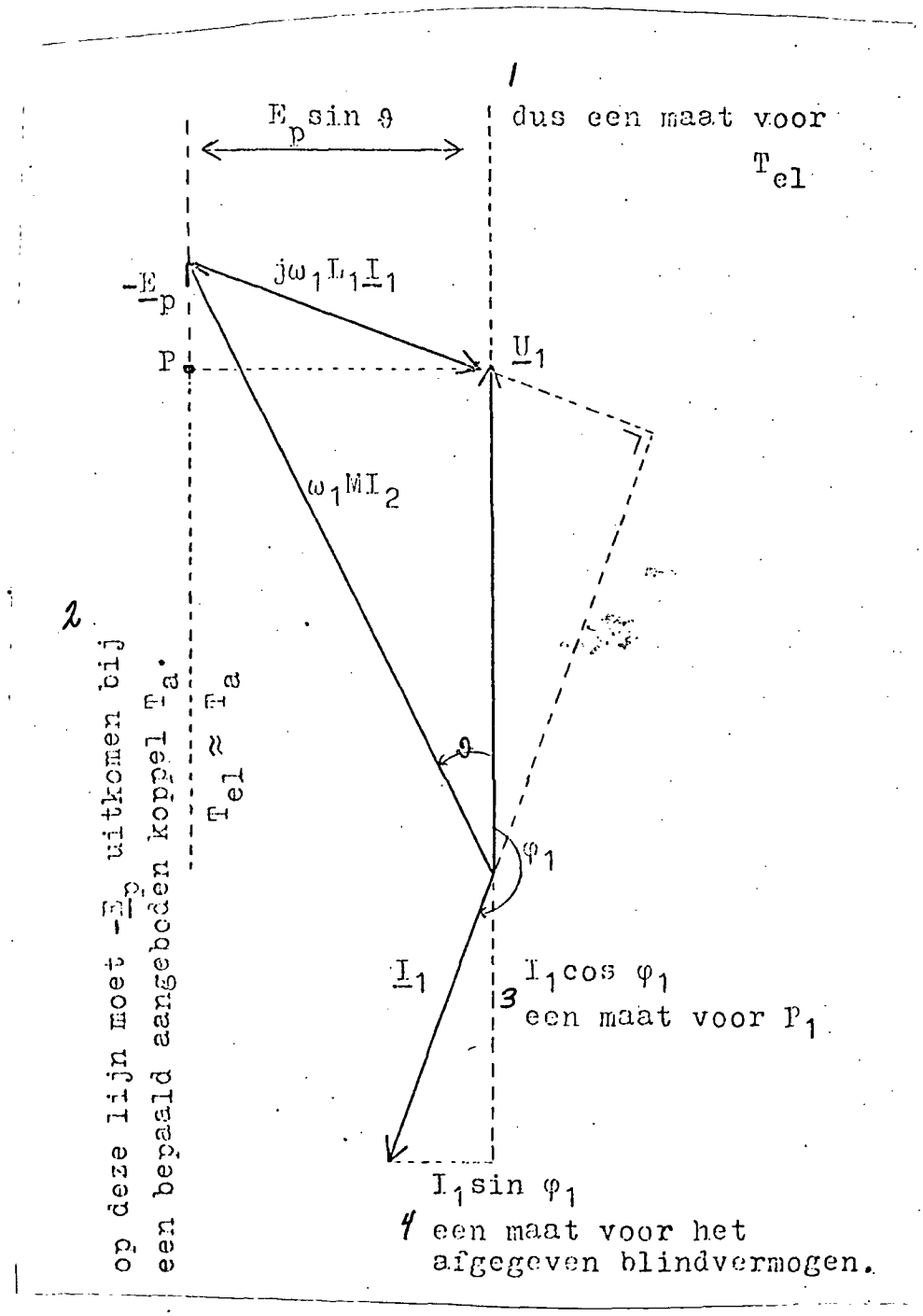
1
$E_p \sin \vartheta$
dus een maat voor
T_{el}
$-\underline{E}_p$
$j\omega_1 L_1 \underline{I}_1$
P
$\underline{U}_1$
$\omega_1 M I_2$
2
op deze lijn moet $-\underline{E}_p$ uitkomen bij
een bepaald aangeboden koppel T_a.
$T_{el} \approx T_a$
ϑ
φ_1
$\underline{I}_1$
$I_1 \cos \varphi_1$
3 een maat voor P_1
$I_1 \sin \varphi_1$
4 een maat voor het
afgegeven blindvermogen.

Fig. 17

Key: 1. Thus a measure for T_{el}
2. $-\underline{E}_p$ must come out on this line for a specific couple produced, T_a
3. a measure for P_1
4. a measure for the given idle power

/48

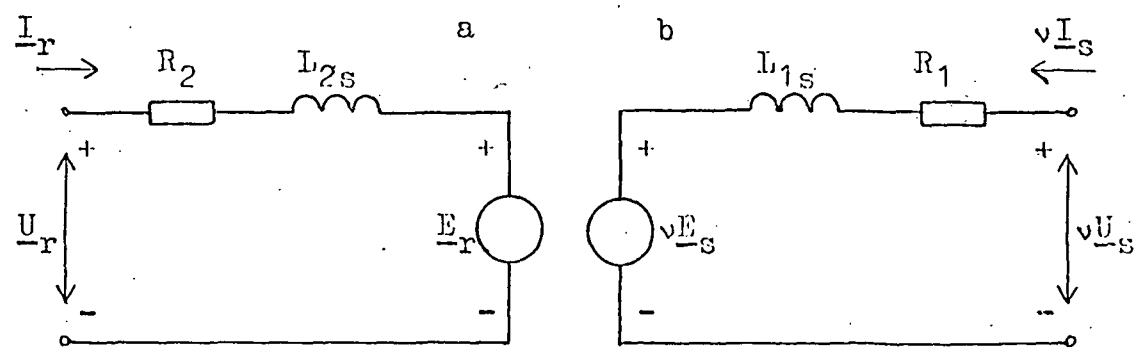

$$\underline{U}_r = R_2\underline{I}_r + j\omega_2 L_{2s}\underline{I}_r + \underline{E}_r \qquad \nu\underline{U}_s = \nu\underline{I}_s(R_1 + j\omega_1 L_{1s}) + \nu\underline{E}_s$$

Fig. 18

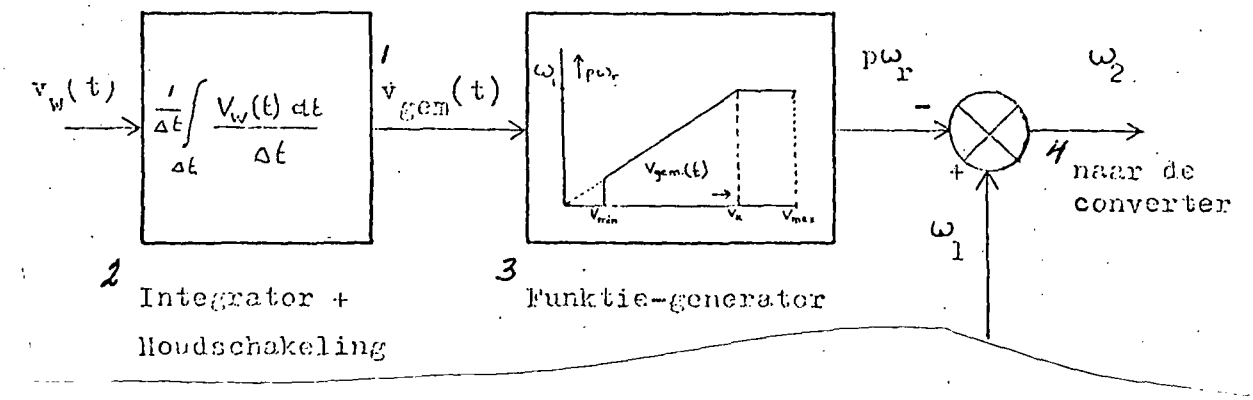

Fig. 19

Key:
1. V_{meas} (t)
2. Integrator + lead connection
3. Function generator
4. To the converter

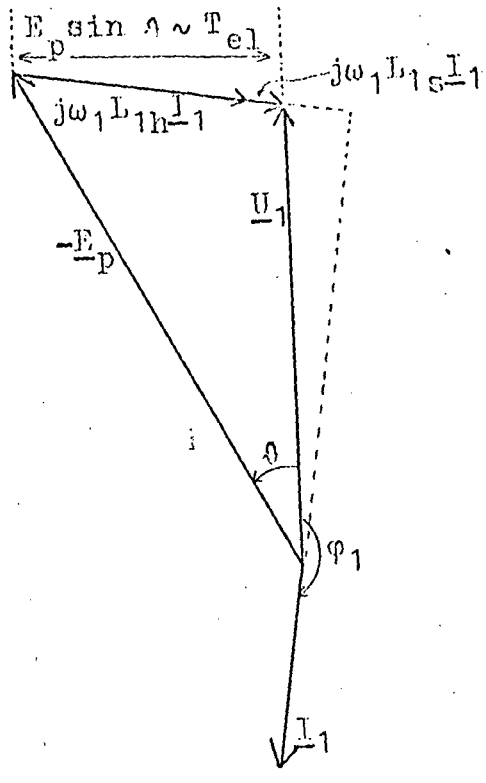
$E_p \sin \vartheta \sim T_{el}$
$j\omega_1 L_{1s} \underline{I}_1$
$j\omega_1 L_{1h} \underline{I}_1$
$\underline{U}_1$
$-\underline{E}_p$
ϑ
φ_1
$\underline{I}_1$

Fig. 20

/61

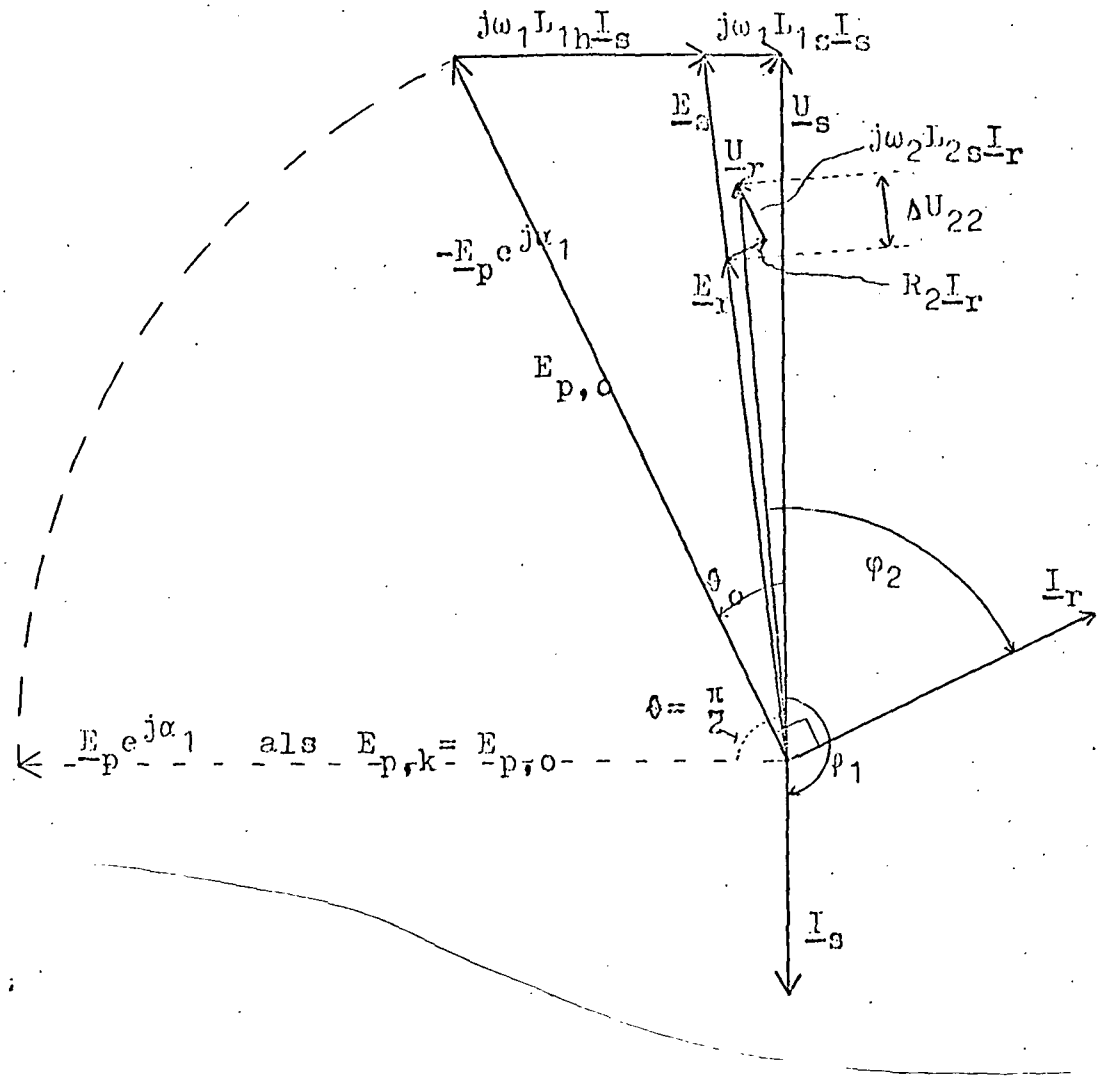
$j\omega_1 L_{1h} \underline{I}_s$
$j\omega_1 L_{1s} \underline{I}_s$
$\underline{E}_s$
$\underline{U}_s$
$\underline{U}_r$
$j\omega_2 L_{2s} \underline{I}_r$
ΔU_{22}
$-\underline{E}_p e^{j\alpha_1}$
$\underline{E}_r$
$R_2 \underline{I}_r$
$E_{p,o}$
ϑ_o
φ_2
$\underline{I}_r$
$\vartheta = \frac{\pi}{2}$
$-\underline{E}_p e^{j\alpha_1}$ als $E_{p,k} = E_{p,o}$
φ_1
$\underline{I}_s$

Fig. 21

/62

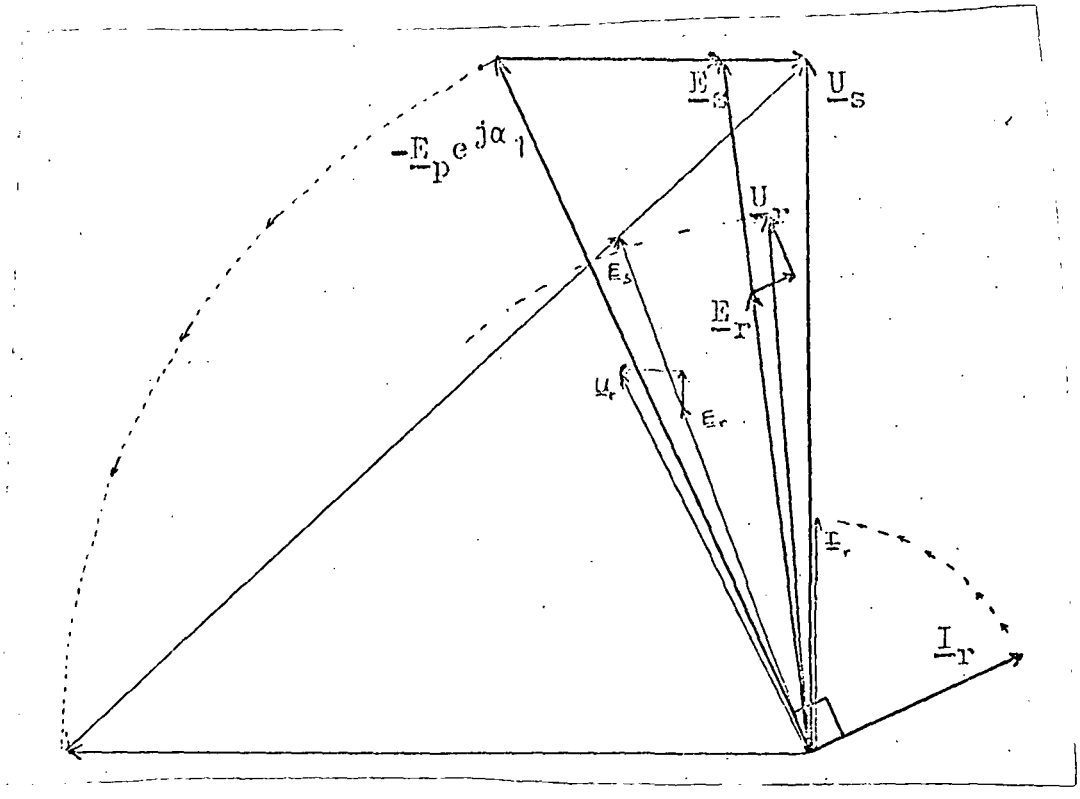
$-\underline{E}_p e^{j\alpha_1}$
$\underline{E}_s$
$\underline{U}_s$
$\underline{U}_r$
$\underline{E}_s$
$\underline{E}_r$
$\underline{U}_r$
$\underline{E}_r$
$\underline{I}_r$
$\underline{I}_r$

Fig. 22

/65

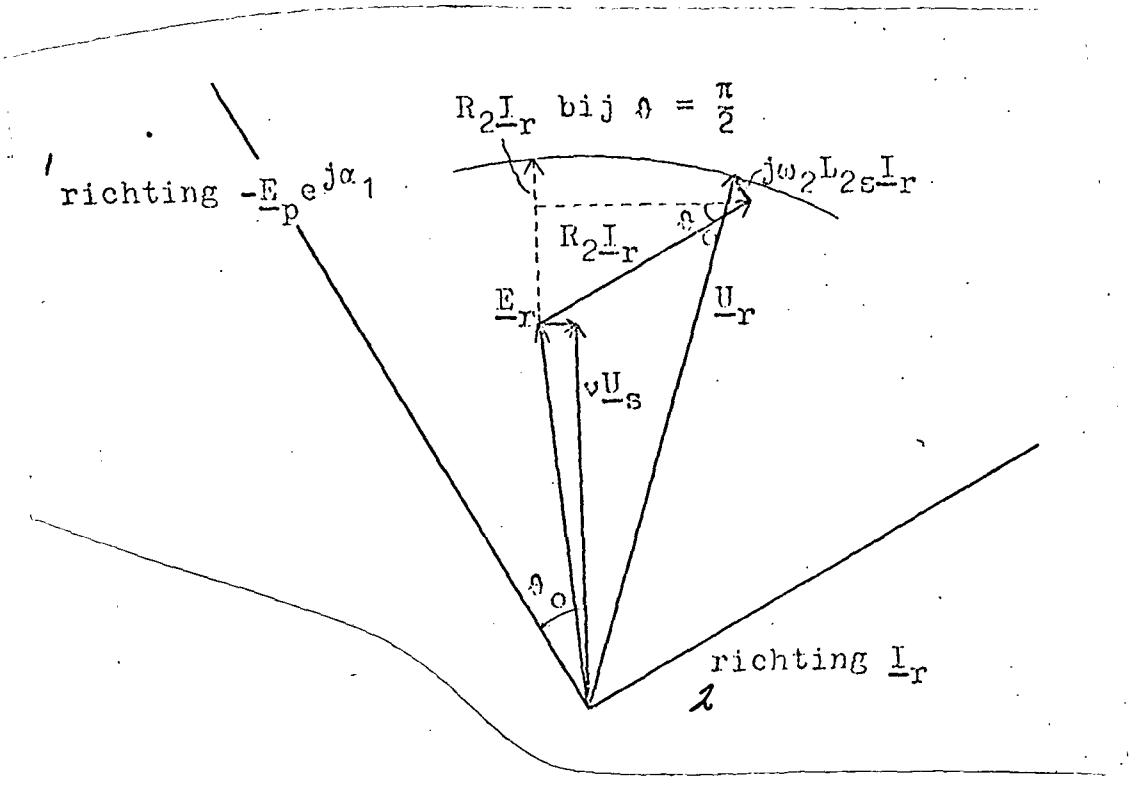

Fig. 23

Key: 1. Direction of $-\underline{E}_p e^{j\alpha 1}$
2. Direction of $\underline{I}_r$

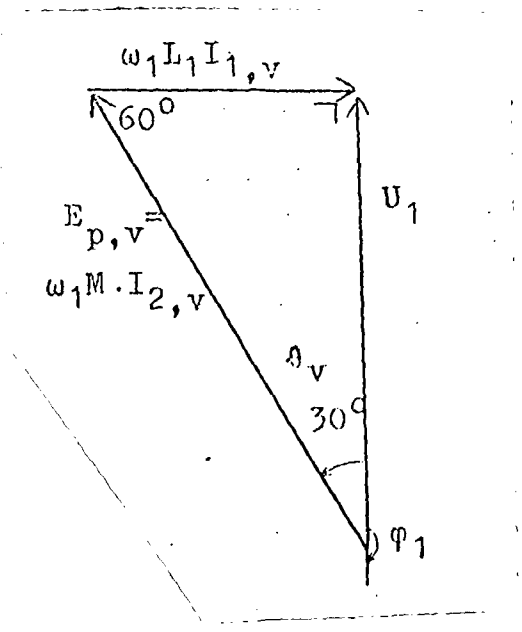
$\omega_1 L_1 I_{1,v}$
60°
U_1
$E_{p,v} = \omega_1 M \cdot I_{2,v}$
ϑ_v
30°
φ_1

Fig. 24

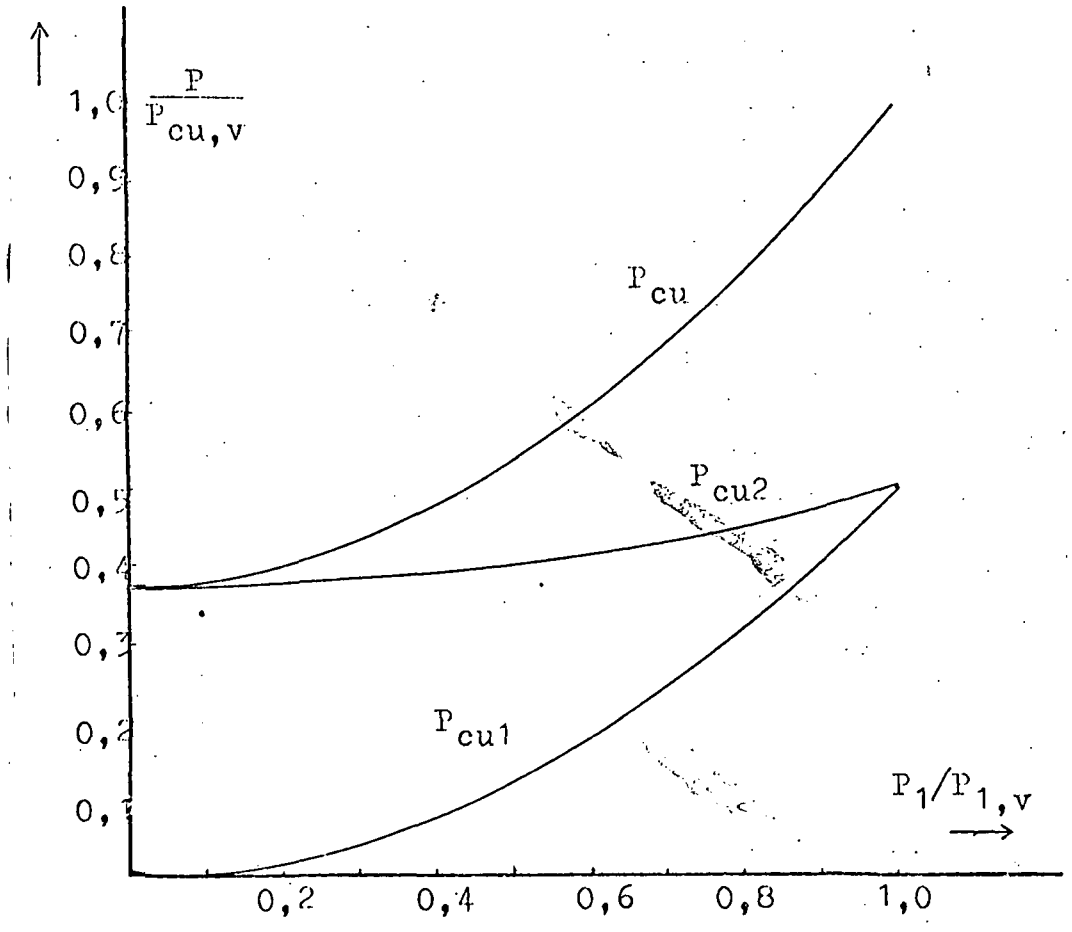

Fig. 25 Copper losses in a DSG as a function of load at $\varphi_1 = 180^o$, $\theta_v = 30^o$, and $P_{Cu1,v} = P_{Cu2,v}$

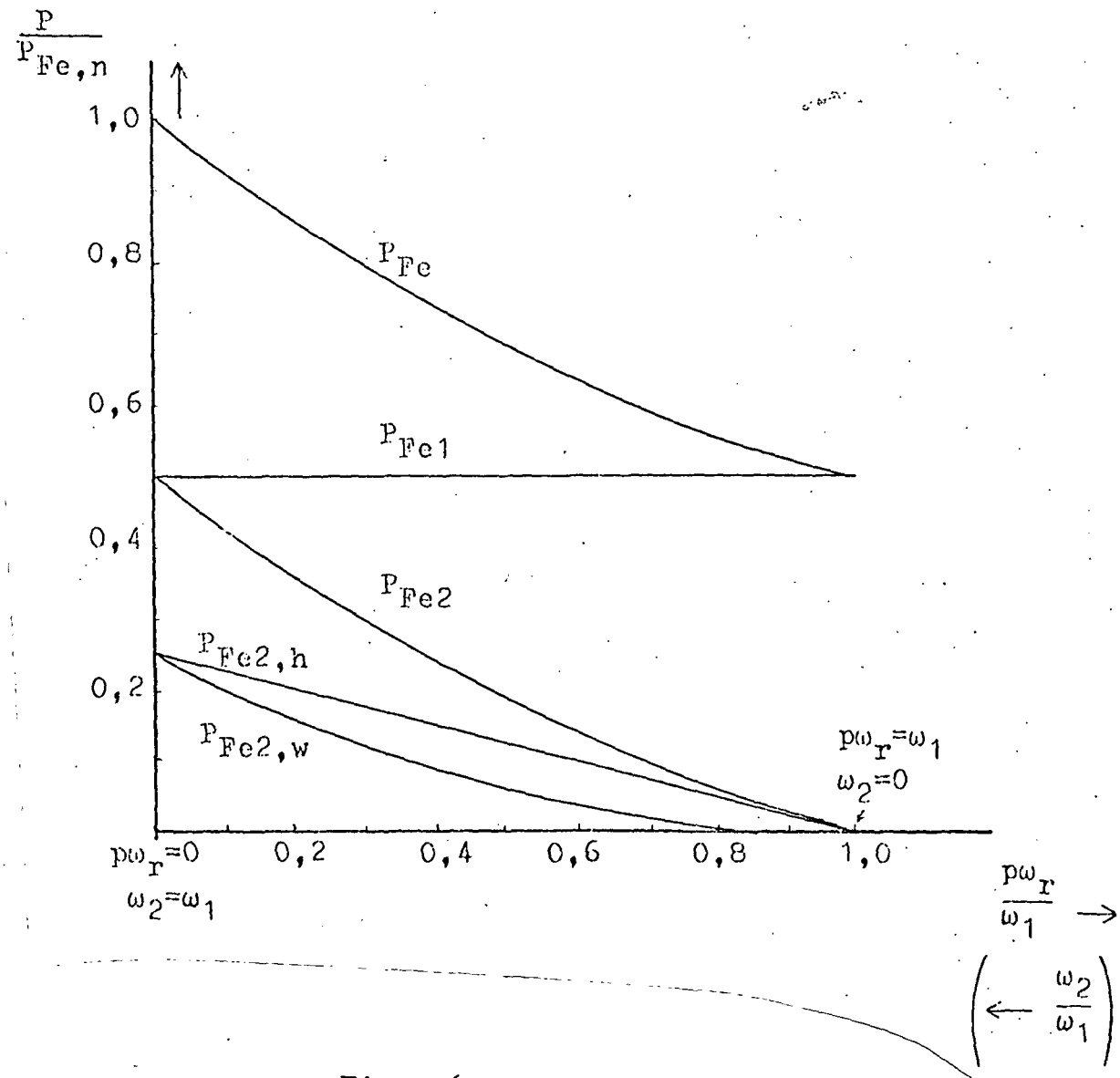

Fig. 26. Iron losses of a DSG as a function of $p\omega_r$ (ω_2) for: $P_{Fe} = 2P_{Fe1} = 2P_{Fe2} = 4P_{Fe2,w} = 4P_{Fe2,h}$ at $\omega_2 = \omega_1$ ($P_{Fe} = P_{Fe,n}$).

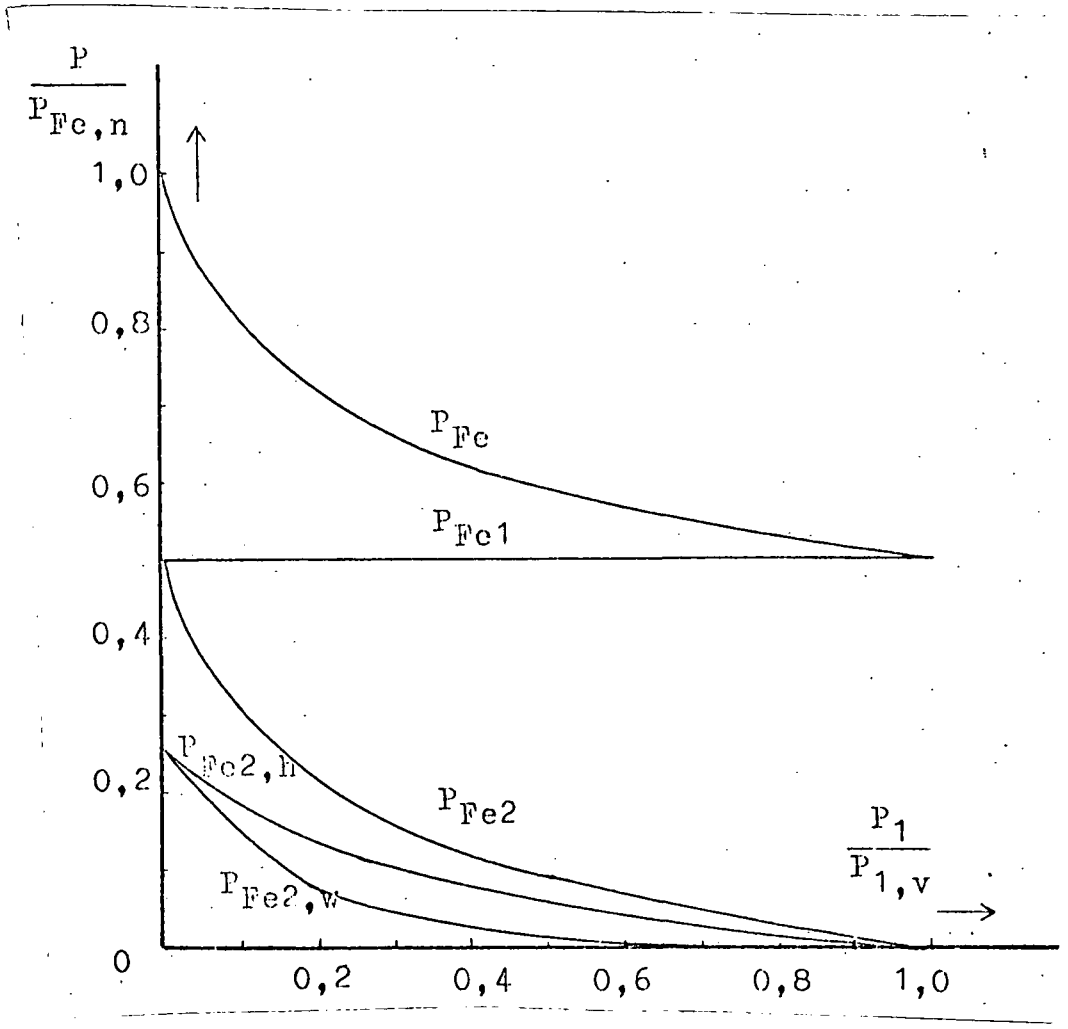

Fig. 27. Iron losses of a DSG as a function of P_1 / $P_{1,v}$; see further under Fig. 26.

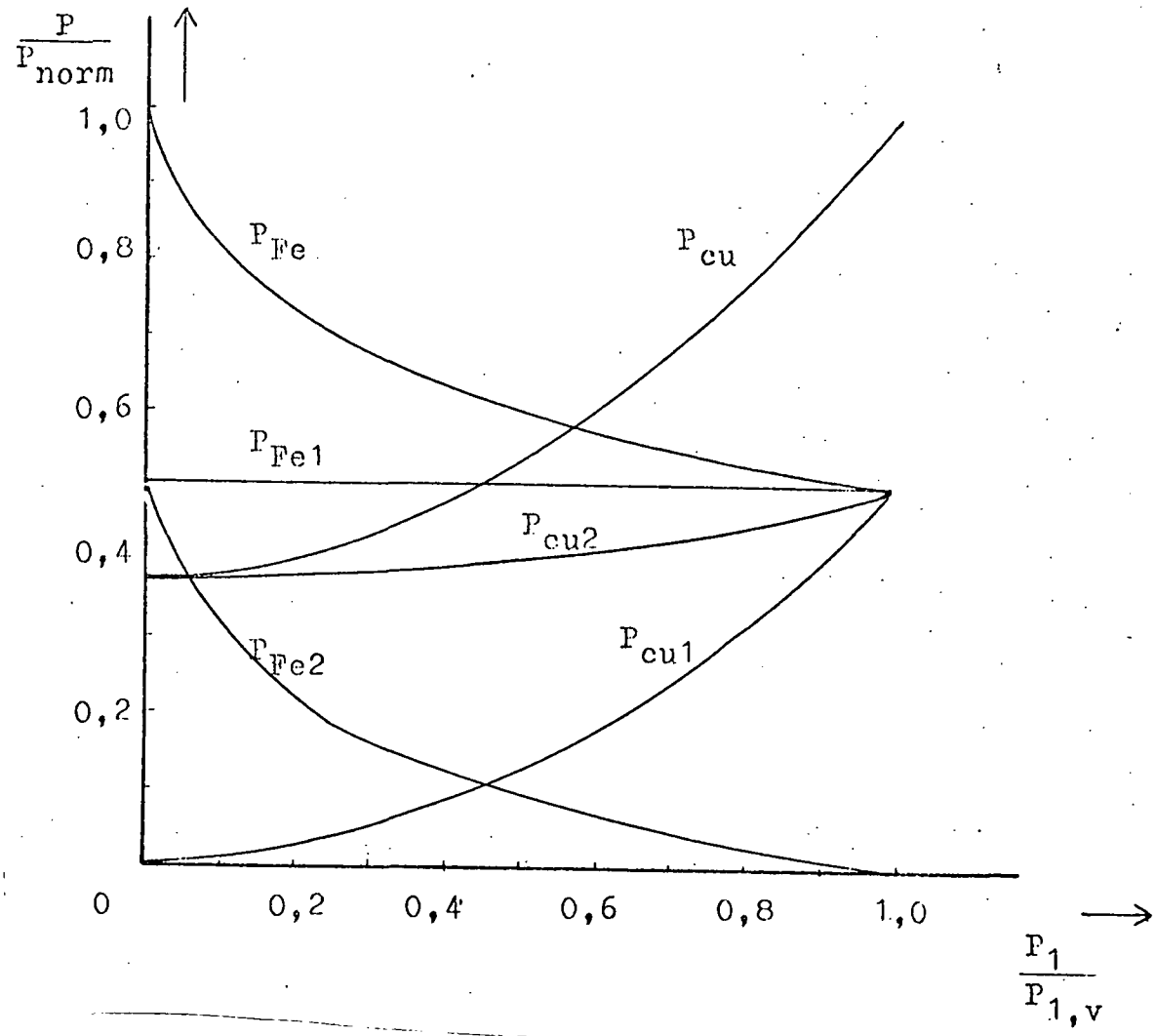

Fig. 28. Copper and iron losses for a DSG, as a function of load at $\varphi_1 = 180°$; $\theta_v = 30°$; $P_{Cu1,v} = P_{Cu2,v}$; $P_1 = c\omega_1\omega_r$; $P_{Fe1} = P_{Fe2}$ at $\omega_2 = \omega_1$; and $P_{Cu,v} = P_{Fe,v}$ thus at $\omega_2 = \omega_1$). (P_{Fe} at zero load,

[Translator's Note: There are no Figures 29 and 30 in the original.]

/76

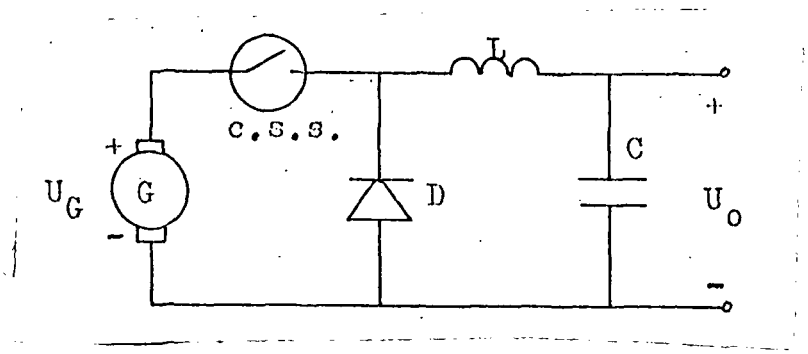

Fig. 9a

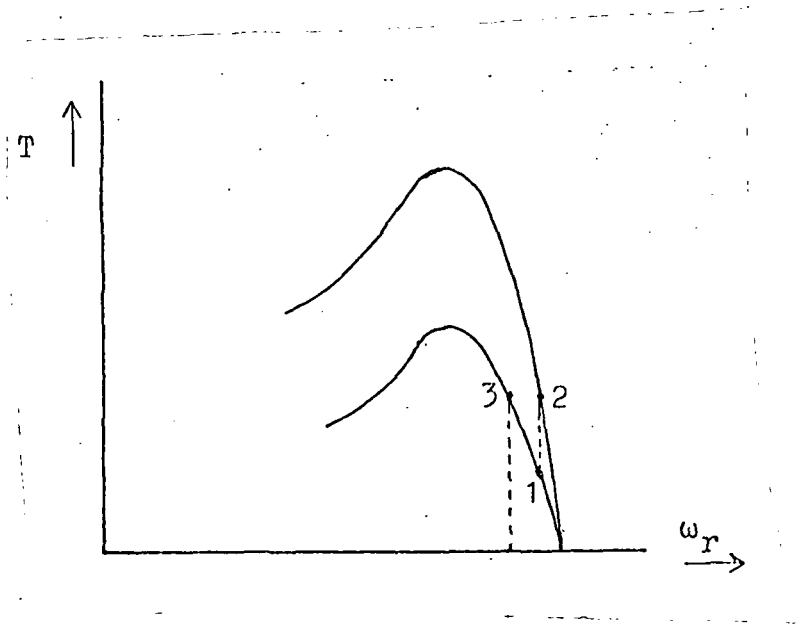

Fig. 31

/79

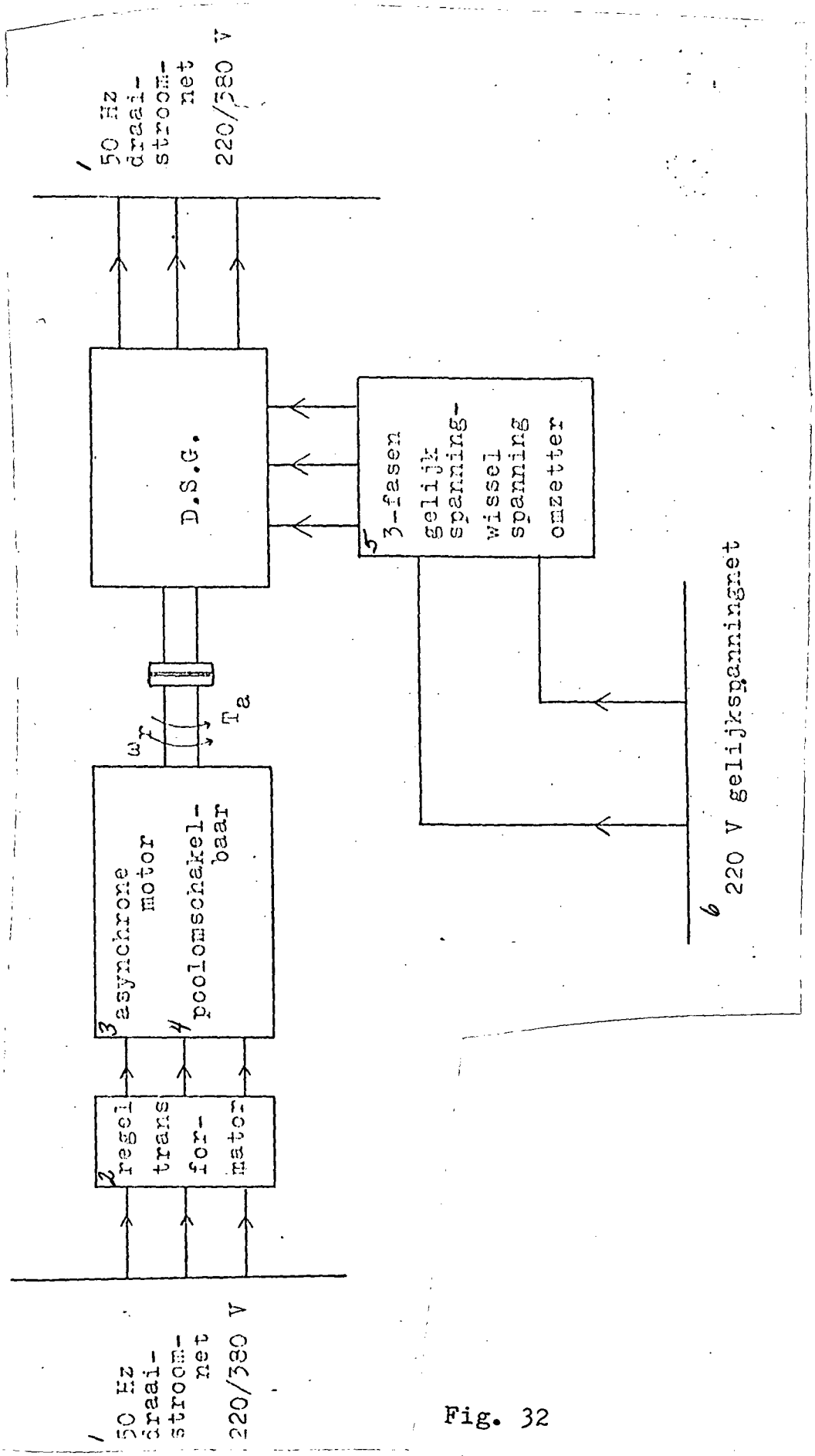
1
50 Hz
draai-
stroom-
net
220/380 V
D.S.G.
5
3-fasen
gelijk
spanning-
wissel
spanning
omzetter
ω_r
T_a
3
asynchrone
motor
4
poolomschakel-
baar
2
regel
trans
for-
mator
6
220 V gelijkspanningnet
1
50 Hz
draai-
stroom-
net
220/380 V

Fig. 32

/81

Key:
1. 50 Hz rotary-current network, 220/380 v
2. Control transformer
3. Asynchronous motor
4. Pole changeover
5. 3-phase, direct-voltage / alternating-voltage inverter
6. 220 v direct-voltage network

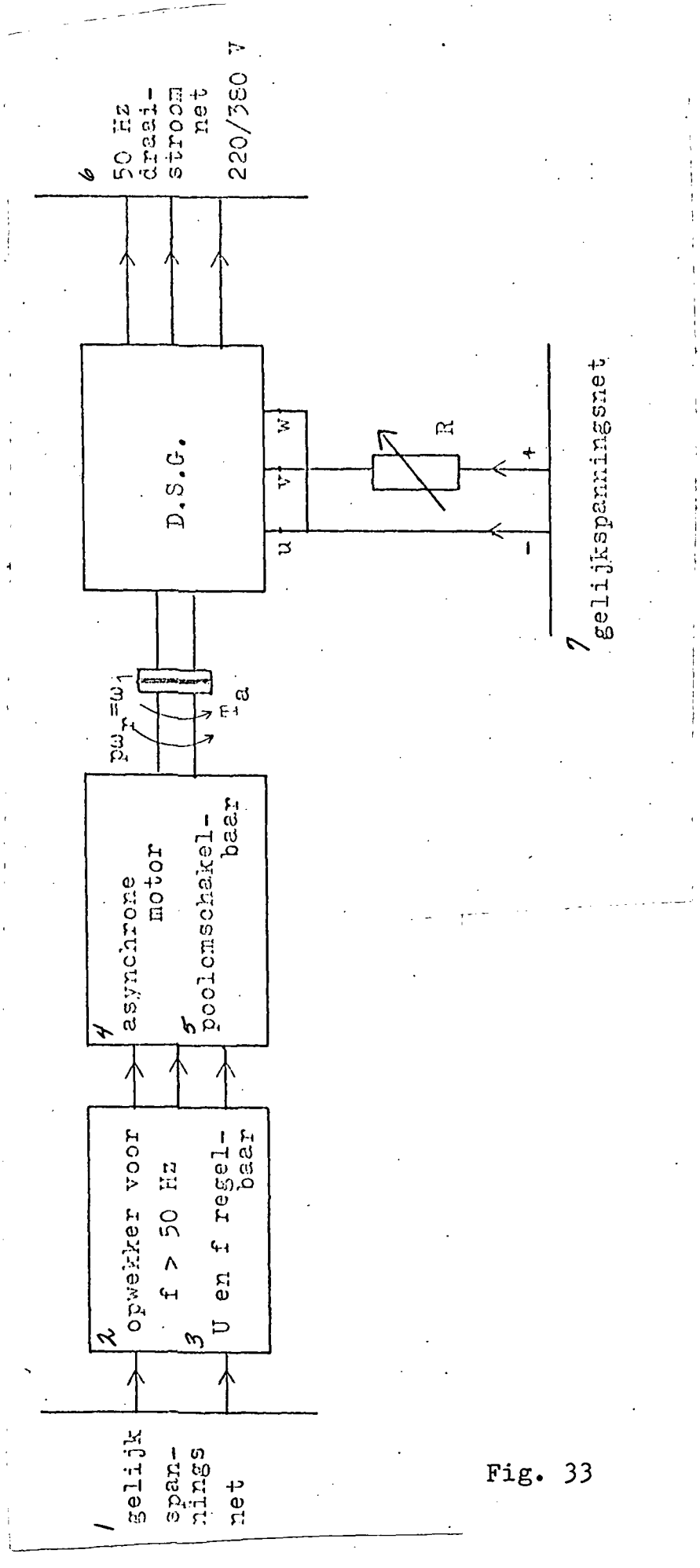
1
gelijk
spann-
rings
net
2
opwekker voor
f > 50 Hz
3
U en f regel-
baar
4
asynchrone
motor
5
poolomschakel-
baar
pω_r = ω_1
F_a
D.S.G.
u
v
w
R
+
-
7
gelijkspanningsnet
6
50 Hz
draai-
stroom
net
220/380 V

Fig. 33

Key:
1. Direct-voltage network
2. Generator for $f > 50$ Hz
3. U and f adjustable
4. Asynchronous motor
5. Pole changeover
6. 50 Hz rotary-current network, 220 /380 v
7. Direct-voltage network

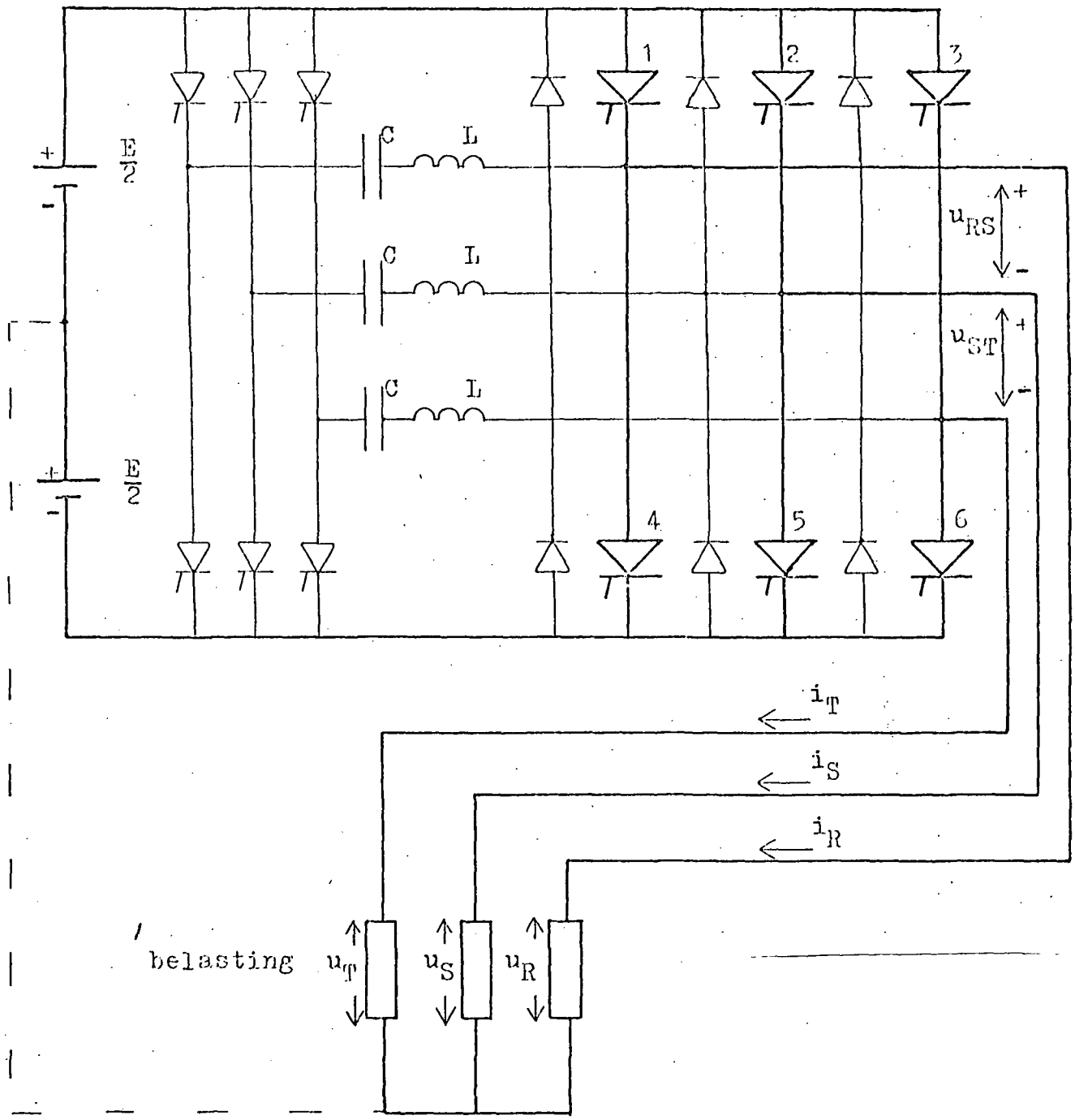

1,2,.....,6 = hoofdthyristoren.

Fig. 34

Key: 1. Load
2. Main thyristors

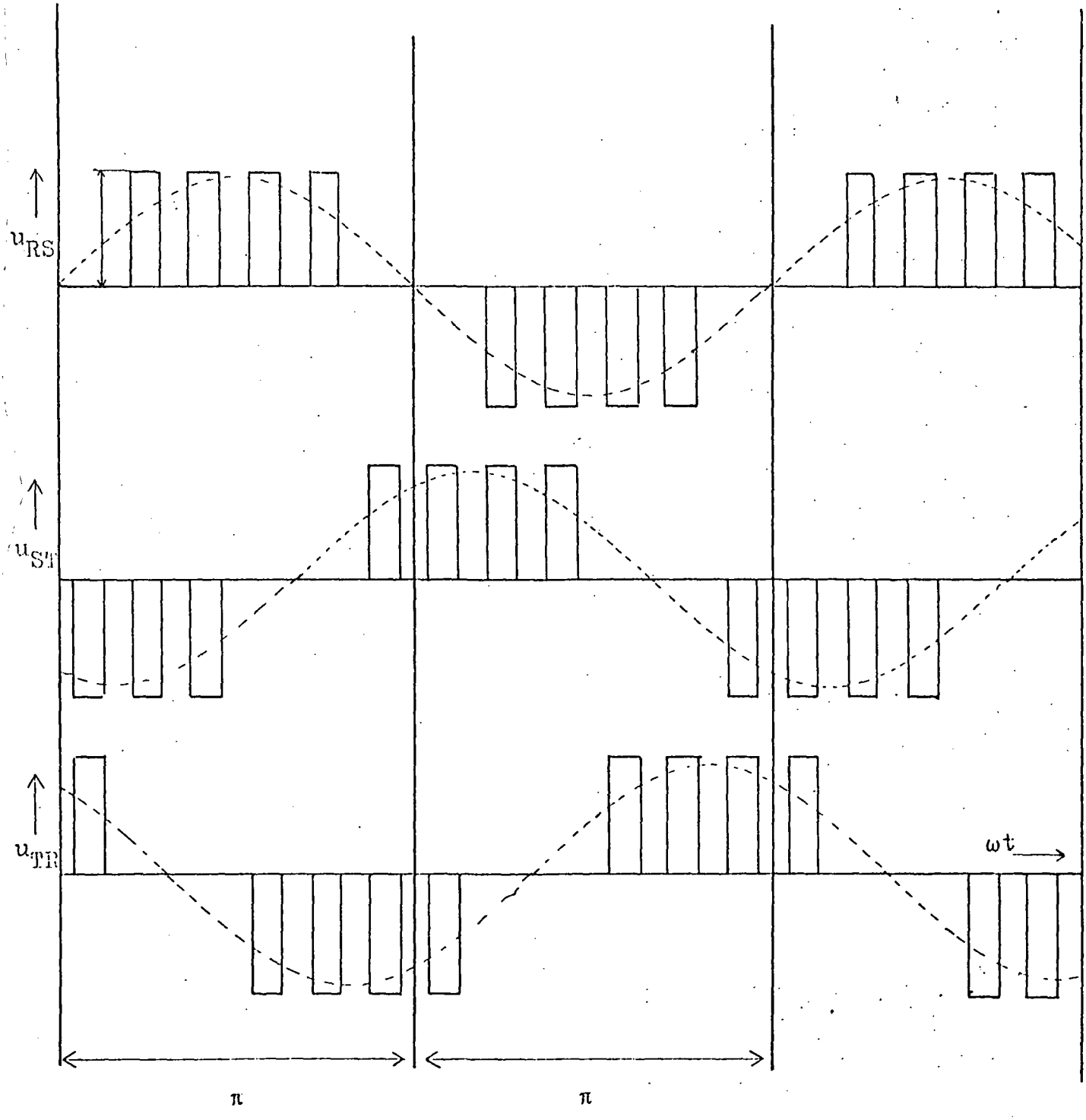

Fig. 35

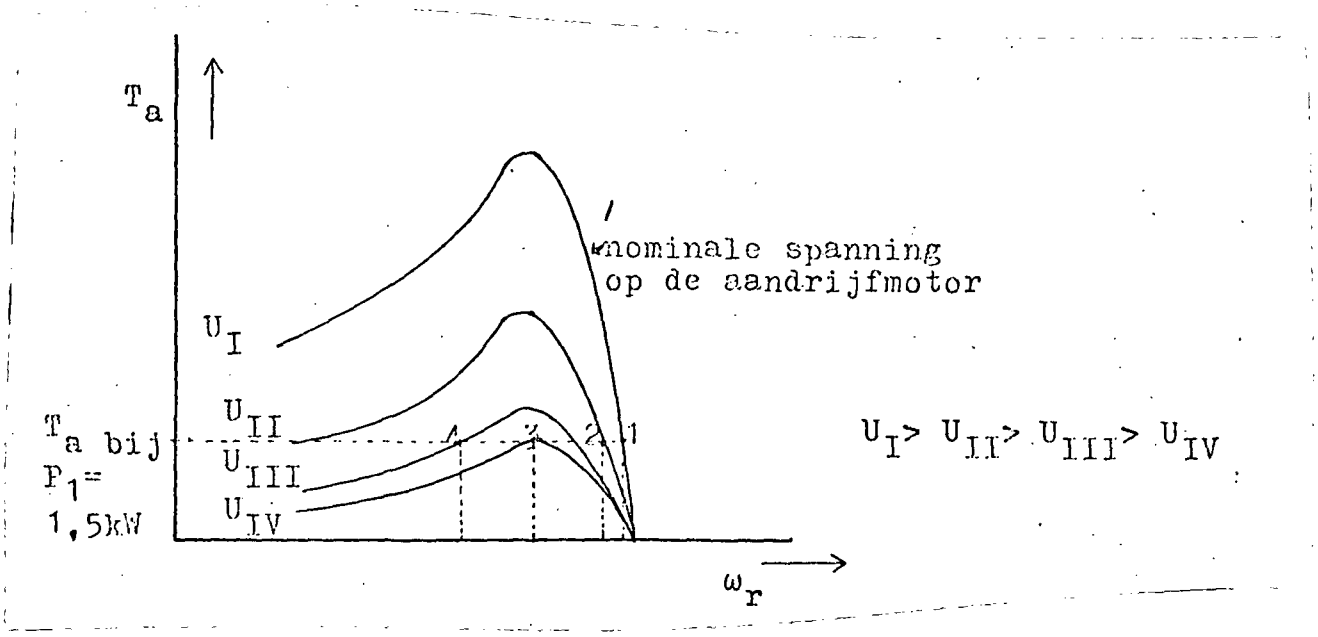

Fig. 36
Key: 1. Nominal voltage at the drive-motor

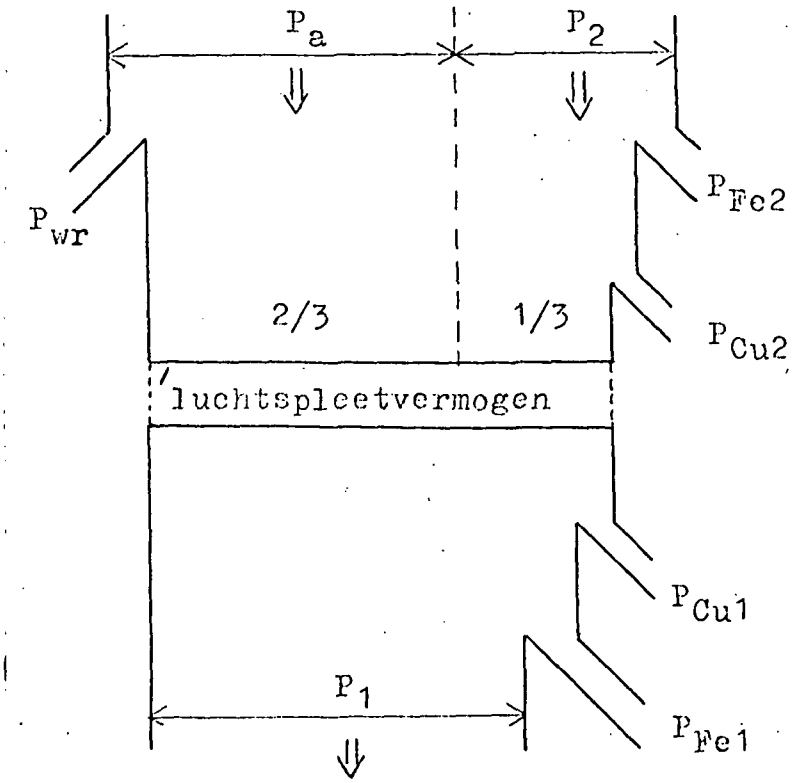

Fig. 37. Power diagram for $\omega_1 : \omega_2 : p\omega_r = 1 : 1/3 : 2/3$.
Key: 1. Air-slit power

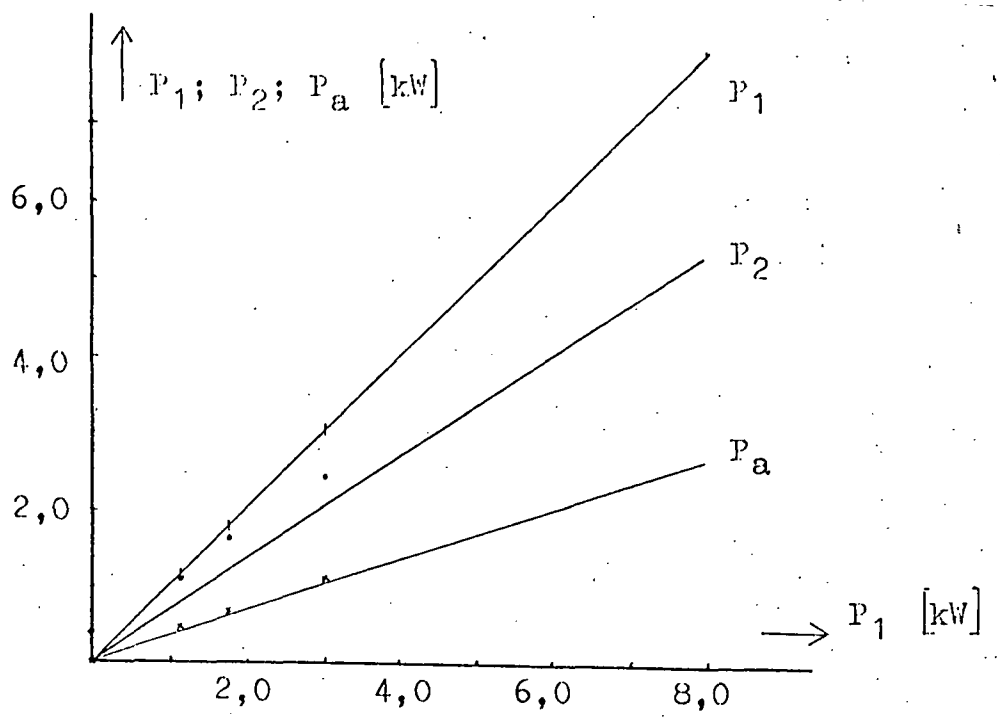

$\omega_2 = \frac{2}{3}\,\omega_1$; $p\omega_r = \frac{1}{3}\,\omega_1$; $n_r \approx 500$ omw/min.

$P_1 : P_2 : P_a = 3 : 2 : 1.$

Fig. 38a
Key: 1. rpm

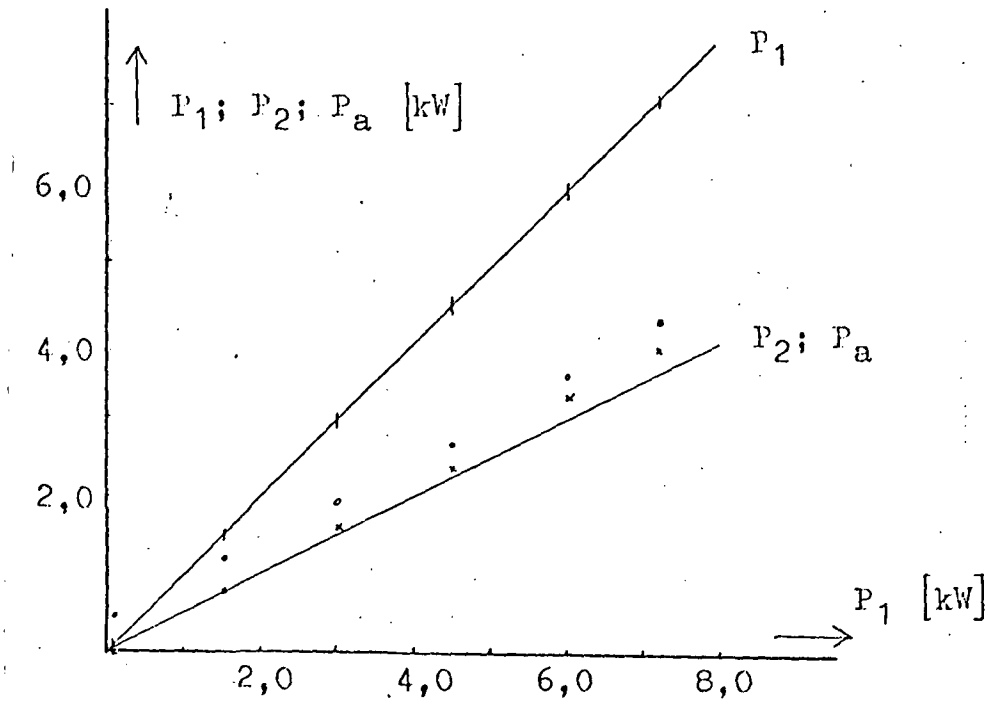

$\omega_2 = \frac{1}{2}\,\omega_1$; $p\omega_r = \frac{1}{2}\,\omega_1$; $n_r \approx 750$ omw/min.

$P_1 : P_2 : P_a = 2 : 1 : 1.$

1 meetpunt P_1

Fig. 38b
Key: 1. rpm

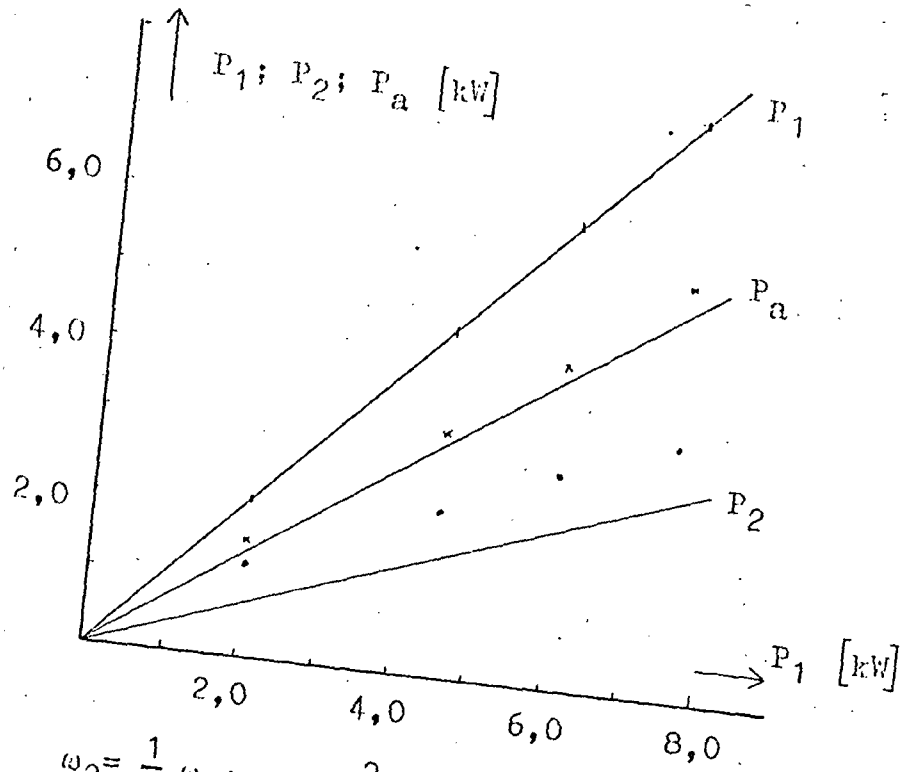

$\omega_2 = \frac{1}{3}\,\omega_1$; $p\omega_r = \frac{2}{3}\,\omega_1$; $n_r \approx 1000$ omw/min.

$P_1 : P_2 : P_a = 3 : 1 : 2$

Fig. 38c
Key: 1. rpm

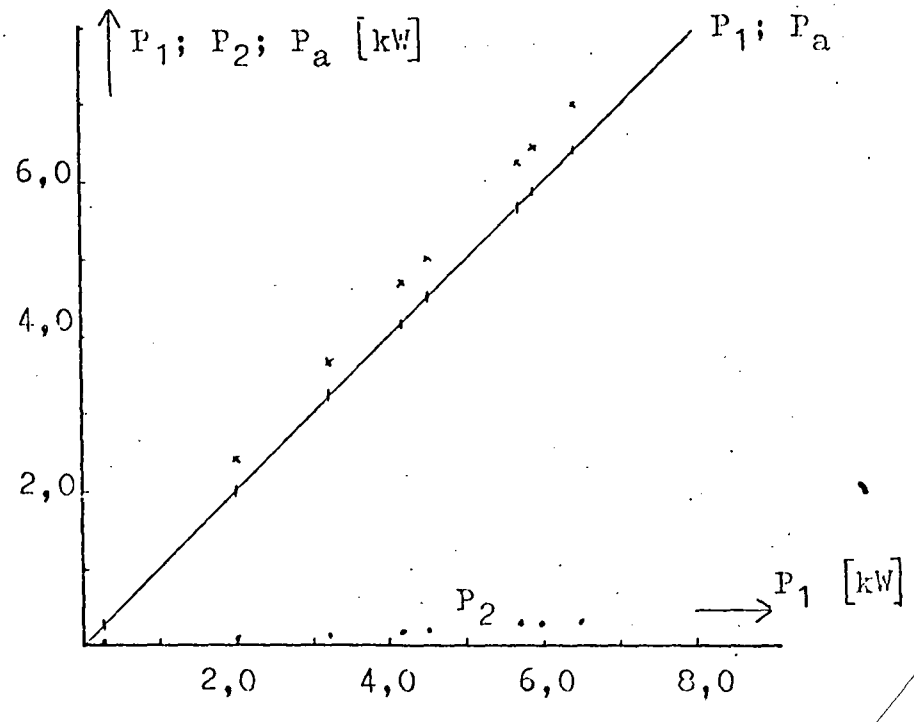

$\omega_2 = 0$; $p\omega_r = \omega_1$; $n_r \approx 1500$ omw/min.

$P_1 : P_2 : P_a = 1 : 0 : 1.$

meetpunt P_1

" P_2

Fig. 38d
Key: 1. rpm

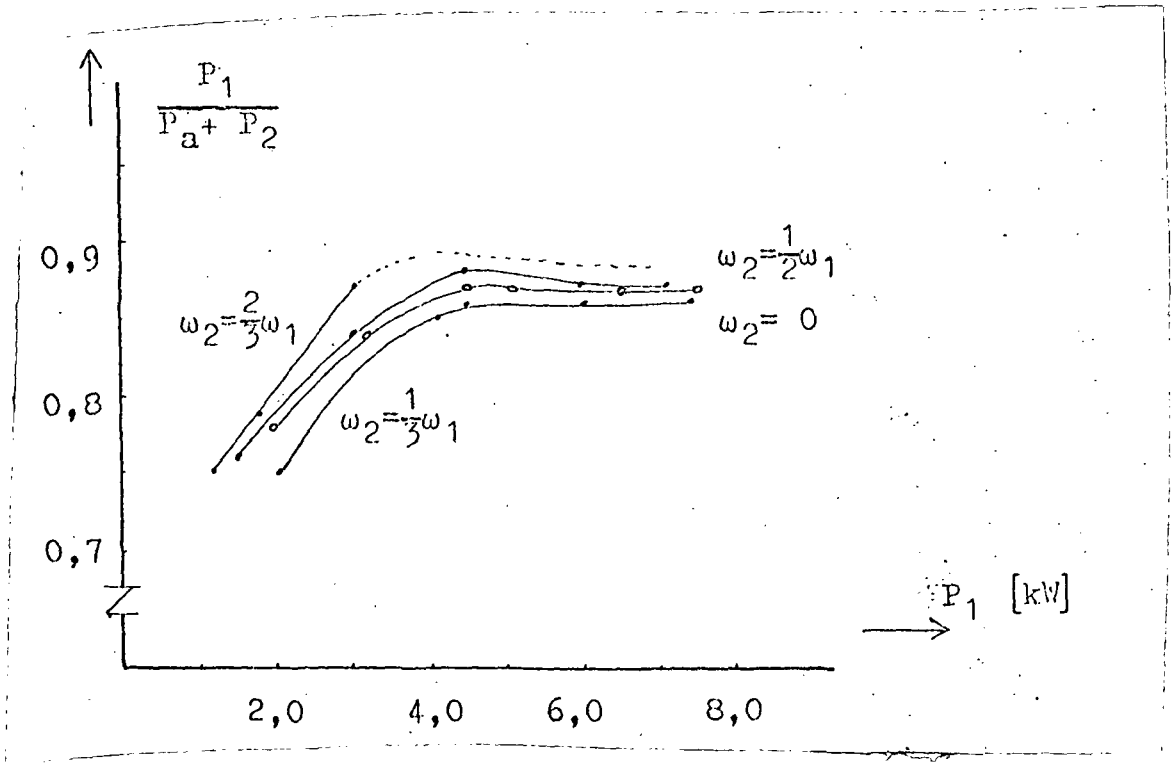
$\frac{P_1}{P_a + P_2}$
0,9
0,8
0,7
$\omega_2 = \frac{2}{3}\omega_1$
$\omega_2 = \frac{1}{3}\omega_1$
$\omega_2 = \frac{1}{2}\omega_1$
$\omega_2 = 0$
P_1 [kW]
2,0
4,0
6,0
8,0

Fig. 39

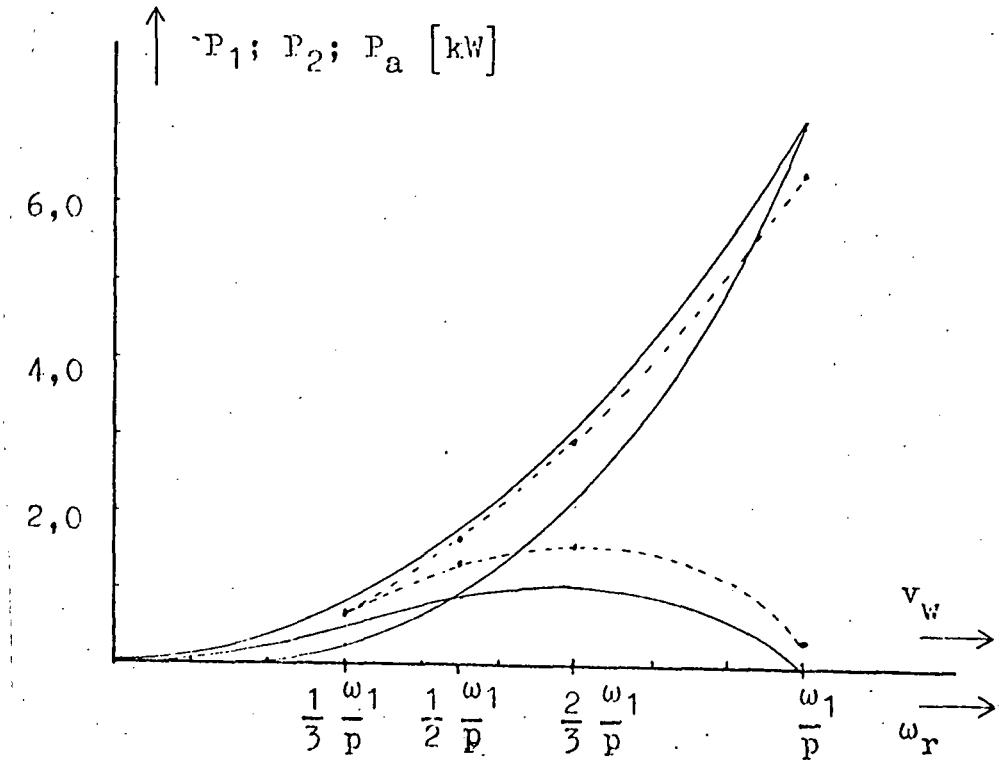

Fig. 40

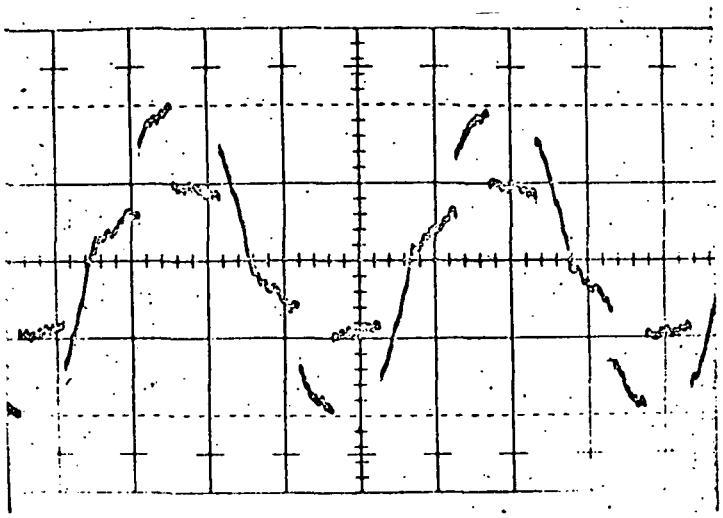

$n_r \approx 1000$ omw/min.

$\omega_r \approx \frac{2}{3}\,\omega_1$

$\omega_2 \approx \frac{1}{3}\,\omega_1$

2 foto 1

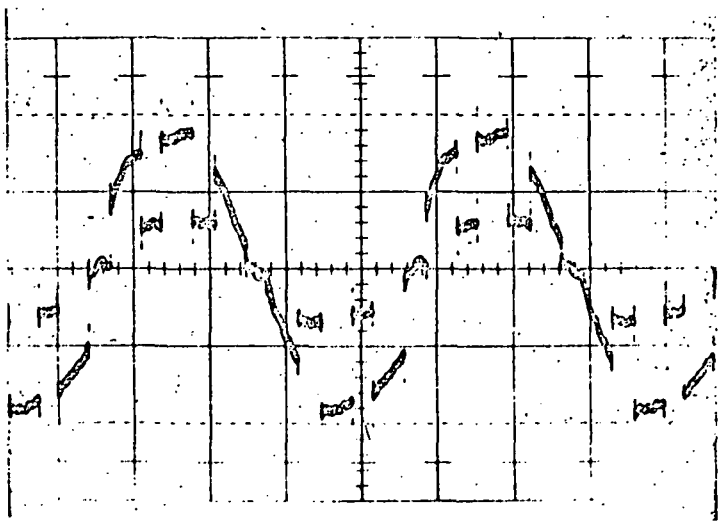

$n_r \approx 750$ omw/min.

$\omega_r \approx \frac{1}{2}\,\omega_1$

$\omega_2 \approx \frac{1}{2}\,\omega_1$

3 foto 2

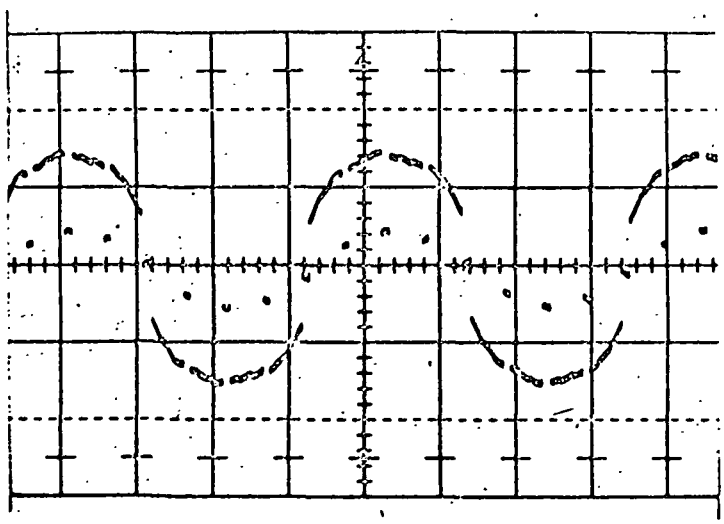

$n_r \approx 500$ omw/min.

$\omega_r \approx \frac{1}{3}\,\omega_1$

$\omega_2 \approx \frac{2}{3}\,\omega_1$

4 foto 3

5 beelden:
200 V/cm; 5 ms/cm.

6 De geïnduceerde statorspanning (220 V eff.) gemeten met open statorklemmen en bekrachtigde rotor.

Key:
1. rpm
2. Photo 1
3. Photo 2
4. Photo 3
5. Images
6. Induced stator voltage (220 v eff.) measured with open stator terminals and rated rotor

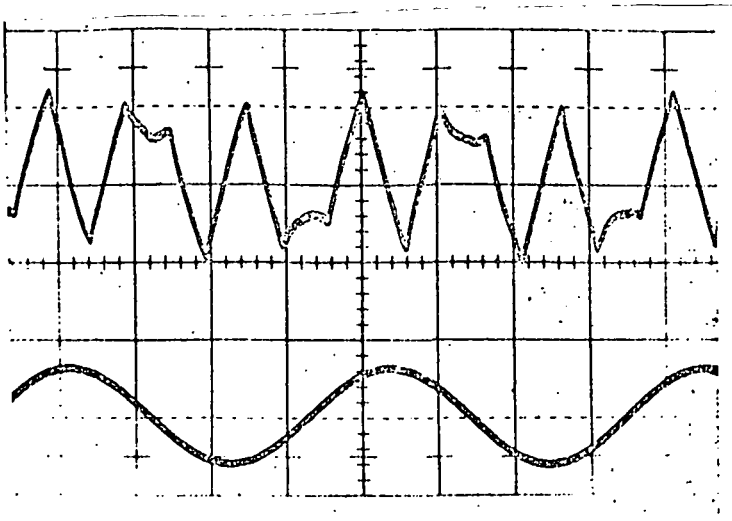

$n_r \approx 1000$ omw/min.

$I_1 = 7{,}9$ A /102

2 foto 4

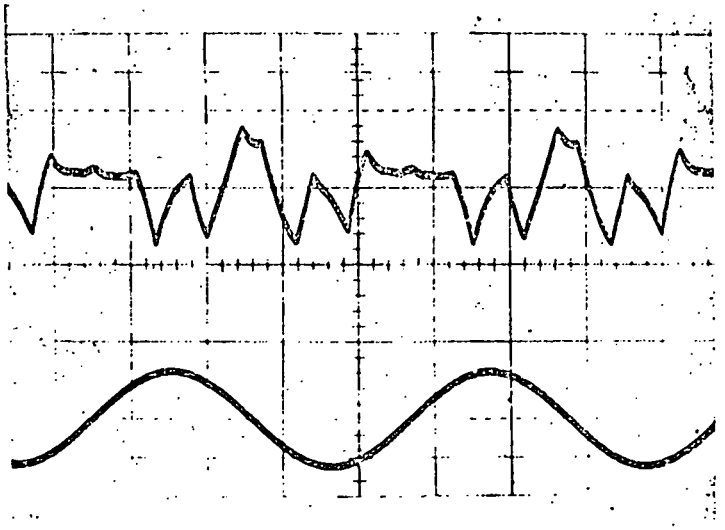

$n_r \approx 750$ omw/min.

$I_1 = 6{,}5$ A

3 foto 5

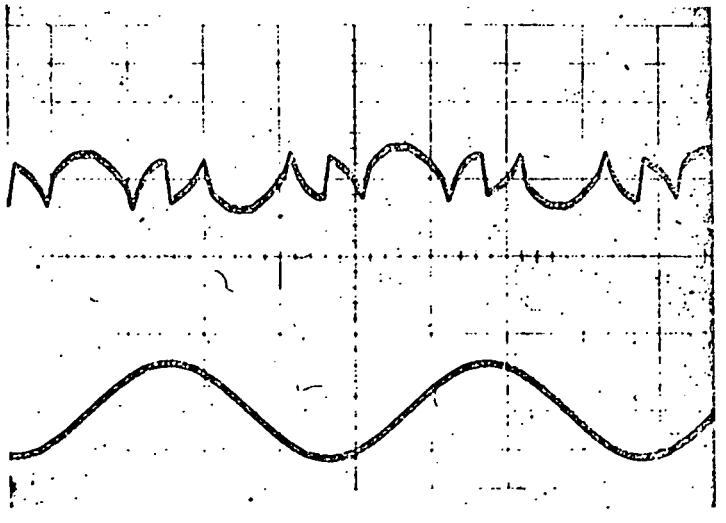

$n_r \approx 500$ omw/min.

$I_1 = 5{,}8$ A

4 foto 6

5 boven: minimaal bereikbare nullaststroom van de D.S.G. beeld ($P_1 = 0$); beeld 20 A/cm; 5 ms/cm.

onder: netspanning, 220 V effektief. beeld

Key:
1. rpm
2. Photo 4
3. Photo 5
4. Photo 6
5. Top image: minimum attainable full-load current of DSG ($P_1 = 0$); image: 20 A/cm, 5 msec/cm
   Bottom image: network voltage, 220 v effective

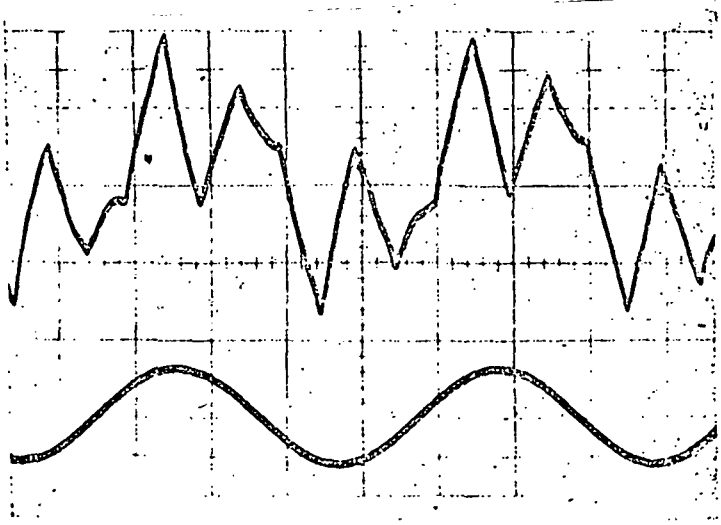

P_1 = 6,0 kW

$n_r \approx$ 1000 omw/min.

I_1 = 12,7 A

2 foto 7

/104

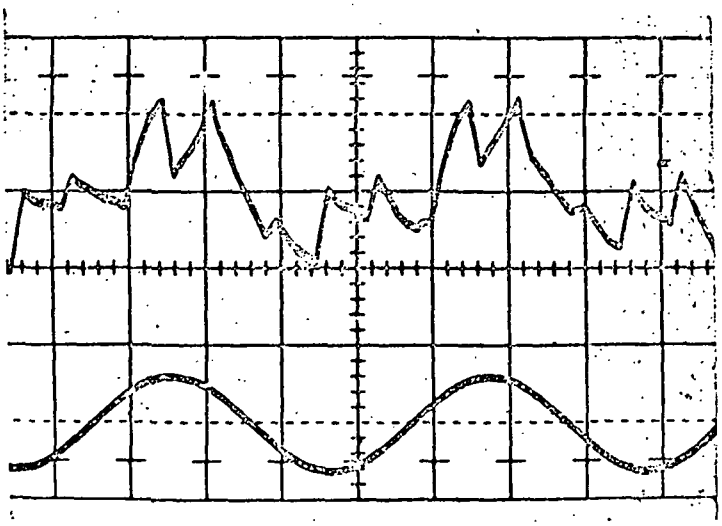

P_1 = 6,0 kW

$n_r \approx$ 750 omw/min.

I_1 = 11,5 A

3 foto 8

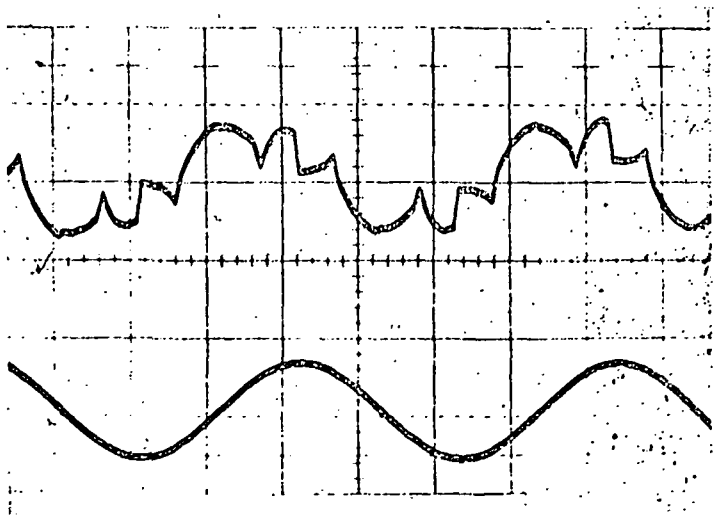

P_1 = 3,0 kW

$n_r \approx$ 500 omw/min.

I_1 = 9,5 A

4 foto 9

5 boven beeld: Door de D.S.G. aan het net afgegeven stroom I_1 bij naast de foto opgegeven P_1; 20 A/cm; 5 ms/cm.

onder beeld: netspanning 220 V effektief,

Key: 1. rpm
2. Photo 7
3. Photo 8
4. Photo 9
5. Top image: current I_1 delivered by the DSG to the network at the P_1 given next to the photo; 20 A/cm, 5 msec/cm
Bottom image: network voltage 220 v effective,

/106

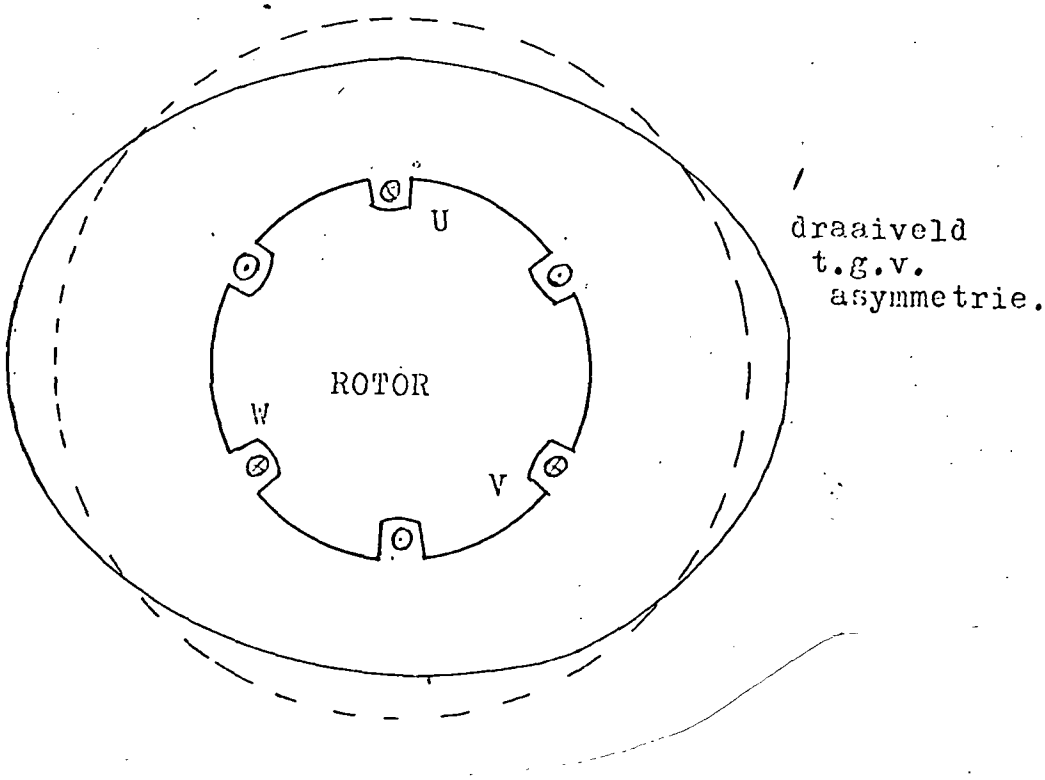

Fig. 41
Key: 1. Rotary-current field under assymetrical conditions

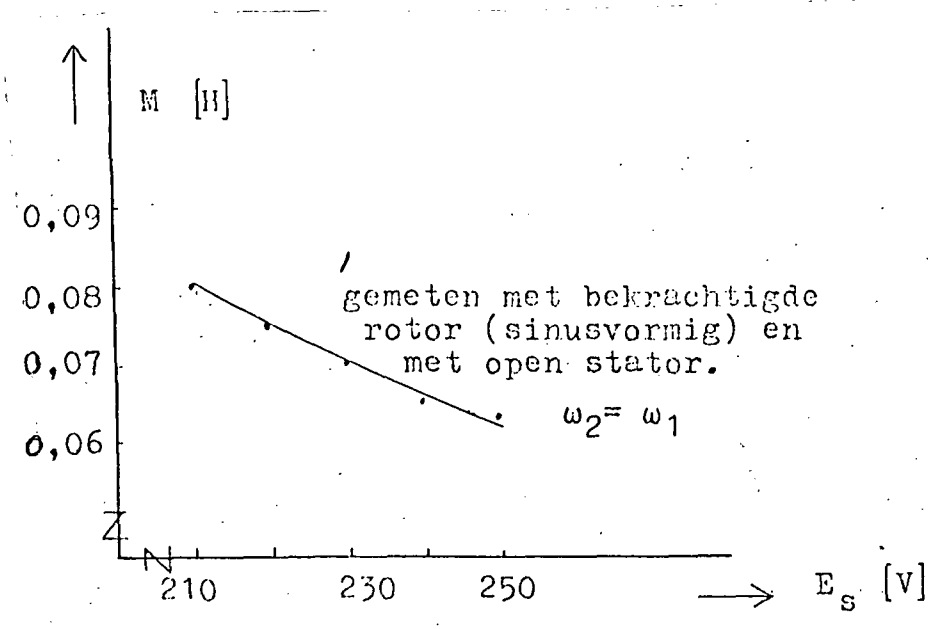

Fig. 42
Key: 1. Measured with rated rotor (sinusoidal) and with open stator

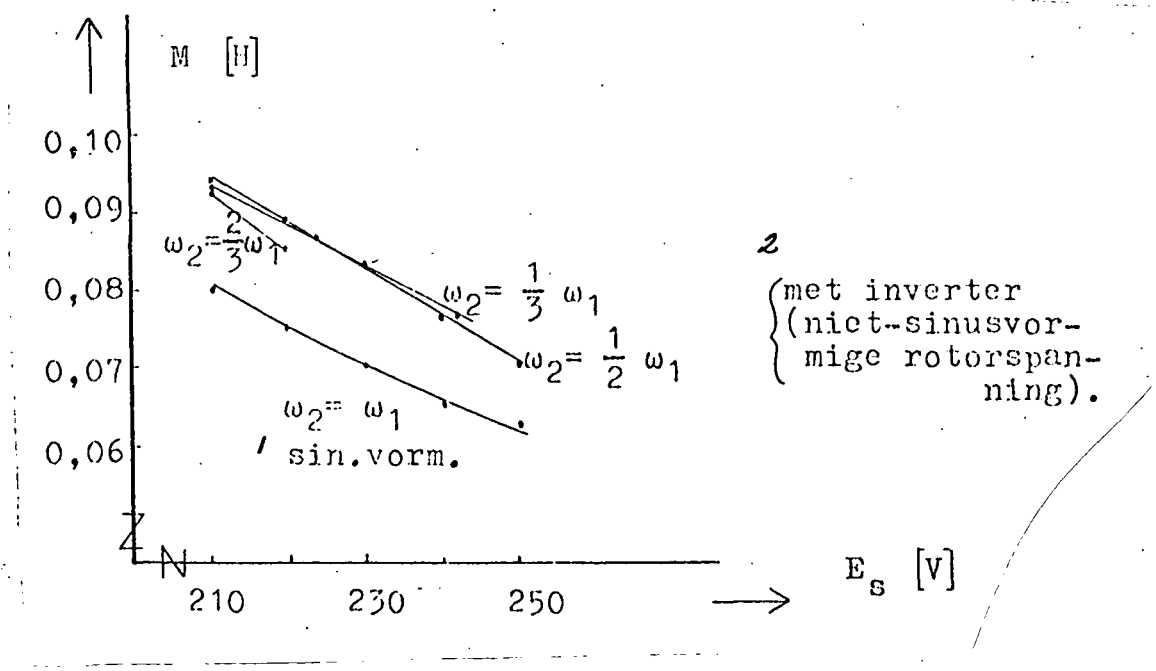

Fig. 43

Key: 1. Sinus.
2. {With inverter (non-sinusoidal rotor voltage

STANDARD TITLE PAGE

1. Report No. NASA TM-75497	2. Government Accession No.	3. Recipient's Catalog No.
4. Title and Subtitle INVESTIGATION OF A GENERATOR SYSTEM FOR GENERATING ELECTRICAL POWER, TO SUPPLY DIRECTLY TO THE PUBLIC NETWORK, USING A WINDMILL		5. Report Date August 1979
		6. Performing Organization Code
7. Author(s) C. Tromp, Power Electronics Laboratory		8. Performing Organization Report No.
		10. Work Unit No.
9. Performing Organization Name and Address Leo Kanner Associates Redwood City, California 94063		11. Contract or Grant No. NASW-3199
		13. Type of Report and Period Covered Translation
12. Sponsoring Agency Name and Address National Aeronautics and Space Administration, Washington, D.C. 20546		14. Sponsoring Agency Code

15. Supplementary Notes
Translation of "Onderzoek aan een generatorsystem voor het opwekken van - direkt aan het openbare net te leveren - elektrische energie met behulp van een windmolen," Delft, The Netherlands, State Univ. of Technology, Power Electronics Lab., Dept. of Electrical Engineering, May 1957, 122 pages.

16. Abstract In this report, an investigation is described for a generator system for generating electrical energy, for direct supply to the public three-phase network, using a windmill.

Besides the task of converting mechanical energy to electrical energy for a three-phase (network) voltage of constant amplitude and frequency, the generator system has the task of controlling the windmill by number of revolutions whereby the power drawn from the wind for a given wind velocity is maximum.

Although this results in a generator revolution which is proportional to wind velocity, the stator of the generator can be linked directly to the network, because a feed converter at the rotor takes care of constant voltage and frequency at the stator.

It is characteristic that the generator itself, in

17. Key Words (Selected by Author(s))	18. Distribution Statement Unclassified-Unlimited		
19. Security Classif. (of this report) Unclassified	20. Security Classif. (of this page) Unclassified	21. No. of Pages 158	22. Price